PROPELLANT ISOLATION SHUTOFF VALVE PROGRAM
FINAL REPORT

JPL Contract No. 953029

TRW 73.4781.6-15

February 1973

Prepared for

The Jet Propulsion Laboratory
Pasadena, California 91103
Under National Aeronautics and Space
Administration Contract NAS7-100

TRW
SYSTEMS GROUP
ONE SPACE PARK • REDONDO BEACH, CALIFORNIA

PROPELLANT ISOLATION SHUTOFF VALVE PROGRAM

FINAL REPORT

JPL Contract No. 953029

TRW 73.4781.6-15

February 1973

Prepared: _____
F. L. MERRITT, Project Manager

Approved: _____
S.F. GIFFONI, Manager
Chemical Propulsion Department

Prepared for

THE JET PROPULSION LABORATORY
Pasadena, California 91103

This work was performed for the Jet Propulsion Laboratory, California Institute of Technology Sponsored by the National Aeronautics and Space Administration under Contract NAS7-100

TRW
SYSTEMS GROUP
ONE SPACE PARK • REDONDO BEACH, CALIFORNIA

FORWARD

This report was prepared by TRW Systems Group, Redondo Beach, California. Described is the analysis and design effort conducted with the objective of determining the optimum configuration for a multicycle isolation valve suitable for application in a fluorine-hydrazine or Flox-MMH rocket engine feed system. The work was accomplished during the period from November 1970 through October 1972. The program was conducted for the Jet Propulsion Laboratory, Pasadena, California under contract JPL 953029. The JPL Program Manager is Mr. Orville Keller.

The work was performed by the Combustion Systems Laboratory in the Applied Technology Division. Mr. Frank L. Merritt of the Chemical Propulsion Department is the Program Manager. Acknowledgment is given for the contributions of Messrs. R. J. Salvinski, G. S. Bell and J. L. Reeve.

ABSTRACT

This report documents an analysis and design effort directed to advancing the state-of-the-art of space storable isolation valves for control of flow of the propellants liquid fluorine/hydrazine and Flox/monomethy-hydrazine. Emphasis is upon achieving zero liquid leakage and capability of withstanding missions up to 10 years in interplanetary space. Included is a study of all-metal poppet sealing theory, an evaluation of candidate seal configurations, a valve actuator trade-off study and design descriptions of a pneumo-thermally actuated soft metal poppet seal valve.

The concepts and analysis leading to the soft seal approach are documented. A theoretical evaluation of seal leakage versus seal loading, related finishes and yield strengths of various materials is provided. Application of a confined soft aluminum seal loaded to 2 to 3 times yield strength is recommended. Use of either an electro-mechanical or pneumatic actuator appears to be feasible for the application. The actuator trade-off study indicates the electro-mechanical approach to offer advantages on an overall system basis and is recommended for ultimate design.

CONTENTS

CONTENTS (Continued)

FIGURES

FIGURES (Continued)

TABLES

1.0 INTRODUCTION

Studies of the propulsion systems required for future long term unmanned spacecraft missions to the outer planets indicate storage of high energy propellants with extremely low leakage for periods of ten years or more must be achieved. Application of specialized isolation valves designed for high sealing reliability for a relatively low number of mission cycles and demanding only slow actuating response provides the best means of assuring propellant storage integrity.

The objectives of the Space Storable Propellant Isolation Valve Program are to investigate methods of internal valve sealing and to provide designs for both the valve and actuator. Theory and design concepts for poppet sealing have been investigated. Included has been an evaluation of materials usable in the propellants liquid fluorine-hydrazine and Flox-MMH, concepts of sealing potentially capable of achieving zero liquid leakage for long periods, and data for design of valves and actuators.

In addition to propellant isolation valves, also included in the program are investigation and design of helium isolation valving. Predicted propellant contamination of the helium on the downstream side of the valve makes necessary consideration of propellant compatibility for the component. This Final Report presents the propellant valve effort. Application of the propellant poppet seal concepts noted in this report appear to be favorable for the helium valve design.

Part of this effort was accomplished early in the program and is documented by Reference 1, Detailed Evaluation Report. In addition a design was provided for a pneumotherally actuated valve using a combined Soft-Hard, Hard-Hard poppet sealing concept. This design is documented in Section 5.0 of this report with changes incorporated in response to subsequent analysis. The last phase of the work was originally published as the Alternate Poppet Seal and Actuator Trade-off Study, Reference 27. This effort forms a part of this report primarily in Sections 2.0, 3.0 and 4.0.

The objectives of the study were to establish the most feasible approach for all-metal poppet sealing providing zero liquid-leakage and to determine the optimum valve actuating mechanism considering both the valve and system characteristics.

The seal study phase of the work is directed to a more detailed analytical evaluation of the mechanisms important to achieving low leakage and predicting seal life. The general analysis of principles is covered in Section 2 and a detailed analysis of designs in Section 3.

The major sealing designs considered are:

1. Soft-Hard metal configurations
2. A hard-hard face seal combined with a shear seal
3. An application using ultrasonic energy at the seal interface

The soft-hard configurations include a reappraisal of the original Soft-Hard, Hard-Hard Seal, pneumothermal actuated design submitted to JPL (Reference 2). A detailed stress analysis directed to the loading of the soft seal insert was completed. The analysis of the Soft-Hard, Hard-Hard Seal revealed design revisions to reduce friction between the outer confining wall and the soft material to be of advantage. Also a change in form of the insert to eliminate the thin cross-section originally used was shown to be desirable.

An alternate soft seal design (Bulk Energized Seal) has been proposed incorporating a method of developing high bulk loading of the seal with relatively lower actuating forces. The most favorable sealing approach for the isolation valve determined from the study lies in either the revised Soft-Hard, Hard-Hard Seal or the Bulk Energized Seal concepts.

Several other soft-hard design configurations which utilize a shear seal approach are included without analysis. Tests are required to establish the relative advantage or disadvantage of the shearing concept for sealing in liquid fluorine. Little data and

analysis is available to establish a comparative evaluation. At the outset the approach of minimum sliding action at the seal face has been assumed to be likely to produce the least wear and chemical activity.

As a result of the study application of the soft-hard metal poppet seal approach is recommended to meet the zero-liquid leakage requirement and to provide particle contamination resistance. The application of more advanced sealing techniques such as ultrasonic bonding described in the report requires feasibility testing before a design can be established. Unless such an exploratory development commitment can be made in the program the approach cannot be considered feasible. Both the Soft-Hard, Hard-Hard Seal and Bulk Energized Seal concepts noted above must be considered as poppet seal candidates.

The actuator trade-off study is provided in Section 4. The study is addressed to both the valve and system interface characteristics. A brief review of a wide range of actuating methods is considered at the outset. The results of the study indicate either pneumatic or electromechanical methods to be feasible. The electromechanical approach provides the greatest advantage with respect to the system. Failure modes do not interact with the system, i.e. leakage of pilot valves supplied from the tank pressurization source. Only electrical connections are required for supply. The mechanisms required for electrical drive are also favorable in characteristic for the low response, low wattage operating characteristic. The environmental extremes of cryogenic temperature and hard vacuum are not new to electromechanical devices. It is recommended the electromechanical actuation approach be adopted for the flight design of both the propellant and helium isolation valves.

2.0 REVIEW OF MECHANISMS OF POPPET SEALING

This section of the study has the purpose of exploring analytical techniques pertinent to predicting the performance of seals. Leakage as related to surface character and the surface effects of wear and chemical reactivity are the primary considerations. Empirical data relating yield strength, unit seal loading and finish to leakage for metal seals in the plastic range is given. Other techniques for application of hard-hard seals and use of energy locally applied to augment sealing are touched upon

2.1 Analytical Approaches to Seal Performance Predictions

2.1.1 Leakage Prediction

This section analytically relates the character of the interface asperities for a seal surface under in-contact conditions to leakage.

The expression for the average leakage area taken from reference 3 (Long Term Performance) is:

$$A_L = \xi_{ms}\ell\left\{(2\pi)^{-1/2}\, e^{-h^2/2\xi_{ms}^2} + \frac{h}{2\xi}\left[1 + \text{erf}\left(\frac{h}{\sqrt{2}\,\xi}\right)\right]\right\}$$

where:
- A_L = leak area
- ℓ = circumferential length of contact area
- ξ_{ms} = rms surface asperity height
- h = gap height between mean surface level and contacting surface
- erf = error function

This analysis applies to a perfectly rigid flat surface which is in contact with a deformable surface with random irregularities as shown in Figures 2-1 and 2-2.

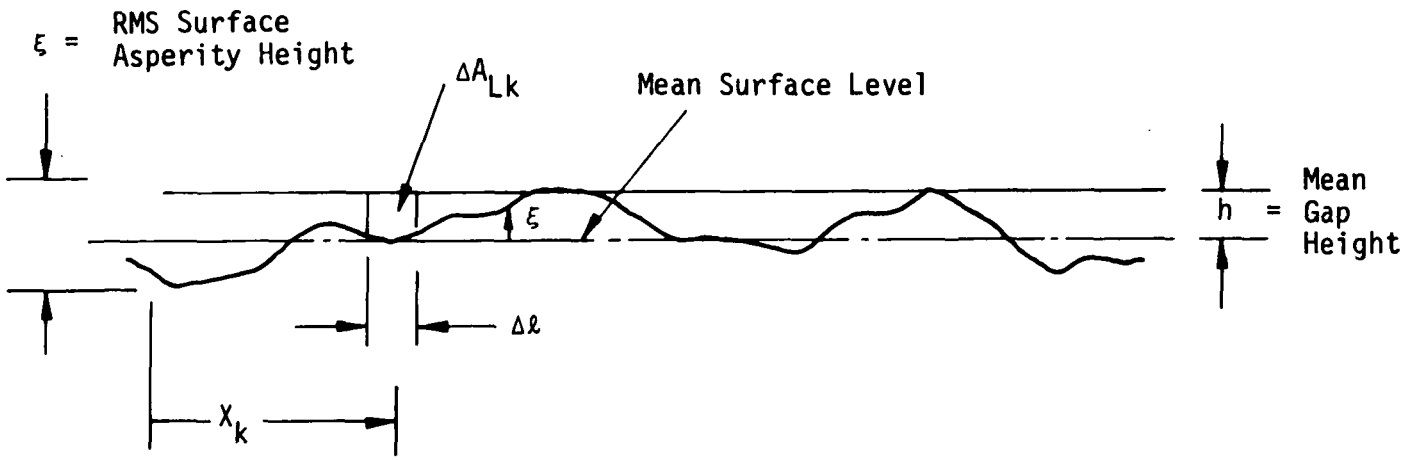

Figure 2-1. Leakage Geometry

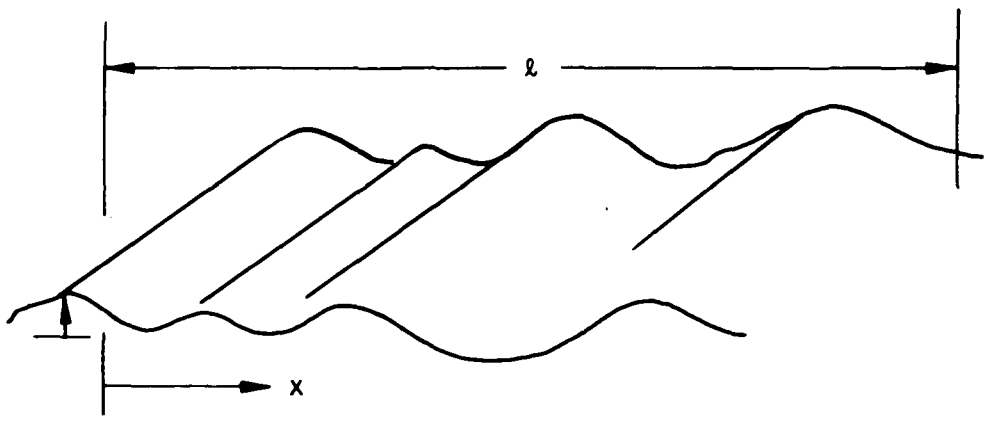

Figure 2-2. One Dimensional Random Surface

This equation is plotted in Figure 2-3 in terms of a dimensionless leak area as a function of a dimensionless gap.

The limiting value for $A/\Delta\ell\xi$ as h/ξ approaches zero is determined by the assumption that the nearness of contact cannot exceed the mean surface asperity level of the machined surface. Figure 2-4 is a plot of the leak rate of helium as a function of the differential pressure across the two surfaces for a given surface finish and gap height. For purposes of the analysis given in the reference the valve seat diameter was chosen as 0.050 inch. Molecular flow with a small entrance path is assumed as the dominating leak mechanism. For larger seat diameters the leakage values must be multiplied by D/.05 where D is the diameter of the large seat.

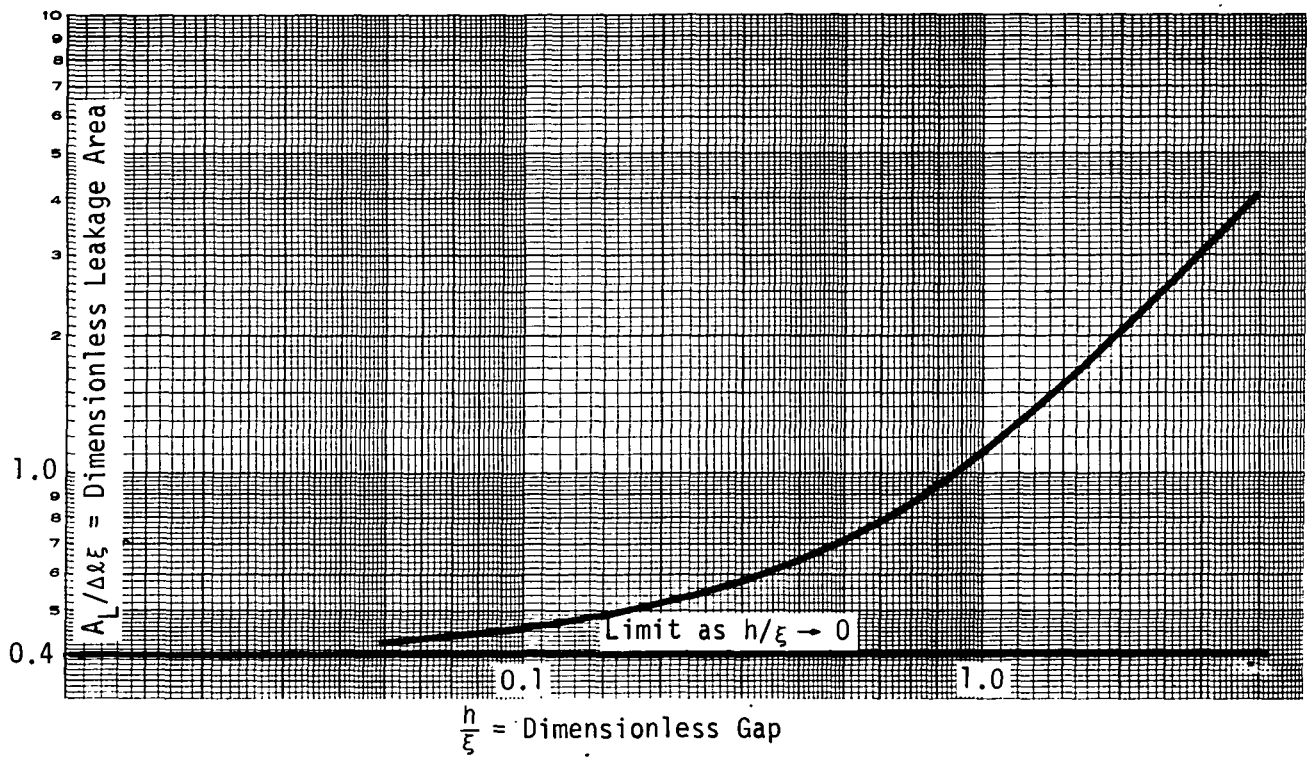

Figure 2-3. Dimensionless Area Vs. Gap

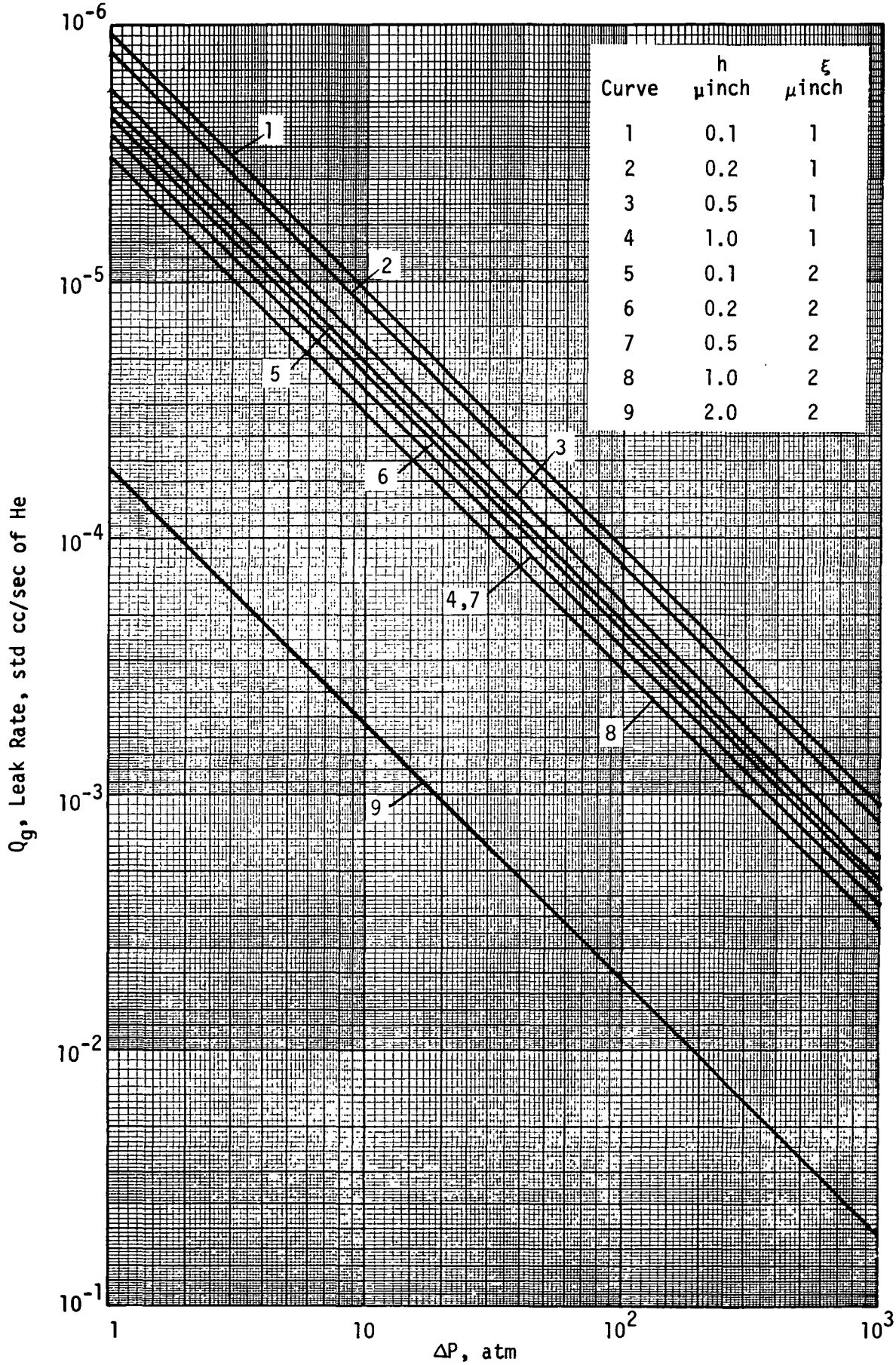

Figure 2-4. Leak Rate Vs. ΔP

Figures 2-5 and 2-6 are taken from Reference 4, The Fluorine Systems Handbook, and are typical computer program output curves of the result of a parametric analysis made in Reference 97 of the reference. The leakage model is constructed with a seal perimeter to seal width ratio of 100. These curves are reported here as additional criteria using steel/aluminum and steel/copper seat combinations with liquid fluorine. What is important to this program is the convergence of the leakage curves as a function of asperity height to a specific seat stress taken to be the yield or plastic range of the soft material. Aluminum requires a lower stress to achieve the same leakage than the copper model. Nothing is said about the oxidation film on leakage as a function of cycles.

Additional curves are given in Figures 2-7, 2-8, 2-9 and 2-10 taken from the same reference. These curves show the effect of important design parameters on the relative leakage. These parameters were optimized in the designs reported in this program and summarized as:

1. Asperity heights approaching 1×10^{-6} inches
2. Surface to be as flat as practical
3. Use low elastic modulus materials
4. Use high seat stresses

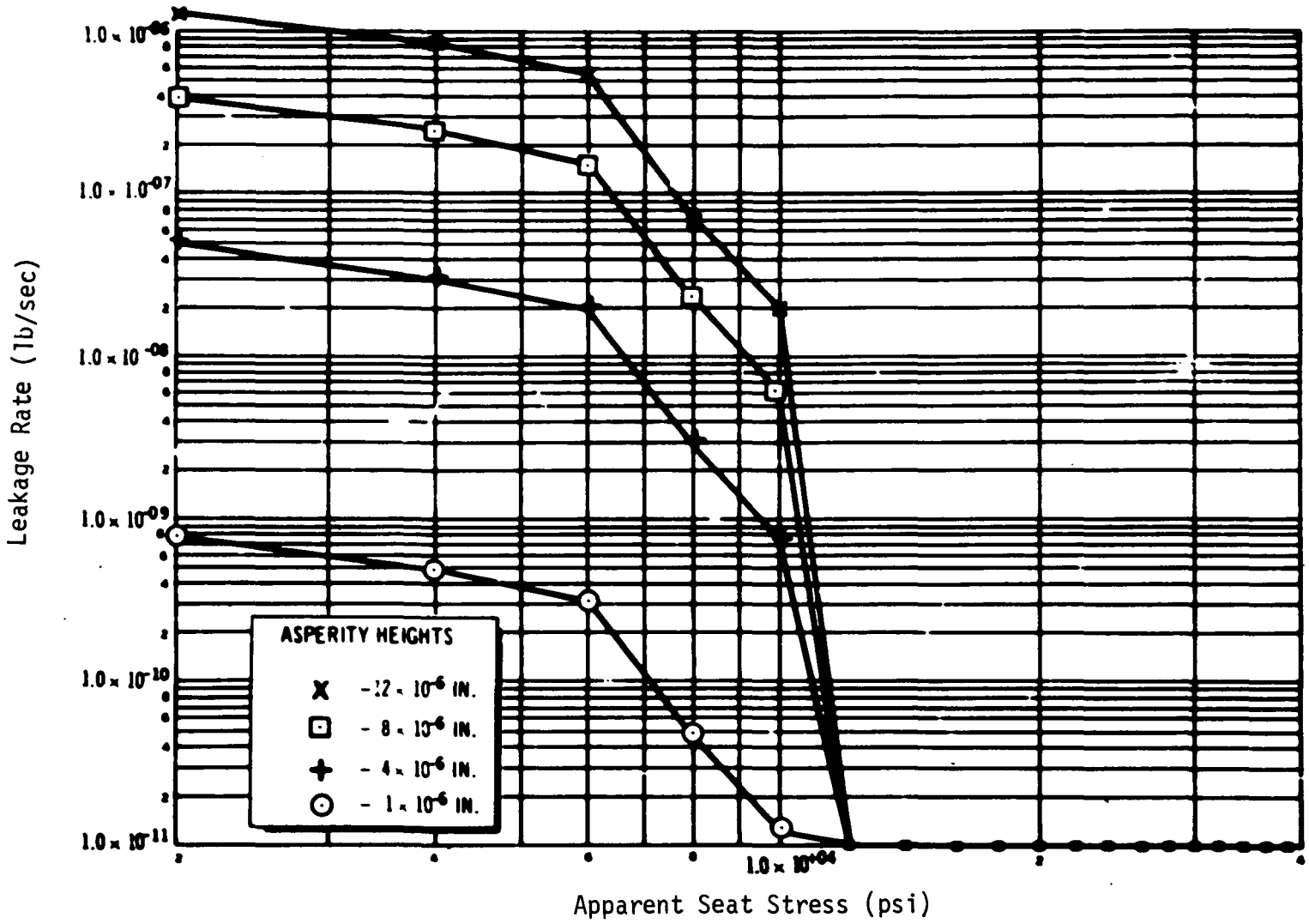

Figure 2-5. LF_2 Seal Leakage (Steel/Aluminum)

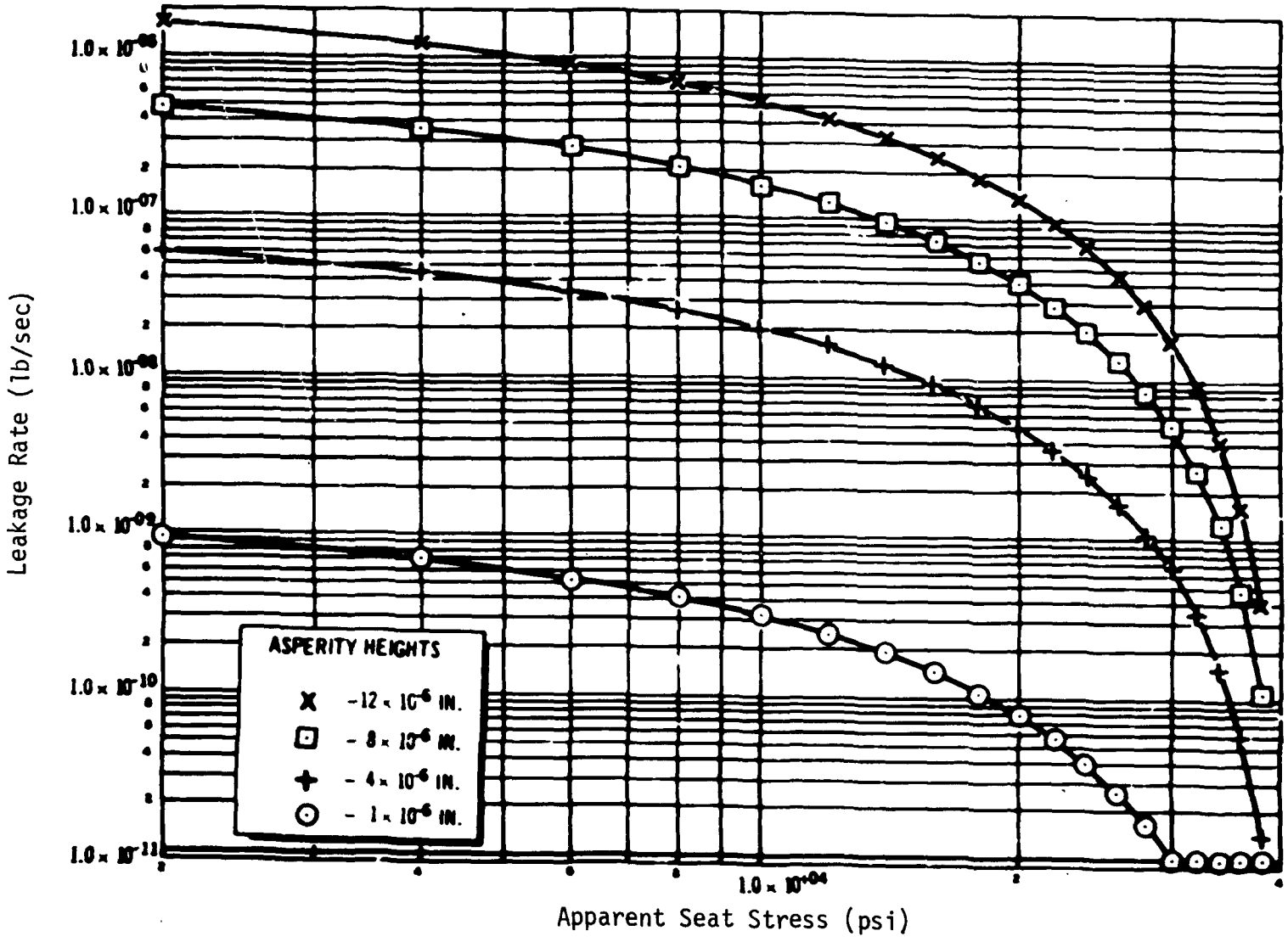

Figure 2-6. LF_2 Seal Leakage (Steel/Copper)

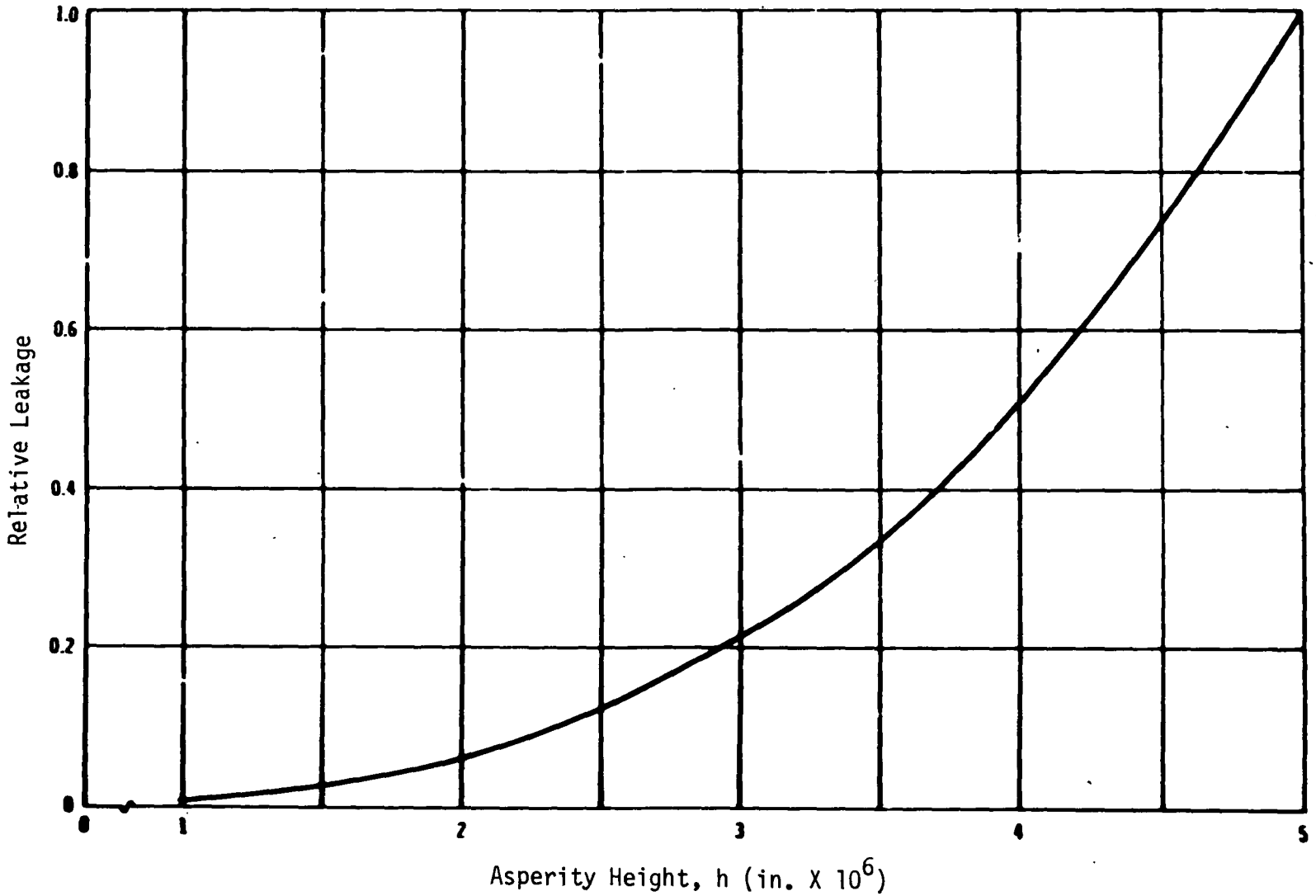

Figure 2-7. Effect of Asperity Height on Leakage

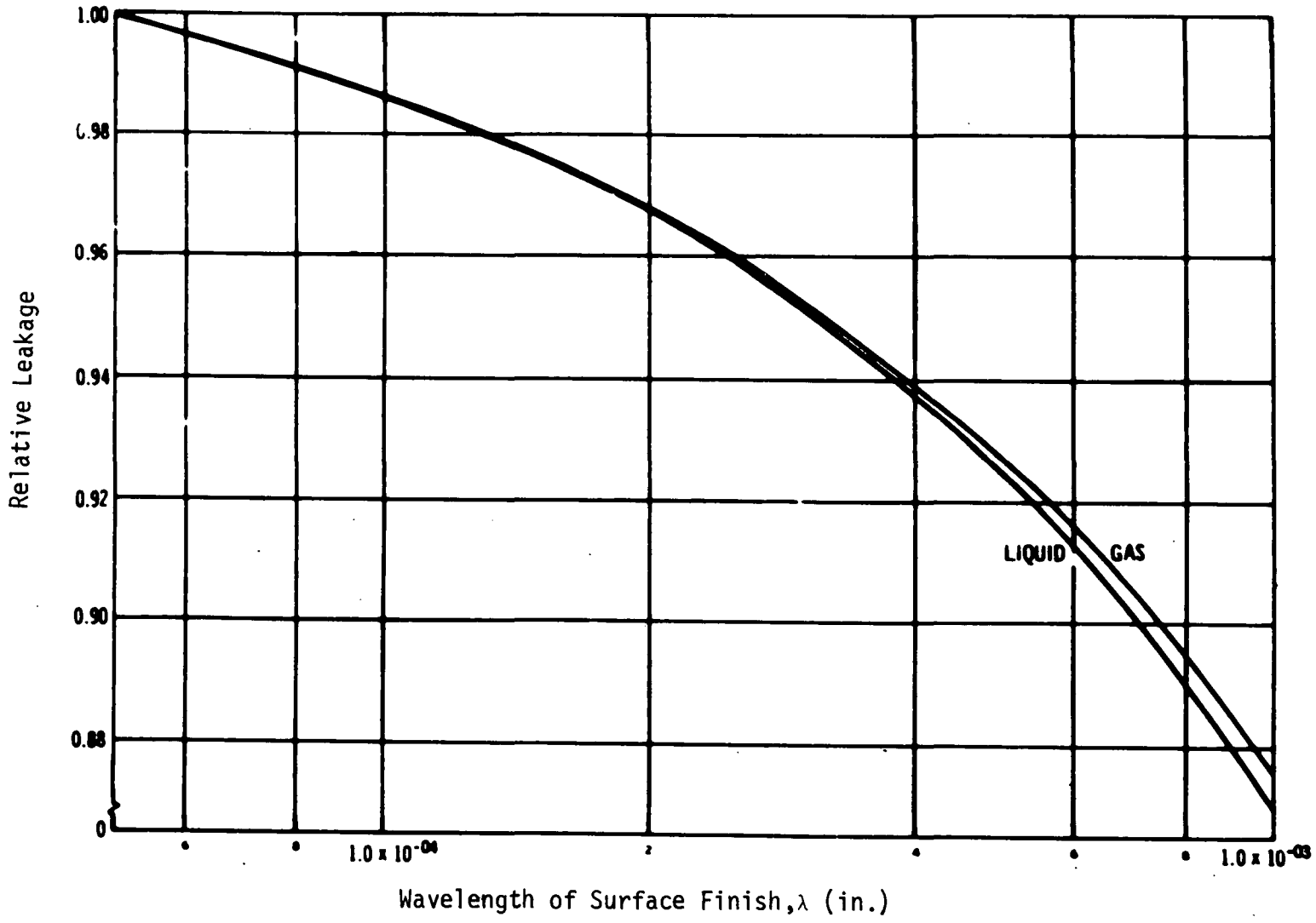

Figure 2-8. Effect of Surface Finish Wavelength on Leakage

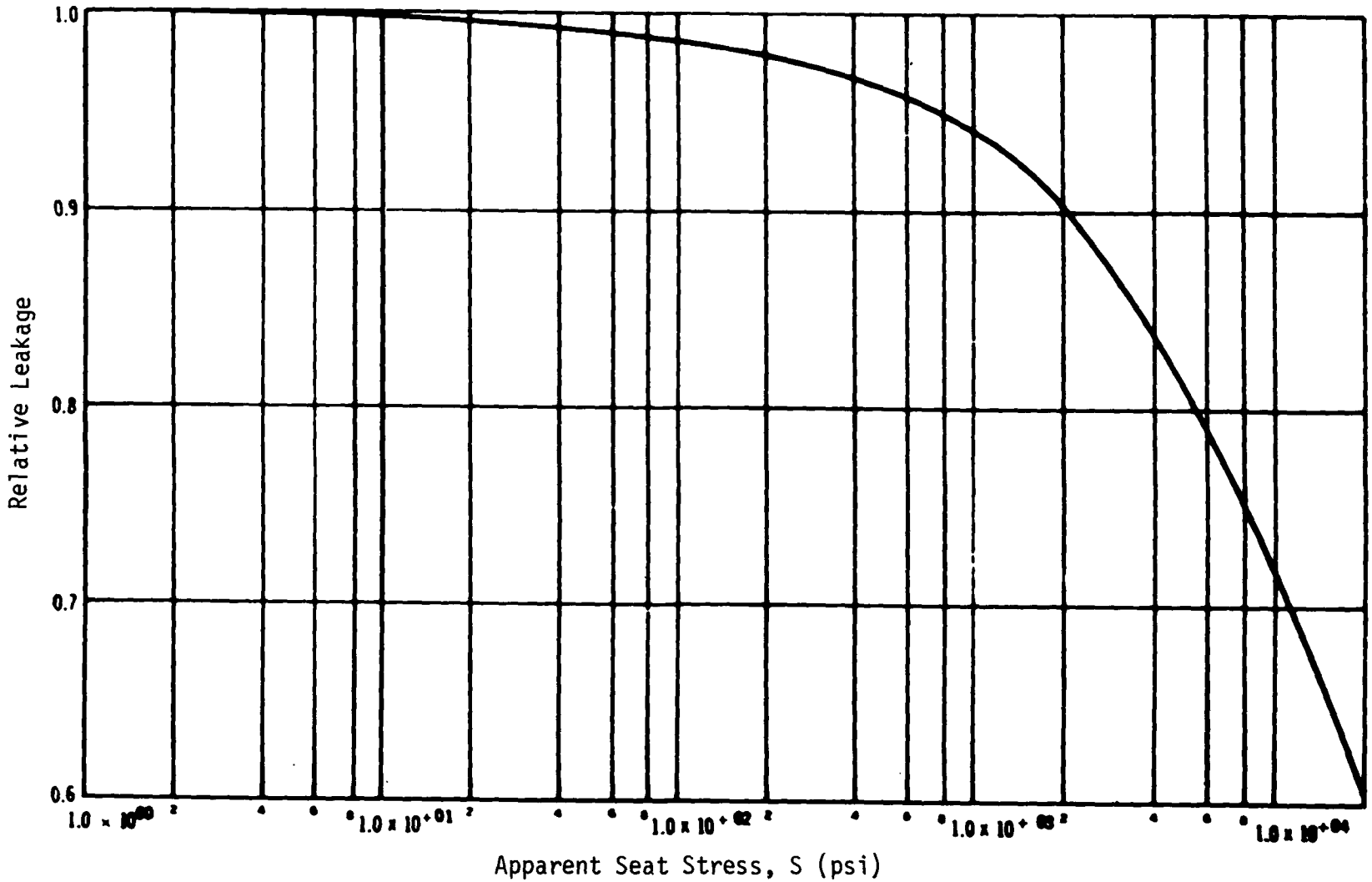

Figure 2-9. Effect of Apparent Seat Stress on Leakage

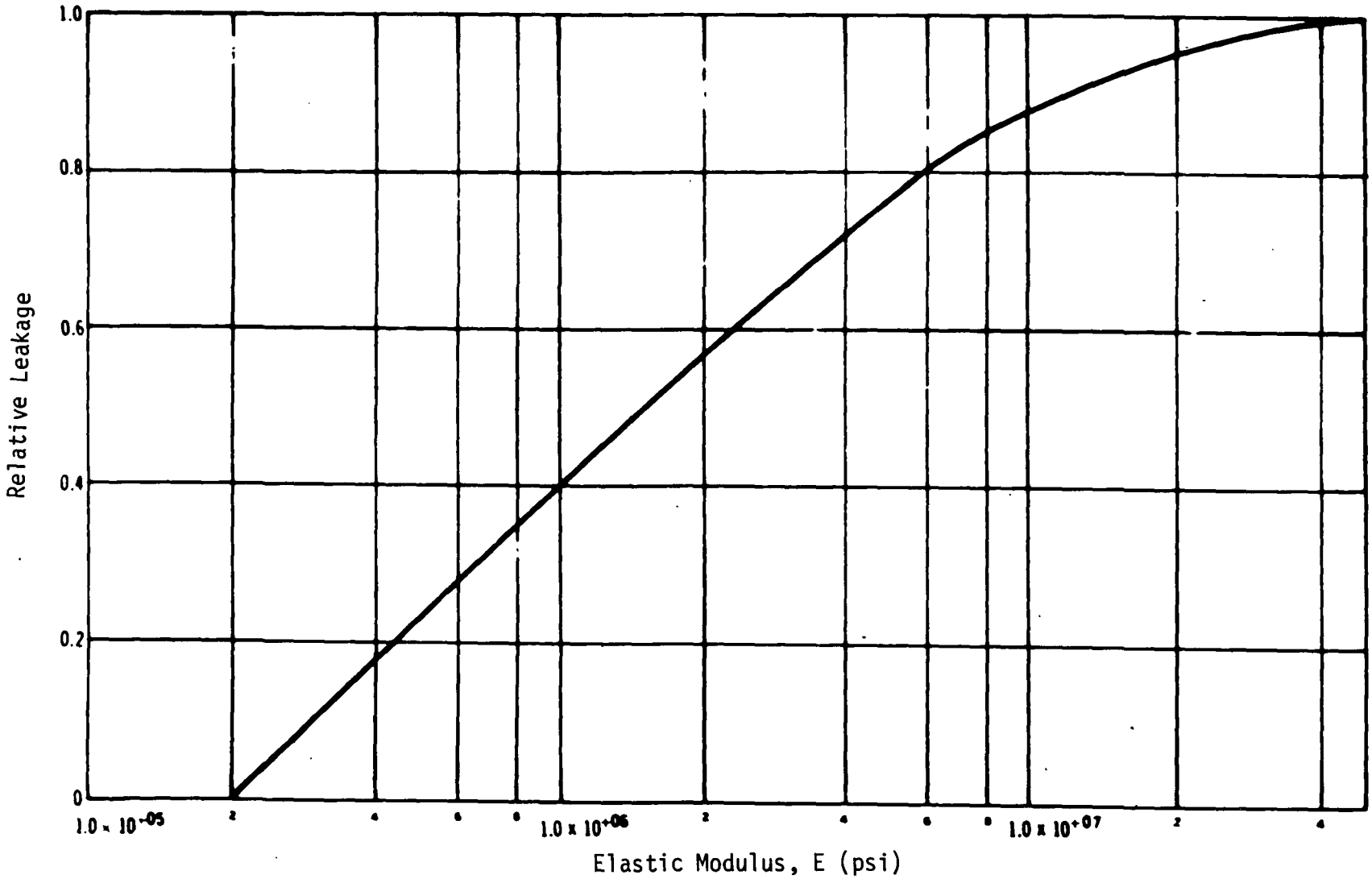

Figure 2-10. Effect of Elastic Modulus on Leakage

2.1.2 Wear Considerations

Wear particle generation in valves can be caused by particulate contamination on the seat surfaces, or by plastic contact of the surfaces. Rabinowicz, Reference 5, has shown that when the contact is plastic, wear particles can be generated due to asperity removal, and that these particles can cause additional damage.

The relationship between particle size and adhesive energy has been developed by E. Rabinowicz, Reference 6, at MIT and is given by the following equation:

$$d = 60\ E\ W_{ab}/\delta_{yp}^{2}$$

where: d = the average diameter of the wear particle
E = Young's modulus
δ_{yp} = yield stress of the material in compression
W_{ab} = the work of adhesion of the materials a & b in contact and is further defined as:

$$W_{ab} = \gamma_a + \gamma_b - \gamma_{ab}$$

where: γ_a = surface free energy of material a per unit area
γ_b = surface free energy of material b per unit area
γ_{ab} = interface free energy per unit area.

It has been found that δ_{yp} is about one-third the hardness P and that $\delta_{yp/E}$ is about $3X10^{-3}$ for many materials, then:

$$d = 60{,}000\ W_{ab}/P$$

Experimental results showing the relation between material and the average wear particle diameter obtained by E. Rabinowicz, Reference 6, are presented in Table 2-1.

Table 2-1. Average Wear Particle Size Under Ambient Atmosphere for Different Materials

Metal	P $\frac{dynes}{cm^2}$	W $\frac{ergs}{cm^2}$	d cm
Lead	4×10^8	440	270×10^{-4}
Tin	6	540	120 "
Bismuth	12	375	50 "
Cadmium	23	600	320 "
Aluminum	30	900	140 "
Zinc	30	750	440 "
Copper	60	1100	250 "
Brass	120	700?	180 "
Mild Steel	200	1000	60 "
Iron (Oxide)	2000?	600?	1 "
Aluminum (Oxide)	2000	900	1 "
Teflon	4	15?	90 "
Nylon	20	30?	? "
Silver	80	920	330 "
Nickel	260	1650	35 "
Glass	550	200?	1 "

Another assumption made is that the wear particle size generated at any given cycle is equal to the surface finish or mean asperity height characterized by the surface of the softer seat. The wear particle size d given by the above equation is the equilibrium size. That is, the particle tends to a certain size and remains at that size. Also the surface finish will generate to a finish equal to the equilibrium size. This equilibrium surface is then the final surface characterized after "wear in", independent of the initial surface condition. In most cases, a valve seat finish is very fine, ranging about 2 rms or greater. If we assume an initial surface finish of .05 microns (2 rms) and using an iron oxide surface model it can be seen that the average wear particle will eventually "wear in" to 1.0 micron. The corresponding finish will be 40 rms. For a valve seat this is a severely rough surface and leakage would be considered gross.

It is necessary to know the equilibrium wear particle diameter generated as a function of cycles. Using the example the 40 rms finish may require a cycle "wear in" of an unrealistic number considering the life usefulness of the valve.

It is important to consider the effect of the reactivity of the environment on the wear particle size. The more reactive the environment the smaller the wear particle. This effect is illustrated in Table 2-2 using copper-copper surfaces in various environments. In vacuum the wear particle would be quite large. For a reactive propellant such as fluorine or FLOX the wear particle should be smaller than those listed in Table 2-1. However, for the fuels such as hydrazine or MMH the wear particle size should be greater indicating a better leakage performance characteristic of metal valve seats for the oxidizer over the seats used with the fuel.

The design implications of the foregoing analysis are apparent. The use of harder seat materials will result in smaller wear particles and subsequently the wear process will result in finer surface finishes. This has previously been reported in Reference 7. By selecting a seat material with a characteristic small wear particle size it should be possible to predict the final surface finish after N cycles. If the surface finish is approximately equal to the wear particle size for a given seat material combination then prediction is easily obtained. However, it appears that surface roughness can be much smaller than the average wear particle size reported in Table 2-1. Therefore, the initial performance of the valve seal should be better than at "wear-in." It remains to develop a relation between wear particle size as a function of cycle life. In addition, the equilibrium wear particle size of a material exposed to the propellant needs to be determined.

Surface roughness and wear particle generation criteria can be used for the leakage model only by assuming that the surfaces at the interface conform in curvature (or flatness) within the dimensions of the minimum surface roughness. If the conformity is larger than the surface roughness the dominant leakage area will be the gaps produced by waviness of the surfaces and will undoubtedly be much higher. This design implication

Table 2-2. Effect of Environment on the Average Wear Particle Size

Environment	Average Particle Diameter Copper-Copper Surfaces Micrometers
Nitrogen	480
Helium	380
Carbon Dioxide	300
Dry Air	224
Oxygen	201
Laboratory Air	177
Wet Air	144
Cetane	12
Silicone DC 200-100 cst.	9.5
Ucon Fluid LB-70X	9.5
Palmitic Acid in Cetane	8.0

favors the use of flat surface geometry for thick seats which can be most easily fabricated with present day fabrication techniques. The use of thin elastic seats such as the lip seal can be made to conform to the poppet, however, the conformity on a micro level is not well known.

Wear fragments can also be transferred from one material to the other contacting element. Adhesive fragments take the form of semiellipsoids of dimensions approximately 1.0×10^{-3} to 4.0×10^{-3} cm wide. The proportion of length and height will be 1.7 and 0.5 times its width. The amount of adhesive wear is generally proportional to the normal load at the interface. Adherent wear fragments can be important since surfaces can be roughened by this process.

An example of the analysis that may be applicable to predicting cycle life vs. surface roughness is given in the following:

> An expression of the number of cycles to equilibrium would relate the number of junctions which must be destroyed (or created) to equal one junction of the same area. This assumes the real area of contact is always constant. Reference 6.

$$A_r = \frac{\pi d_i^2}{4} N_i = \frac{\pi d_e^2}{4} N_e$$

$$N_i = \frac{d_e^2}{d_i^2} N_e$$

where N is the number of junctions and d is the diameter of the loose particle generated. The subscripts i and e are representative of the first cycle and at equilibrium.

The total adhesive energy for a given set of junctions is:

$$W = \frac{d\ P}{60{,}000} N$$

The adhesive energy required to change N_i junctions of average diameter d_i to N_e junctions of average diameter d_e is:

$$\Delta W = \frac{d_i P}{60{,}000} \frac{d_e^2}{d_i^2} N_e - \frac{d_e P}{60{,}000} N_e$$

Assuming only one junction at equilibrium, then:

$$\Delta W = \frac{P}{60{,}000} \frac{d_e}{d_i} (d_e - d_i)$$

Further assuming that an equal adhesive energy is used to create a wear particle per cycle, then:

$$C_e = \frac{\frac{d_e}{d_i} (d_e - d_i)}{d_i} = \frac{d_e}{d_i} \left(\frac{d_e}{d_i} - 1 \right)$$

Taking d_e to be 2.0μ and d_i to be .05μ then,

$$C_e = 40\ (39) = 1{,}560 \text{ cycles.}$$

The reader should be cautioned that this analysis is based on assumptions that have not been validated by test or documented by others.

It is useful to plot a relationship between wear particle diameter and cycles. Figure 2-11is a plot of these parameters based on the above analysis, however C_e and d_e are now taken to be C_n and d_n where:

C_n = number of cycles to develop d_n and,

d_n = diameter of wear particle at n cycles

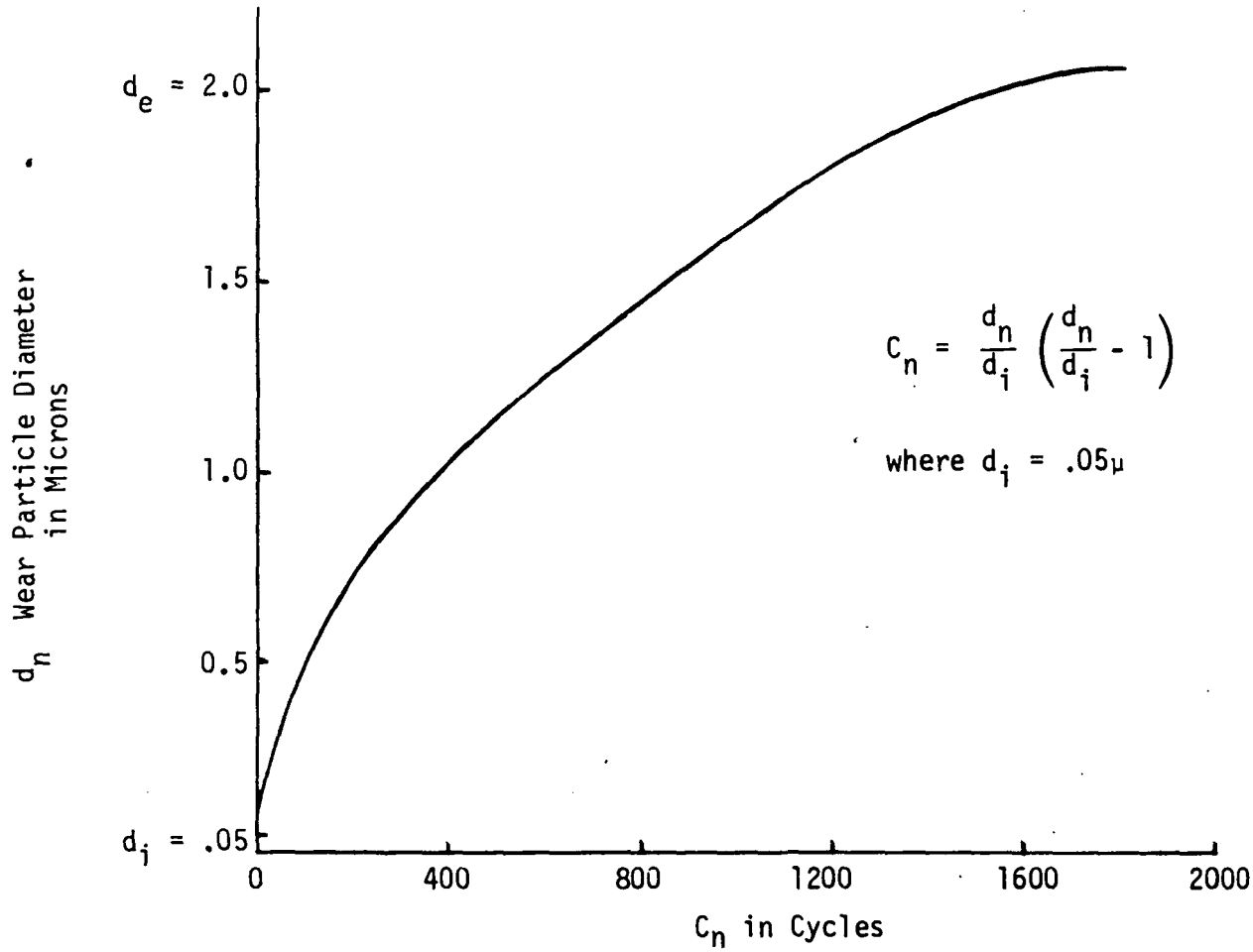

Figure 2-11. Estimated Wear Particle Diameter as a Function of Cycle Life

2.1.3 Propellant Chemical Effects

A general evaluation of materials suitable for application over the range of space storable oxidizers and fuels of interest in the program was conducted under the Detailed Design Report, Reference 1. The effort was directed to consideration of materials usable for common use in both propellants and for application in soft-hard seals in which a very soft material is desired. A broader compilation of candidate materials is included in Reference 4, Fluorine Systems Handbook.

Evaluation of materials for sealing of necessity involves a very detailed knowledge of the effects of chemical reactivity at the metal surfaces and at the edge of a bimetal interface.

Corrosion data to the level of detail desired is generally not available. This is primarily a problem with the oxidizer. It is necessary then to establish material selections based upon data that is available which includes corrosion rates in fluorine, observations of the effect of fluorine on actual valve parts following propellant tests, and determination of the nature of oxide and fluoride films on various alloys. Some of the information presents conflicting results for given materials exposed to apparently like conditions. In general it must be assumed if good results such as extremely low corrosion rates were ever obtained in any one experiment that this result can be repeated once all factors are controlled. The primary element affecting chemical reactions involve contaminants in the fluid, impurities in the alloys or in the reacting propellant lapping compounds imbedded in surfaces or in platings and other coatings applied to surfaces.

In general, this discussion points up the need for extreme care in processing materials for use in fluorine. To a degree, the controllability of a given alloy may be more important than the capability of exhibiting the absolute peak of compatibility. The consistency and purity of the commercially available alloy is the primary factor in control. This aspect of compatibility was considered for the materials previously selected in the program.

The materials specified for the presently submitted isolation valve design were Inconel 718 for seal contact surfaces and 1060-0 or 1100-0 aluminum for the seal insert. No platings or brazes were used on the basis that the fewer processes involved with fluorine or FLOX propellants the more reliable the long term compatibility of the component. Differences in heat treat were assumed to provide a degree of differential hardness at bearing interfaces. This coupled with fluorine oxidation of the surface has been proven to provide an adequate solution to lightly loaded guide bearing applications (Reference 8). Good results in application of Inconel 718 in fluorine service is documented by McDonnell Douglas by Reference 9. Based upon the above logic and experience, no change in the body materials is suggested. The choice of soft seal materials must involve mechanical considerations as well as the yield strength range required for a given poppet mechanism and the cold work characteristics acceptable for cycle life.

Some coatings do offer advantages, if sufficient process testing can be accomplished to assure consistent long term results. Work by Aerojet on a metal-to-metal sealing shutoff valve (Reference 10) indicates the condition of a gold plated CRES 304L to be good following a limited exposure. The use of Beryllium nickel as the substrate is suggested as being a better choice over 304L. This data indicates a plated gold to be a stable surface and could be considered at least as a protective finish within the isolation valve. The gold was electrodeposited to .0015 in thickness and finish polished to 2 micro-inches. The only noticed effect was a dull or cloudy appearance of the gold following fluorine exposure.

Passivation Coating

Marquardt conducted an investigation into the oxide-fluoride surface reactions of a number of hard materials (Reference 11). The concept was advanced that a material which reacts to a gaseous fluoride would have advantage in not building up surface corrosion products. A disadvantage to a long term use however is that no protective fluoride coating forms and the material will continuously react. Tungsten, Boron, Platinum and

Carbon are examples of elements forming fluorides that are gases at normal temperature. Nickel chromium, copper, iron and aluminum all form solid fluorides.

Indications are also apparent that the fluorides are 2 to 5 times less dense than the parent metals indicating an increase in bulk on formation at the surface. Most all metals change to a different crystal form on reaction to a fluoride. Also the bond characteristics with the surface are also changed from a metallic to an ionic bond. The thickness of the fluoride coating and the equilibrium characteristics finish for a given material due to extended exposure must be experimentally established to determine the result of the process. Experimental evidence indicates fluoride films to be in the order of 2 to 20 Å in thickness for aluminum and other materials of good compatibility. This is relatively insignificant compared to typical asperity heights of microinches.

Experience cited by McDonnell Douglas reference (9) shows the results obtained for both a hard-hard and soft-hard poppet seal combination on LF_2 exposure. The combinations used were A286 steel on Inconel 718 and a 23+ carat gold plated seat on Inconel 718. Inspection following propellant exposure indicated the seal surface to be in good condition with only stains appearing on the metal in the static seal areas.

A consideration pertinent to materials compatibility of seals for the isolation valve is that exposure times are far less than the entire mission period. Using a design affording total confinement and protection of the soft seal element as well as seal surfaces, only extremely small areas are exposed at structural intersections. For a total of 30 mission cycles and open time duration of 6 hours each, the total open time would be 180 hours in a full 10 year period. The direct exposure of the seal for resealing demonstration could be conducted in a relatively short time if the closed time was neglected. The closed time could be evaluated with static seal samples over long periods.

Conclusions

A review of experience with seals in LF_2 indicates good results to be potentially achievable. The primary area of uncertainty lies in the

area of detail material surface reactions in the oxidizer. At this point it is apparent the choice of material must remain open among the originally proposed materials, Reference 1. In general, it must be assumed aluminum will require verification of the effects of hard surface fluorides in re-appraising the sealing function. Test data indicates generally good results with gold platings indicating pure gold to be a candidate for a seal insert. Gold platings can also be used for minimizing metal pickup on bearing surfaces in other areas.

2.2 Soft on Hard Metal Sealing

2.2.1 Experimental Sealing Data

The logic pointing to the application of the soft on hard sealing approach was presented in Reference 1. At the outset the ground rules of the effort limited materials exposed to propellants to metals or ceramics. Experimental evidence from a number of sources have shown the leakage requirement of 10^{-6} sccs He cannot be met by conventional hard on hard flat seats because of the effects of even a small amount of particulate contamination.

As a starting point for this effort a review of soft on hard sealing experience of other investigations was undertaken. The work done in the past was largely directed to static seal application. One instance was noted where repeated use of a single gasket was demonstrated. The efforts investigated were accomplished by G.E. and ITTRI.

The first aspect of sealing investigated was to determine the unit seal loading versus leakage for various materials and initial finishes. Some of the data is provided in the following paragraphs. Surface model analyses of the relationships of yield strength, loading and finish is then presented to establish a basic correlation and insight into the mechanisms involved at the interface.

Some of the important factors involved in achieving a good seal were reviewed in Reference 12. As would be expected the use of smooth surfaces and low yield strength materials provided a high degree of sealing with the lowest contact loading. The need for a substantial plastic flow of the softer material is indicated.

The effects of strain hardening of the material was also considered. The principle is illustrated in Figure 2-12 for the case of repeated loading. The figure illustrates a typical stress-strain curve. The cold work effect for a given material is determined by the shape of the plastic portion of the curve. On reloading, a higher stress must be applied to achieve yielding. Typical stress-strain curves for aluminum and copper are given in Figures 2-13 and 2-14 from Reference 28. Data is given for both normal and cryogenic temperatures. It is evident from these curves that the slope of the 1100-0 aluminum in the plastic region is much flatter than that for copper over the temperature range. From this, aluminum appears to be a better choice. In addition, the yield strength of the aluminum is much lower allowing plastic flow at lower stress levels. Table 2-3 from Reference 13 gives a comparison between standard yield strength data (tensile test data) for various materials and apparent yield strength obtained by experimentally yielding a typical gasket shape (leak test data). The Y* values are obtained by plotting the intersection of the elastic and plastic stress-strain curves. In general it is apparent higher yield values can be expected in compression of a gasket compared to typical tensile data. The effects of high friction, and potential anisotropic characteristics of the materials can explain the differences obtained.

Another measure of the cold work characteristic of materials can be obtained by Meyer Hardness measurements. These are expressed as Meyer Hardness σ_m or Meyer Index μ. The Meyer Index is defined by the relationship:

$$P = kd^{n'}$$

where: n' = material constant related to strain hardening

k = a material constant representing the resistance of a metal to deformation.

P = the applied load

The Meyer Index is related to the slope of the plastic portion of the stress-strain curve. The higher the value the greater the slope. Table 2-4 lists relative hardness values and indices for several soft materials.

The data gives a general relationship between materials. The Meyer Index values given cannot be rigorously applied however as hardness values have a greater influence on choice of materials.

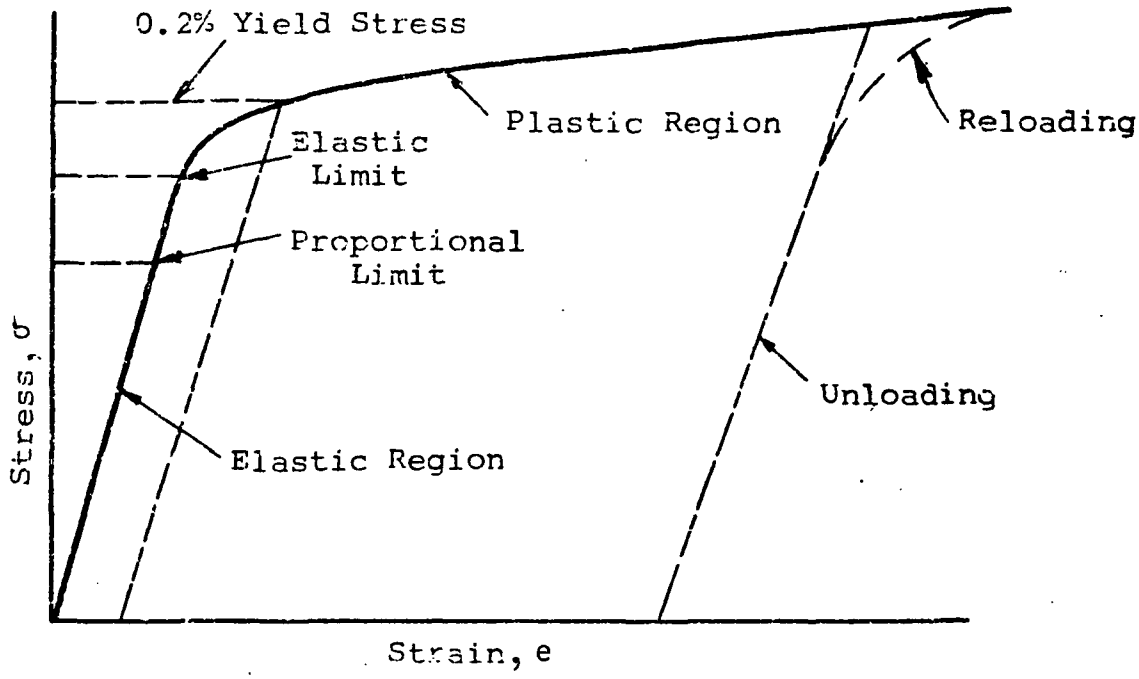

Figure 2-12. Typical Stress-Strain Diagram

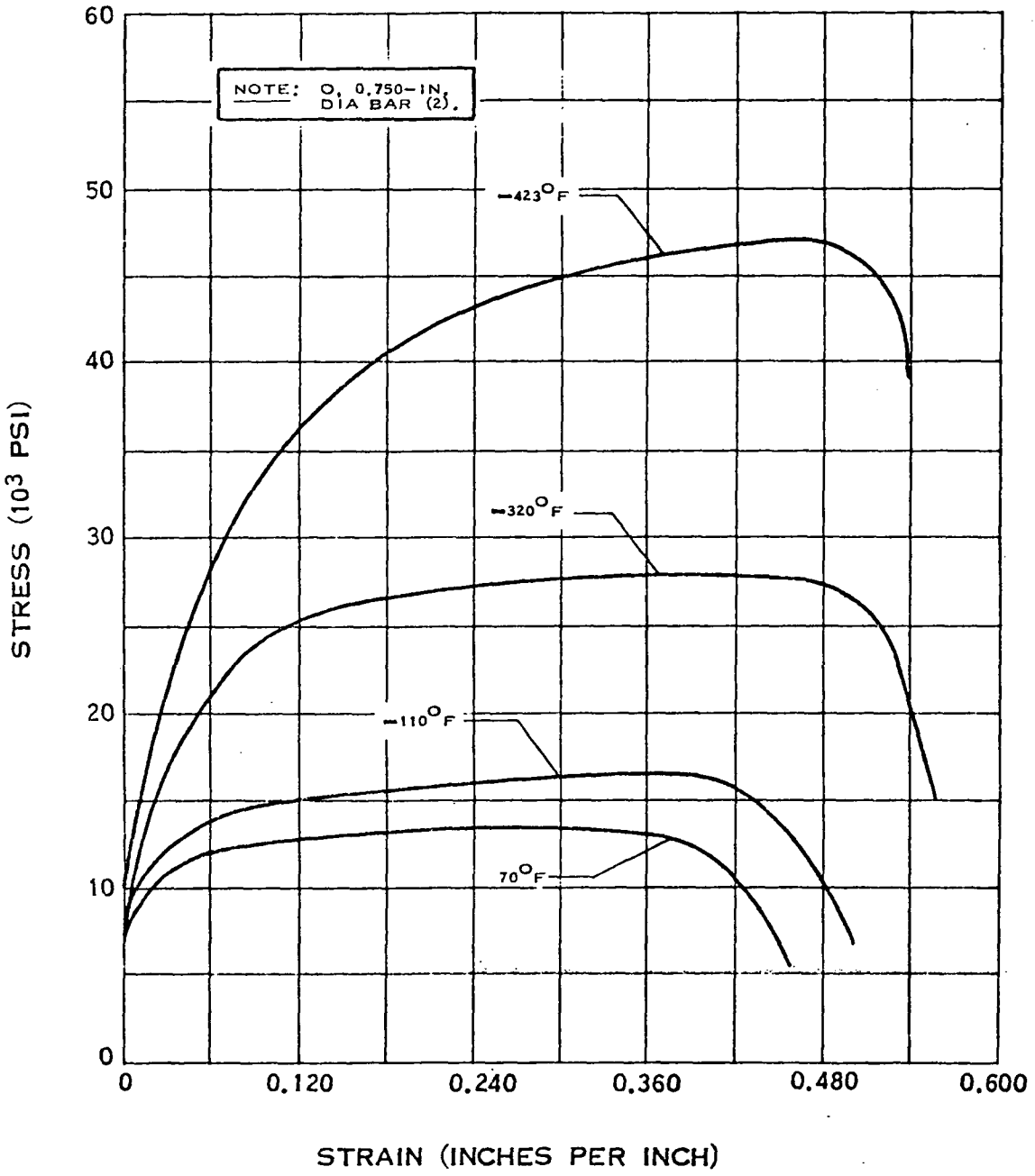

Figure 2-13. Stress-Strain Diagram for 1100 Aluminum

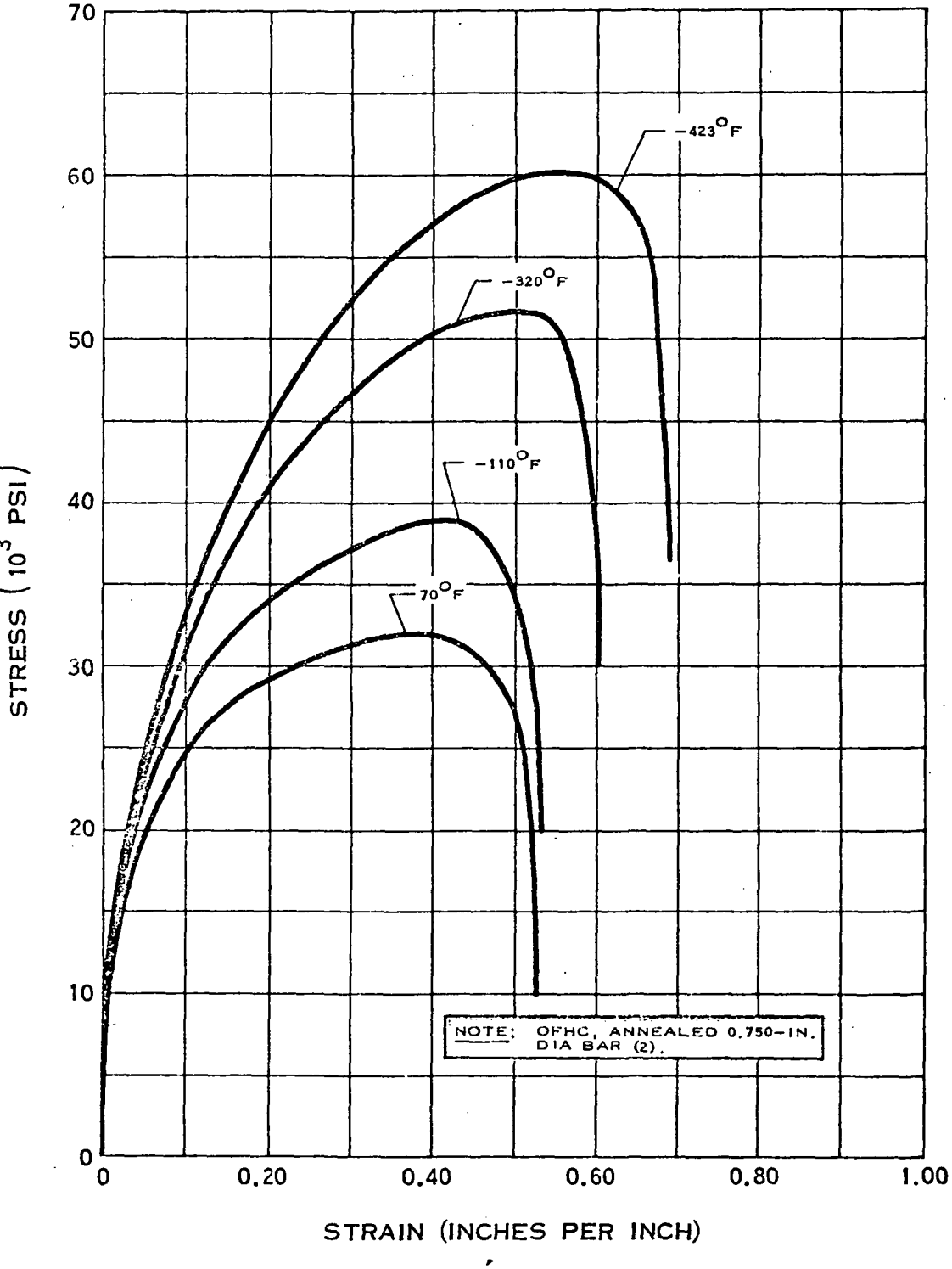

Figure 2-14. Stress-Strain Diagram for Copper

Table 2-3. Yield Strengths of Gasket Materials

Material	Tensile Test Data			Leak Test Data
	0.02% Y.S.	0.2% Y.S.	Y*	Y*
Lead	1040	1425	1518	2090
Aluminum	3388	4400	3930	5350
Copper	6140	7770	7200	12700
Nickel	10200	13230	12530	29100

Y* gained directly from load-deflection curves: intersection of extensions of elastic and plastic portions of the curves. 0.02 and 0.2 standard offset yield values are noted.

Table 2-4. Meyer Hardness and Index for Various Materials

Material	Meyer Hardness (psi)	Meyer Index
102 Copper	109,000	2.09
1100 - 0 Al	48,700	2.19
2024 - 0 Al	89,600	2.44
5086 - H32 Al	139,000	2.14
6061 - T6 Al	159,000	2.00
2024 - T351 Al	202,000	2.00
7075 - T6 Al	262,000	2.00
Teflon	3,870	2.80
Lead	4,390	2.33
321 CRS	202,000	2.35
C1141 Steel	308,500	2.22

This data serves only to illustrate the character of the soft materials potentially usable in the program. The data describes the function of the material as might be applied in the mechanisms of loading the seal. It has been shown the apparent reaction of asperities at the interface can depart considerably from these typical properties. The effects of particulate contamination and the character of surface reactants (oxides or fluorides) can greatly affect sealing results.

A sealing curve for 1100 aluminum on 347 SS is provided in Figure 2-15 from Reference 14. From this curve it is apparent a seal better than 10^{-6} SCC He/sec was obtained with loading equal to yield stress. Conclusions reached under the same effort indicated gaskets for use at 1150 psi must be loaded to 2.25 times yield stress to reduce leakage below 10^{-6} SCC He/sec. For a pressure differential of 6000 psi 2.5 times yield is required. This data was based on seals approximately 3 inches in periphery sealing on both sides. The seals were unconfined. It was also found that materials of equal coefficient of expansion maintain a better seal at low temperatures. Also it was found that once a seal was established the load could be reduced considerably before an increase in leakage occurs.

Another test reported in Reference 15 and shown in Figure 2-16 relates the leakage obtained relative to surface finish for aluminum and steel. For a 15 RMS finish a leak rate of 10^{-6} SCC He was obtained with a load of approximately 1.25 times yield. At 50 RMS a load of 3 times yield was required.

The effects of resealing a soft on hard seal were experimentally established in work done under Reference 16. The data is presented in Appendix A. The configuration is shown in Figure 2-17. Opposing knife edge sealing surfaces load a soft copper gasket of approximately 1.1 inch diameter contact circle. The seal was relocated on each cycle. Leakage tests were repeated after each of 6 sealings. The results are summarized in Table 2-5. The results indicate a high degree of potential in resealing a soft-hard interface. The conditions of the demonstration must be considered to be relatively severe although not involving propellant exposure. The seal loadings were high in the order of 700#/inch of seal perimeter. The loading was the same for each resealing.

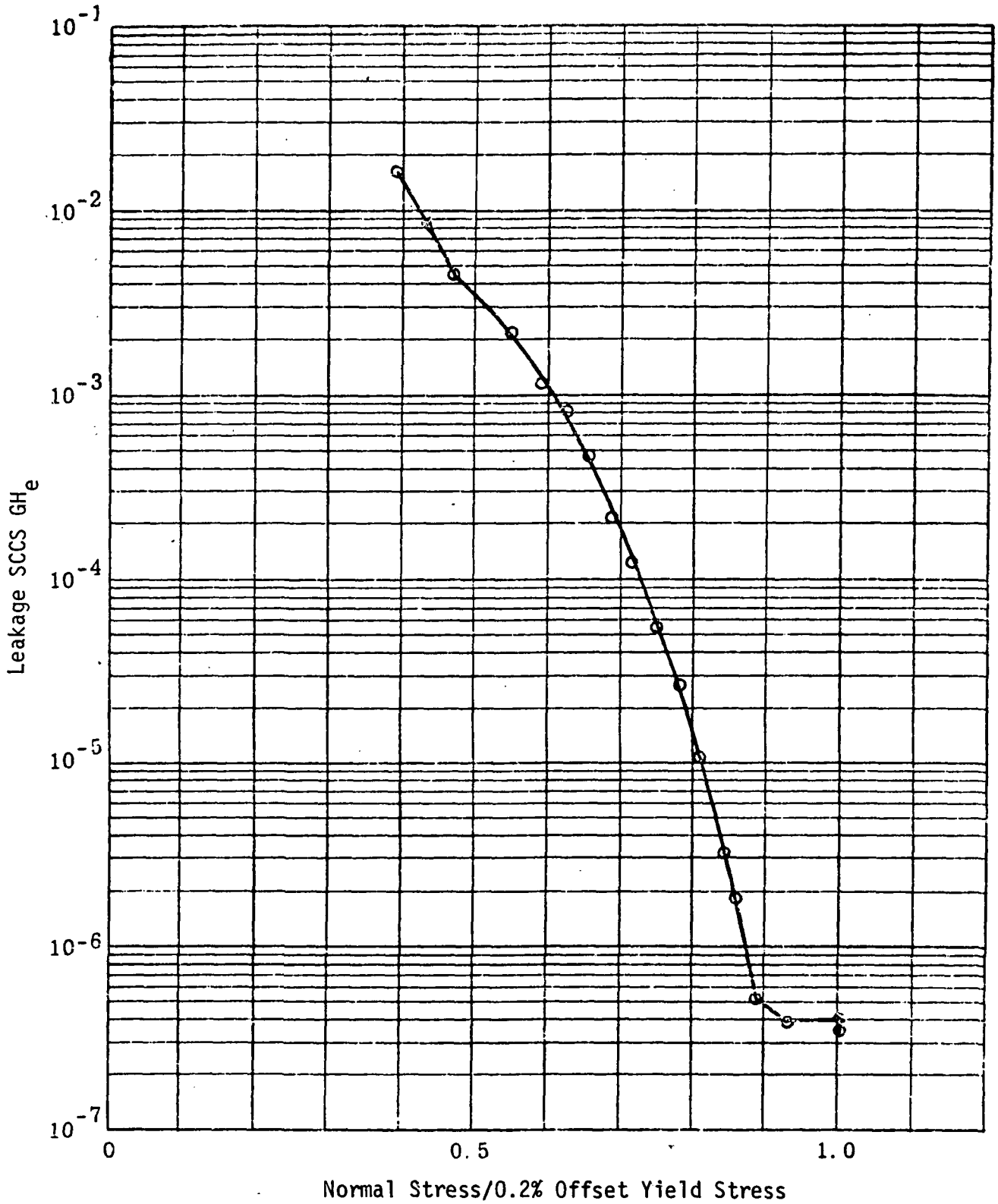

Figure 2-15. Leak Vs. Normalized Stress for 1100-0 Aluminum With 347 SS Seal Surfaces, Fine Circumferentially Machined

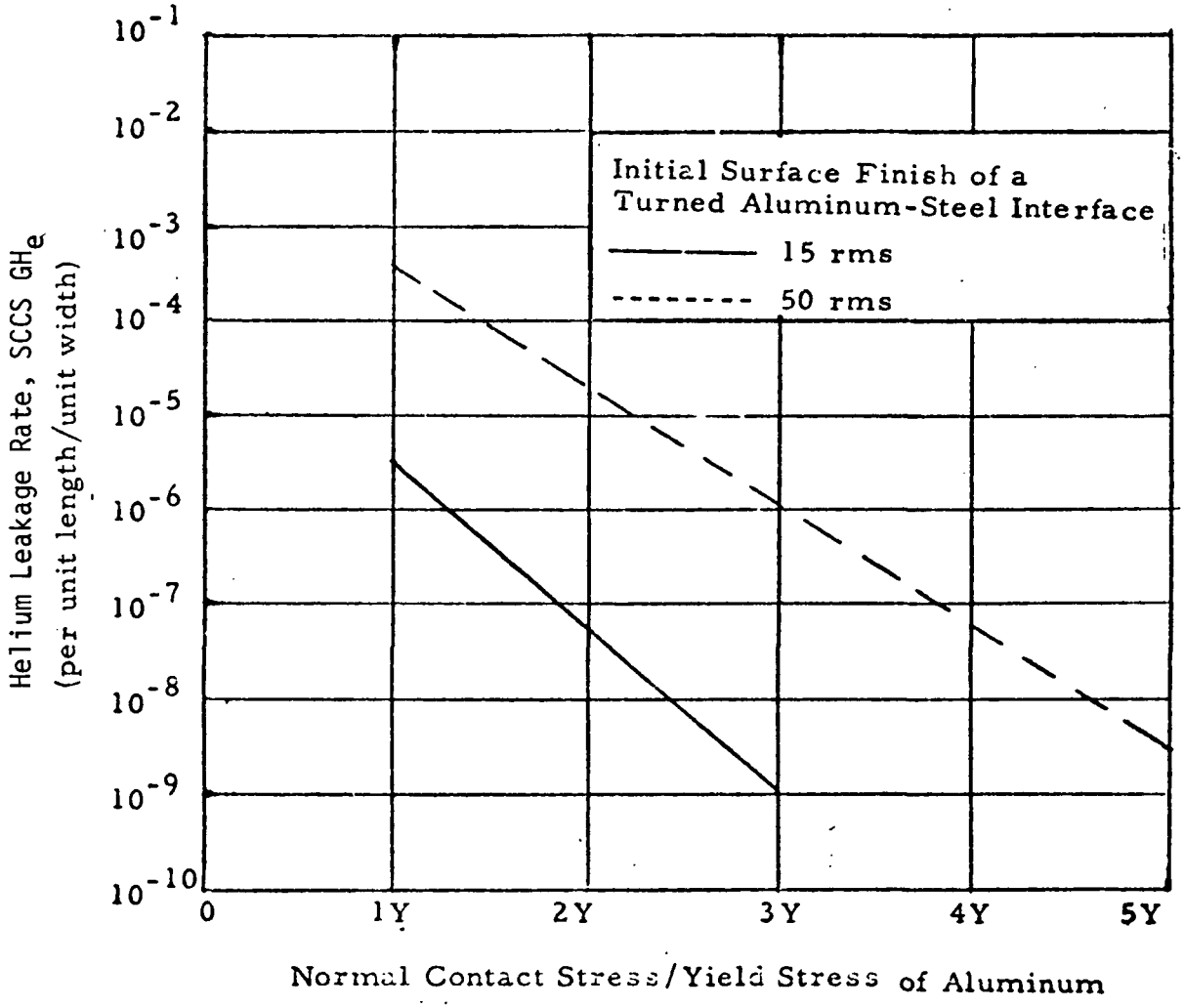

Figure 2-16. Typical Comparison of the Leakage Characteristics For Two Different Initial Surface Finishes. A 10 psi Pressure Difference Across the Interface is Assumed.

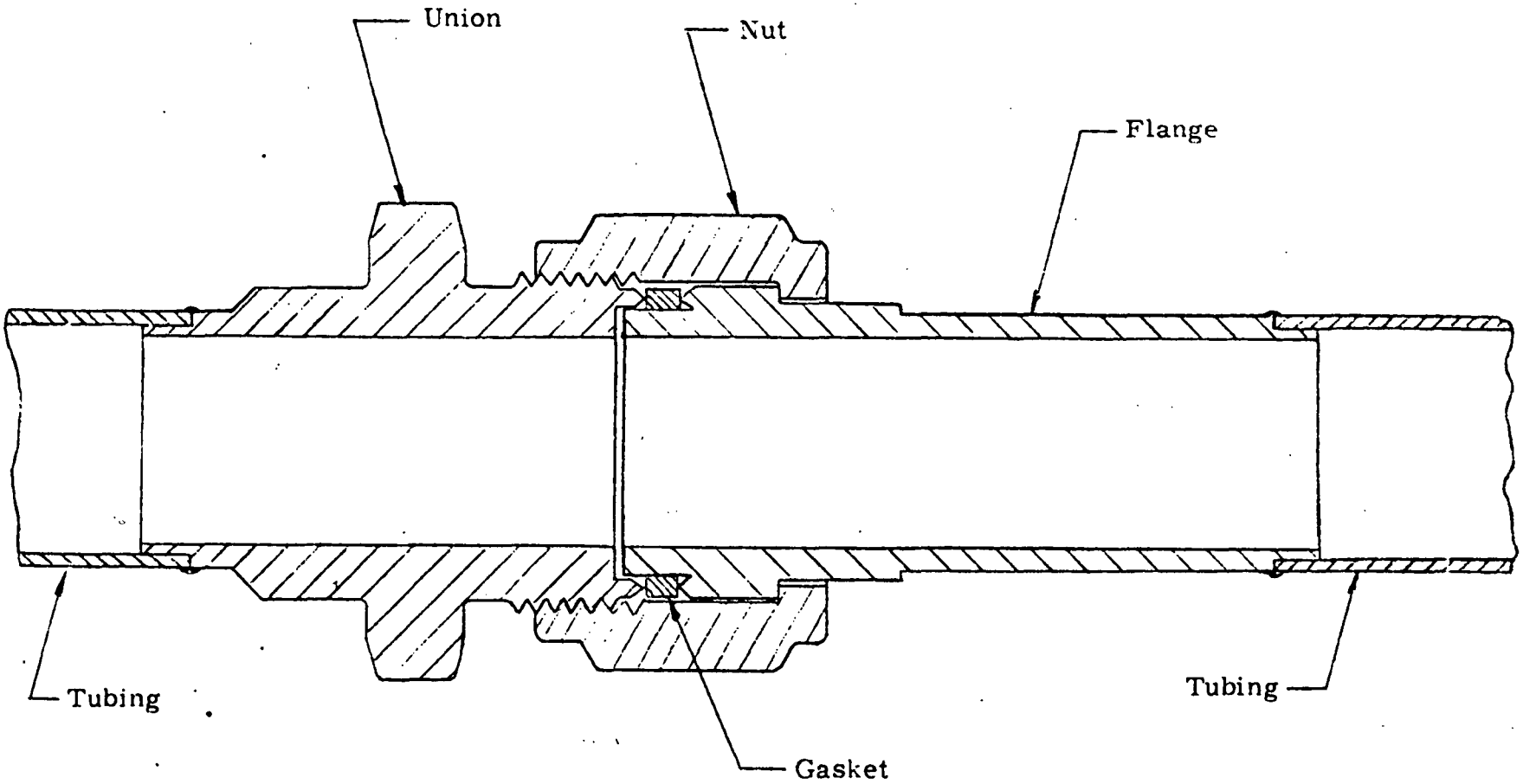

Figure 2-17. Welded Knife-Edge Connector

Table 2-5. Knife Edge Seal Leakages

Cycle	Leakage 1500 psid scc He/sec	Seal Loading lbs
Initial Assembly	$< 9 \times 10^{-7}$	2300
Reseal 1	$< 9 \times 10^{-7}$	2200
" 2	3×10^{-4}	2200
" 3	2×10^{-5}	2200
" 4	$< 3 \times 10^{-6}$	2200
" 5	2×10^{-6}	2200

2.2.2 Analysis of Sealing Mechanisms
Sealing Stress Requirements

Empirical design practice for hard to hard metal valve seats and static metallic gaskets commonly dictates a seating stress of two to three times the compressive yield stress of the softer material to achieve low leak rates (Reference 17, p. 6.3.2-6). Plastic metal working theory was applied to the problem of forcing a soft plastic material into the asperities of a hard elastic material. These stress models were originally developed to predict the pressures required to force macroscopic blanks into hard dies, but should apply as well on the microscopic level as the geometric parameters they contain are non-dimensional. Suitable allowance must of course be made for changes in bulk material properties at the contacting surfaces. Cyclic work hardening and oxide and fluoride films may increase the effective yield stress of the soft material at its surface, which is of interest in predicting asperity conformance. In metal working practice the material is deformed a distance equal to many times the thickness of surface films, so the yield stress of the bulk material may be used. It may be possible to evaluate this increased surface yield stress by correlation of Vickers microhardness test results on annealed material with similar data on samples exposed to mechanical cycling and propellant environments.

The predictions of two separate plasticity models are summarized in Figure 2-18. Here a random asperity contour is idealized to a sawtooth pattern of opening angle 2α . When the two sealing surfaces are brought into light

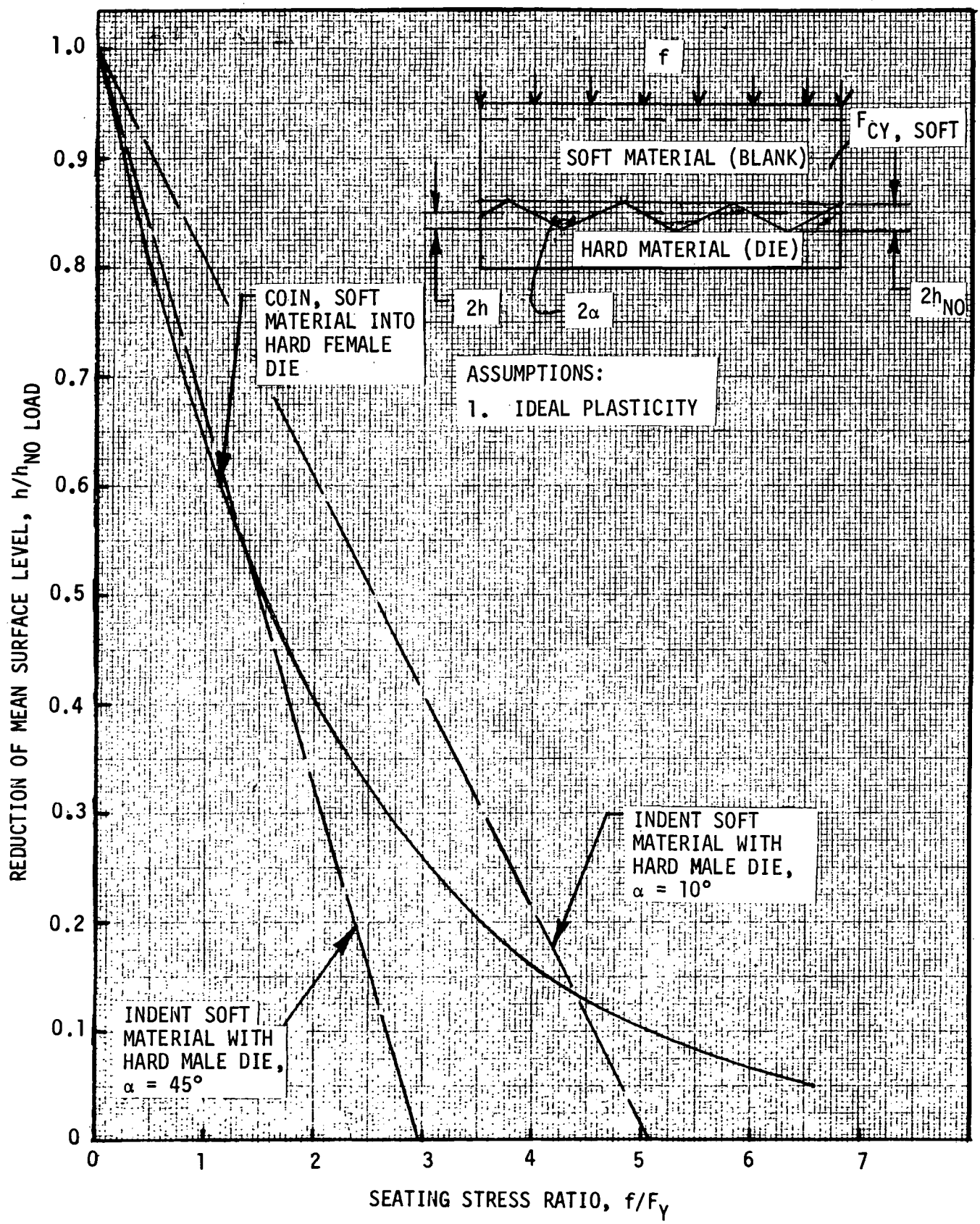

Figure 2-18

RELATION OF MEAN SURFACE HEIGHT TO APPLIED SEATING STRESS BY PLASTIC COINING AND INDENTATION THEORY

contact, the hard material has asperities of effective depth of $2h_{NO\ LOAD}$. As the mean contact stress is increased to several times the compressive yield stress of the soft material, the soft material is forced into the asperities of the hard materials. The decrease in effective height of still unfilled asperities is indicated on Figure 2-18. The solid curve shows the prediction of a coining model (Reference 18) in which a flat soft blank is forced into a depression in a hard die. By this model, the required contact stress is not affected by the angle of the sawtooth and must be very large to fill the last 10 percent of the die depth. The dashed curves of Figure 2-18 represent the prediction of a punching model (Reference 19) in which a single sharp punch is indented into a soft blank. It can be seen that at applied stresses between two and four times the yield stress the predictions are similar, but the punching model predicts a dependence on asperity sharpness as well as depth. This dependence is shown in Figure 2-19. Consideration of limited data on the asperity angles encountered in practice indicates that at worst real surfaces would be on the relatively flat portion of this curve.

In an actual soft/hard contact the soft material, as well as the hard will have a significant surface roughness. None of the plastic models in-being treat a non-flat soft blank, but presumably very little increase in the contact stress should be necessary to crush down peaks and valleys in the soft surface if it is already being forced into the hard surface at several times yield.

In addition to the soft and hard surface contours, wear particles composed of soft material, hard material and/or their compounds will be trapped between the seats. An upper limit on the depth such particles will be indented into the soft surface can be found with another punching model, in this case a blunt radiused punch. Figure 2-20 shows the indentation depth versus contact stress for this case. Of particular interest is the stress necessary to indent an approximately spherical wear particle a distance equal to its own diameter into the soft surface, which would presumably end its detrimental effect on leakage rate.

In design, a leakage analysis would be performed to determine what mean surface height under load would be acceptable in a given application so as not to exceed the allowable leakage criteria. Then Figures 2-18 to 2-20 and test data would be used to find the seating stress required to maintain this surface height over the required number of actuation cycles with wear particles present.

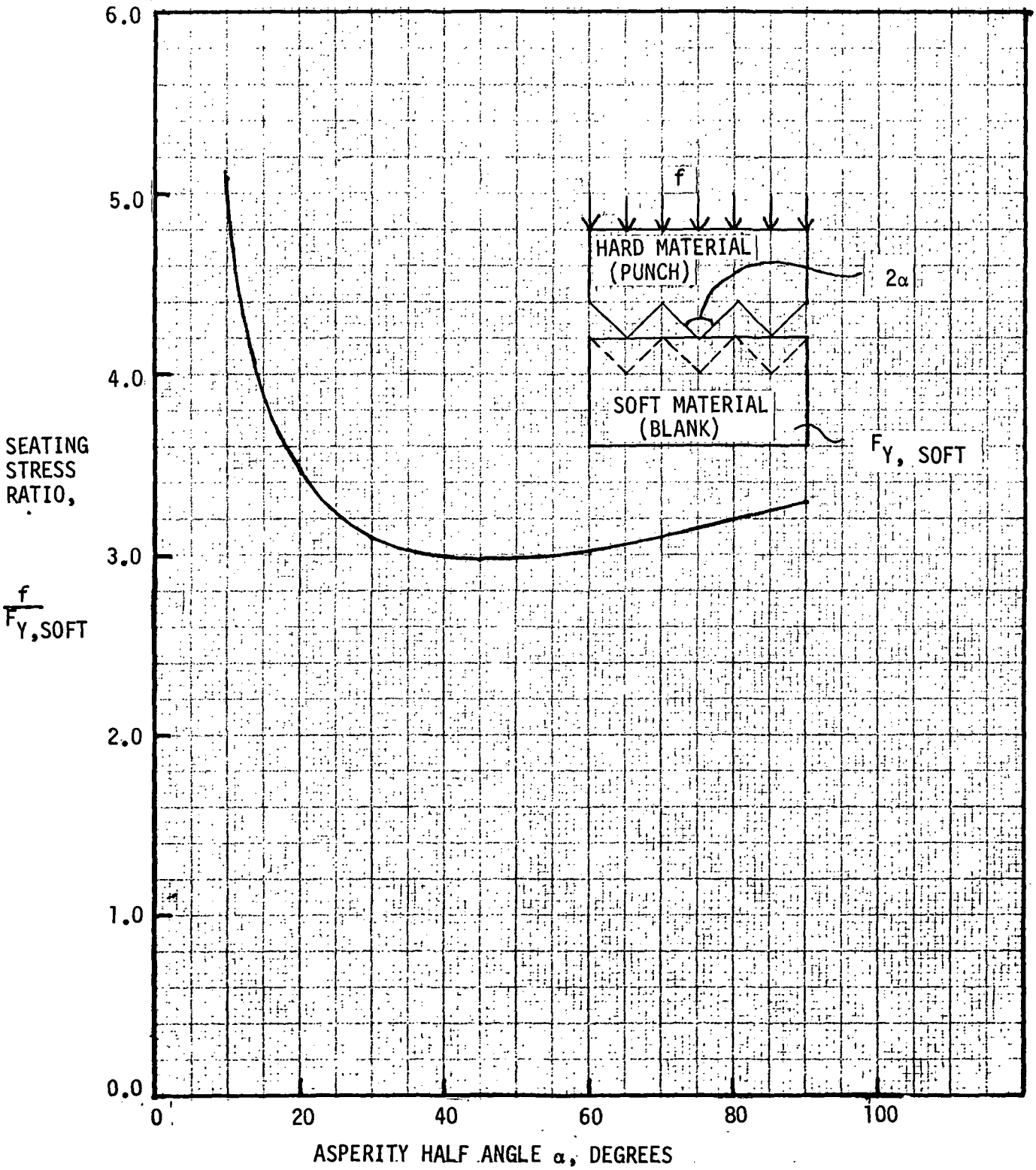

Figure 2-19

EFFECT OF ASPERITY SHARPNESS

ON REQUIRED SEATING STRESS

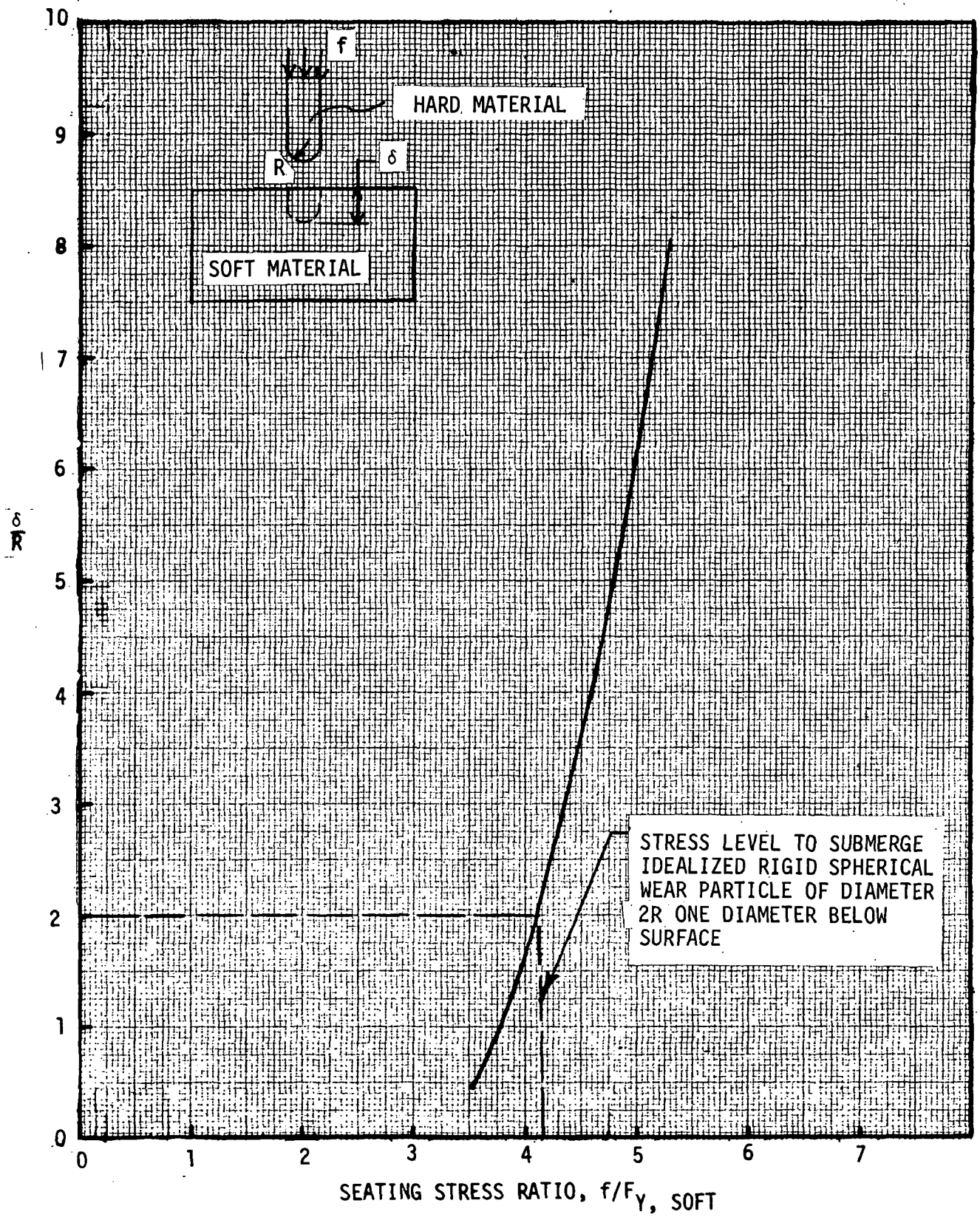

Figure 2-20

INDENTION OF HARD RADIUSED PUNCH INTO SOFT MATERIAL

Bulk Compression Seal Analysis

The general analysis of the bulk compression concept centered on determining the effect of confining the soft seal metal with actual hard walls having finite wall thicknesses and moduli of elasticity. Figure 2-21 shows the effect of relative modulus of elasticity on the apparent bulk compressibility of a soft metal confined within hard metal cavities of two different shapes. The apparent bulk compressibility is defined in this context as the slope of curve of pressure in the cavity as a function of incremental volume change of the soft material (caused by a small piston, for example). This apparent compressibility is non-dimensionalized by the theoretical bulk compressibility of the soft material. The cavity walls are assumed to be infinitely thick in Figure 2-21. If, for example, a sphere of soft aluminum is surrounded by a thick wall of hard steel and compressed, Figure 2-21 shows that the system will appear to be 43 percent softer than the bulk compressibility of aluminum since the modulus of elasticity of aluminum is one third that of steel. The example is noted in the Figure. The additional flexibility introduced by walls of finite thickness is illustrated in Figure 2-22 for a thin annular cavity. The lower curve reflects a factor of two decrease in the initial volume of the soft material assumed in plotting the upper curve.

Extrusion Seal Analysis

Figure 2-23 shows the dimensional requirements on gaps between adjacent parts surrounding a soft metal seal according to plastic extrusion theory. For a typical seal width dimension of 0.012 inch and a seating stress of three times yield, the curve indicates that such a gap should be kept narrower than 0.0009 inch which is stringent but achievable.

The actuation loads involved in opening an extrusion seal after once seating it are investigated in Figure 2-24. If the hard walls confining the soft metal seal are rigid, only elastic strains will be produced in the soft material. When the seating load is released it will return to its original dimensions and can be slid open without any frictional resistance. On the other hand, if the hard walls can deflect laterally as the soft seal is loaded axially, the soft material will be laterally thickened. When the seating load is withdrawn the deflected hard walls will tend to maintain a lateral pressure against the soft metal. This pressure can equal several times the yield stress of the soft material. Significant actuator loads in the valve opening direction can be required to overcome frictional binding caused by this lateral pressure.

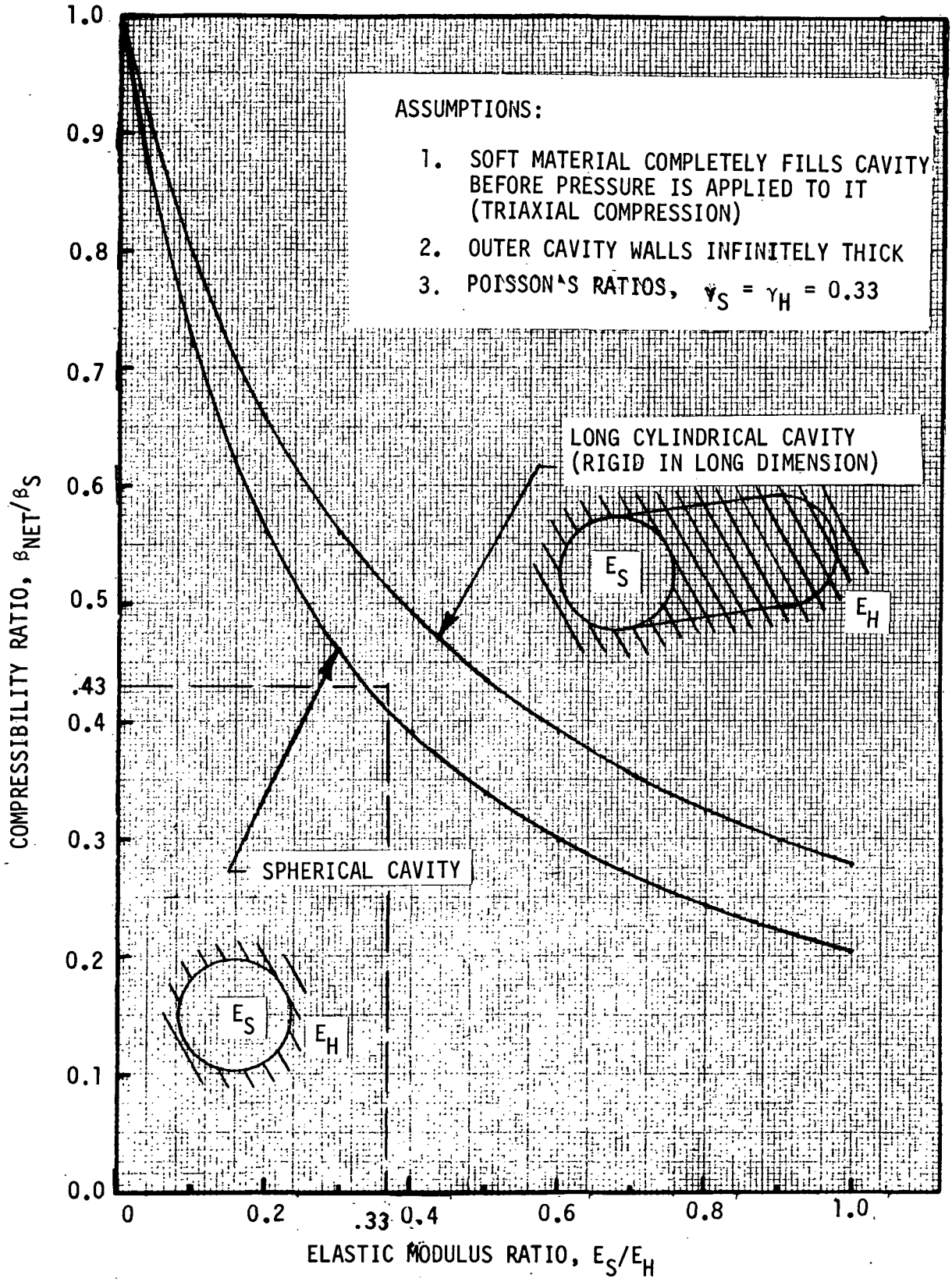

Figure 2-21

EFFECT OF HARD CAVITY WALL FLEXIBILITY ON APPARENT BULK COMPRESSIBILITY OF SOFT SEAL MATERIAL

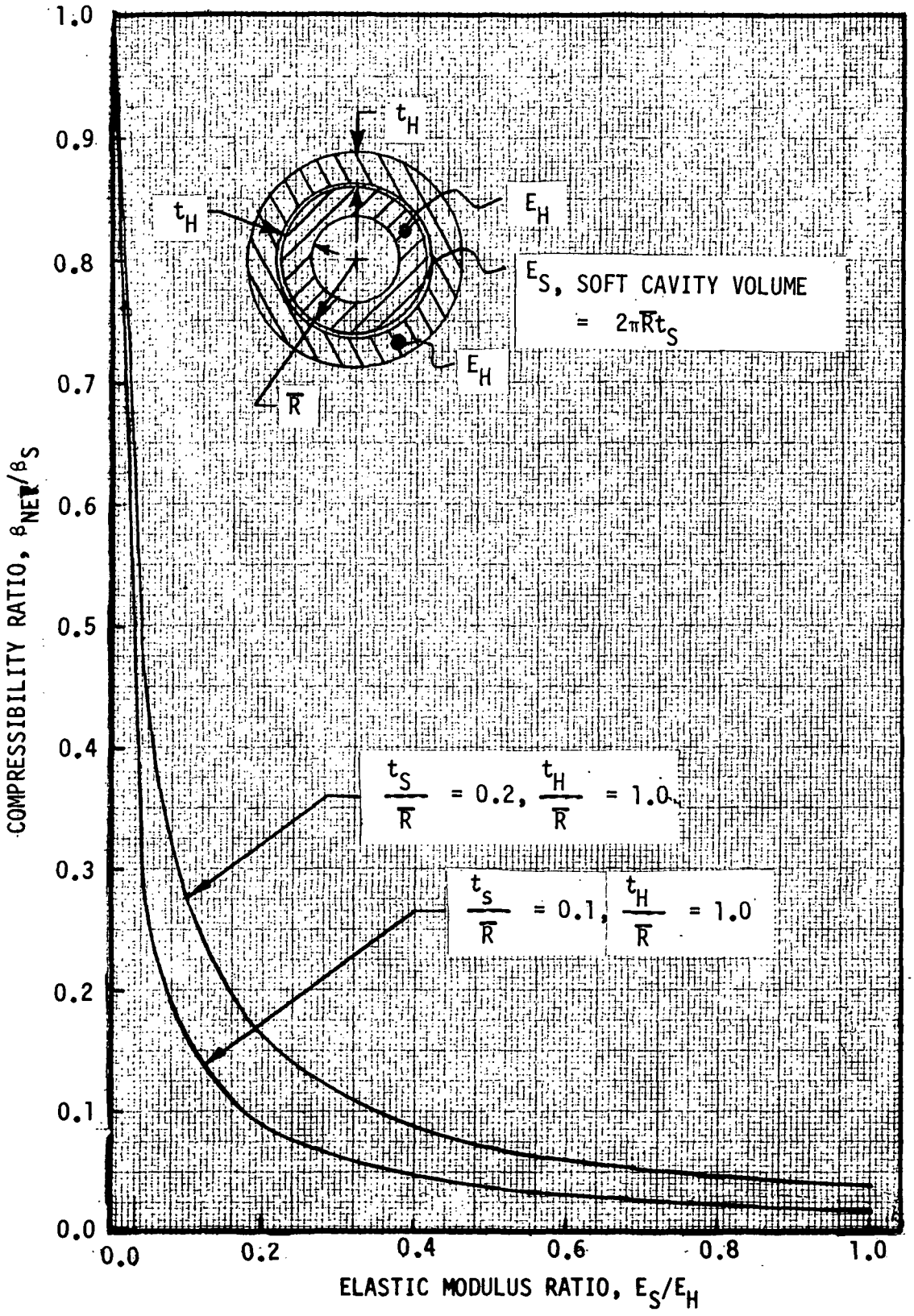

Figure 2-22

EFFECT OF FINITE HARD CAVITY WALL THICKNESS ON APPARENT BULK COMPRESSIBILITY OF SOFT SEAL MATERIAL ENCLOSED IN ANNULAR CAVITY

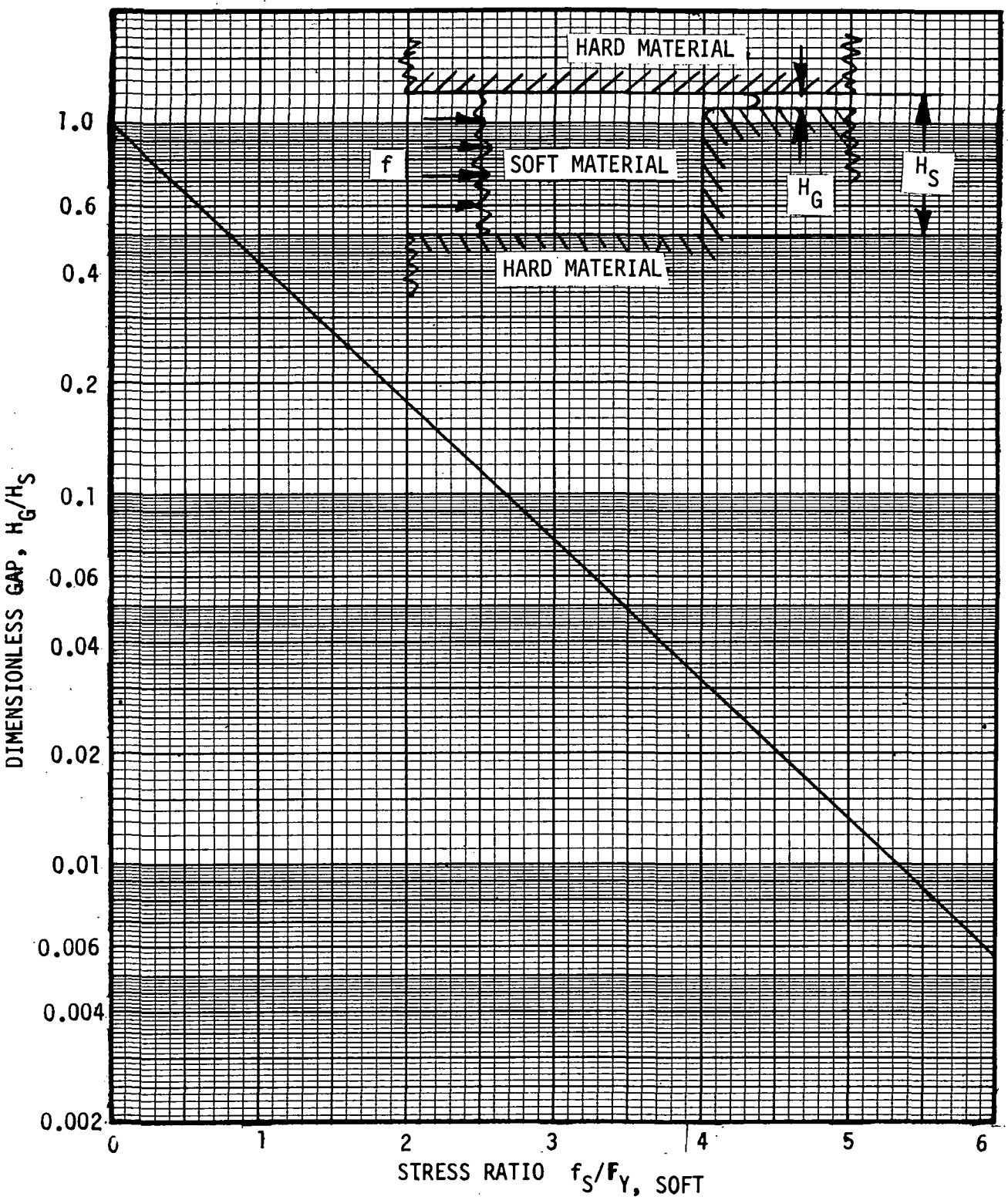

Figure 2-23

MINIMUM GAP REQUIREMENTS BETWEEN ADJACENT PARTS TO PREVENT EXTRUSION OF SEAL MATERIAL BETWEEN SLIDING SURFACES

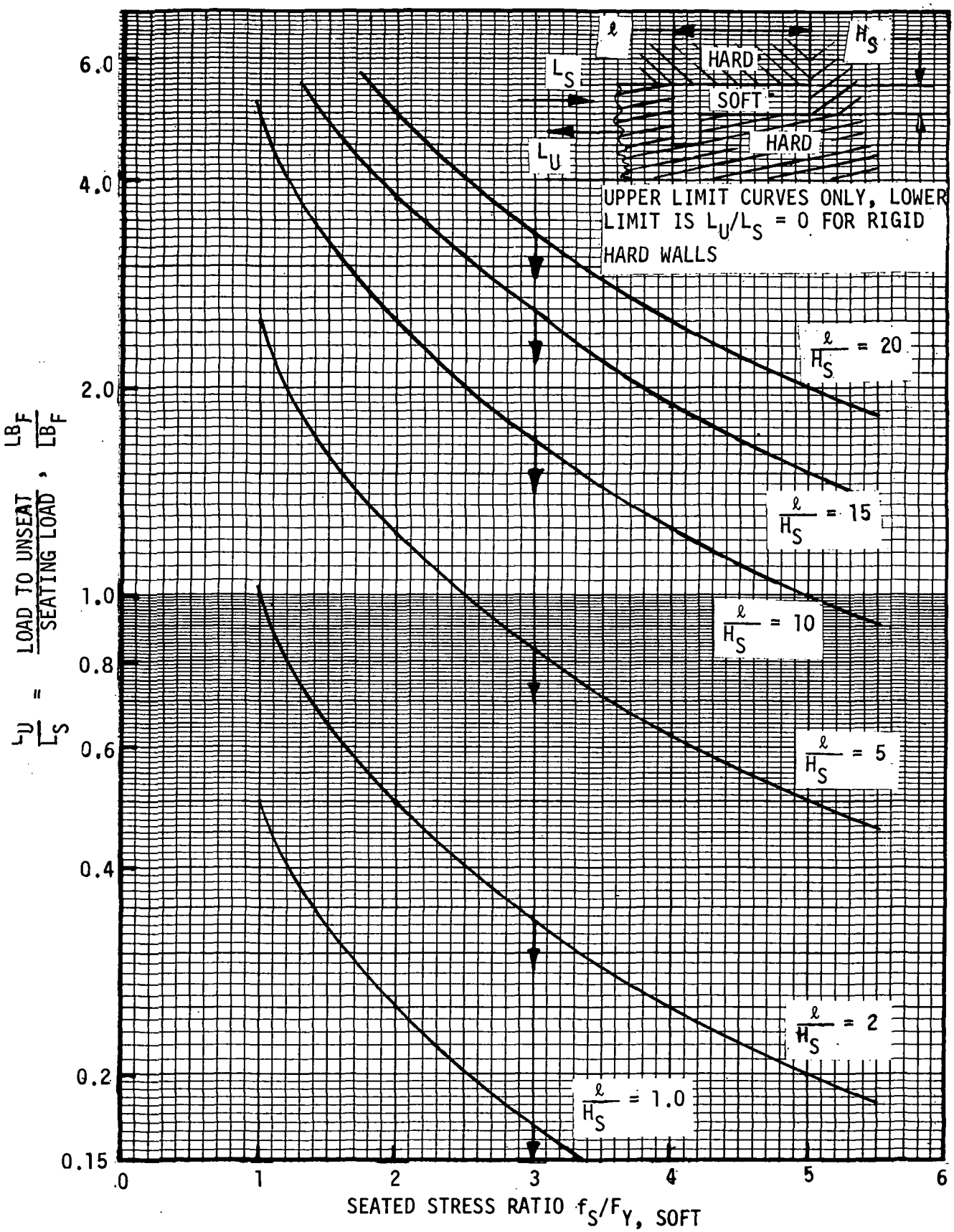

Figure 2-24

LOAD REQUIRED TO OVERCOME FRICTIONAL FORCES

WHEN OPENING EXTRUSION DESIGN VALVE

The upper bound frictional load is that necessary to exceed the shear yield stress along the transverse length of the seal, ℓ. Figure 2-24 shows this upper bound load required to open the seal, ratioed to that required to close it. It seems reasonable to limit designs to geometries that produce values of this ratio below 1.0 to avoid overly severe actuator force requirements.

2.2.3 Detailed Analysis of Seal Designs

Once a particular design layout is available and a certain soft-hard material pair has been selected, more detailed structural analysis must be performed using the geometry of the particular configuration. Factors to be investigated include:

1. Valve seating load requirements
   a. Required stress in soft material at operating temperature with work hardening
   b. Frictional forces during closing
   c. Redundant load paths
2. Valve opening load requirements.
3. Deflection and stress analysis of hard seal confining walls when valve open and closed.
4. Deflection and stress analysis of soft seal material on initial and subsequent actuation cycles.
5. Comparison of calculated stresses with fatigue allowables for desired number of actuation cycles.
6. Comparison of calculated stresses with creep allowables at service temperature to find degree of stress relaxation over service life and its effects.
7. Assess durability of valve in anticipated vibration environment.
8. Evaluate long term effects of propellant reactivity on surfaces.

3.0 CANDIDATE SEAL CONFIGURATIONS

A number of seal configurations are described in this section with analysis directed primarily to the soft on hard metal designs. A brief conceptual description and a cursory evaluation is provided for a combined hard seat and shear seal design and a technique applying ultrasonic energy at the seal interface to establish more intimate contact between the surfaces as a means of reducing leakage.

3.1 Soft-Hard Metal Seal Designs

The mechanisms considered for soft-hard metal sealing were evolved out of the theory and test information presented in Section 2. The designs given primary attention are the original Soft-Hard, Hard-Hard (S-H, H-H) configuration and a Bulk Energized Soft Seal design using an area ratio principle to increase unit loading of the soft material. Several additional configurations have been introduced without analysis as approaches that may be considered if shear action at the interface proved to be of advantage.

The detailed analyses of the S-H, H-H seal model and the bulk compression energized model valve seal is given in Appendices B and C. The major difference between the two designs is the force-stroke relationship in providing high interfacial stresses. The S-H, H-H Seal Seal design requires high force and low displacement whereas the bulk energized seal requires lower forces but higher displacement of the poppet. In both cases friction plays an important but somewhat unpredictable role in the force requirements.

Estimated Leakage Limits With Wear

Referring to Figure 2-11, the wear particle size is assumed to be 1.6 microns (approximately 64 microinches) at 1000 cycles. Referring to Figure 2-4 and taking the gap height to be 1 microinch and the rms surface finish at 2 microinches, curve 8, the leakage is predicted to be 3×10^{-6} scc/sec He at a ΔP of 15 psia. Figure 2-4 was plotted using an orifice diameter of 0.05 inches. This leakage must be multiplied by 12.5 (.625/.05) to obtain the equivalent leakage for a 0.625

diameter orifice. Thus the 3×10^{-6} leakage becomes 3.6×10^{-5} scc/sec He for the larger size assuming the gap h no load of Figure 2-18 to be 64 microinches at 1000 cycles, then to attain a leakage of better than 10^{-5} scc/sec He (1 microinch) requires a h/h_{NO} ratio of 1/64 or .016. This ratio is too low for practical consideration but is useful in the limiting case since the applied stress/yield stress (f/Fy) increases asymptotically. This would be the case for metal surfaces having the stated roughnesses on the first stroke or under conditions of stresses in the elastic range.

The other limiting case is that the rms finish of the soft metal does not exceed that of the hard seat which is a reasonable assumption based on the coining theory of plasticity. The hard seat finish of 2 microinch surface is within practical boundaries at least initially. Assuming a change to about 4 microinches due to fluoride film or oxide film buildup the h/h_{NO} ratio (Figure 2-18) now appears to be close to 0.3 where h_{NO} = 4 microinch and h is made to be about 1.0 microinch resulting in a leakage rate of about 2×10^{-5} scc/sec He (Figure 2-4). The applied seating stress according to Figure 2-18 to achieve this value is of the order of 2.8 times the yield stress. Assuming aluminum yield stress at 15,000 psi the applied stress would be 42,000 psi. The leakage values stated above are for a ΔP of 15 psia. Higher ΔP values will increase the leakage values according to Figure 2-4.

Figure 2-5 taken from Reference 4 is a computer program output curve. The leakage is based on a seal perimeter to width ratio of 100. Leakage of 10^{-11} lbs/sec of LF_2 requires stresses of about 10,000 psi for the steel/aluminum case. To achieve the same result for the steel/copper seal of Figure 2-6 a stress of about 40,000 psi is required.

This analysis indicates the importance of the bulk plastic range of the softer metal in achieving low leakage. However, testing will be necessary to determine the true value of the analysis under the actual operating environments.

3.1.1 Soft-Hard; Hard-Hard Redundant Poppet Seal (Redundant Seal)

The function of the redundant poppet seal has previously been described in Reference 1. In the form submitted as part of the design package, Reference 2, the seal utilized a thin metal sleeve of soft material as shown in Figure 3-1.

A detailed analysis of the function of the seal is described in Appendix B. An evaluation was made of frictional forces between the soft insert and the restraining walls, deflection of the enclosing shell and of stresses in the soft material.

The function predicated in the original design assumed the hard seat sleeve was initially loaded on the seat at a nominal 50 pound force. The center plug then moved forward confining the soft seal against the seat face at an additional force of 493 lb, resulting in a loading of 25,800 psi.

As a result of the stress analysis and evaluation of friction effects, changes in the soft seal insert and hard seal sleeve configurations were indicated. Figure 3-2 illustrates the changes recommended from the the analysis. They are as follows:

1. The soft insert length was reduced to lower the contact area with the hard seat sleeve. On the basis of bulk loading of the soft sleeve the normal force resulting in friction is proportional to area.

2. The radial thickness of the insert was increased to lower stresses in the thin section of the first design. The seal contact area is retained unchanged. This change provides a greater bulk of material to withstand tensile stresses that could be imposed in the soft material on opening the valve. In view of the level of friction predicated at 328 pounds in the original design, it can be assumed the 50 pound hard seating spring will not move the hard seat sleeve on the soft seal. This action will not be necessary however as the normal actuating force to close the valve is capable of breaking out this friction force to insure seating of the seal. The requirement for the 50 pound spring is then only to assure the hard seat contact and confining action to take

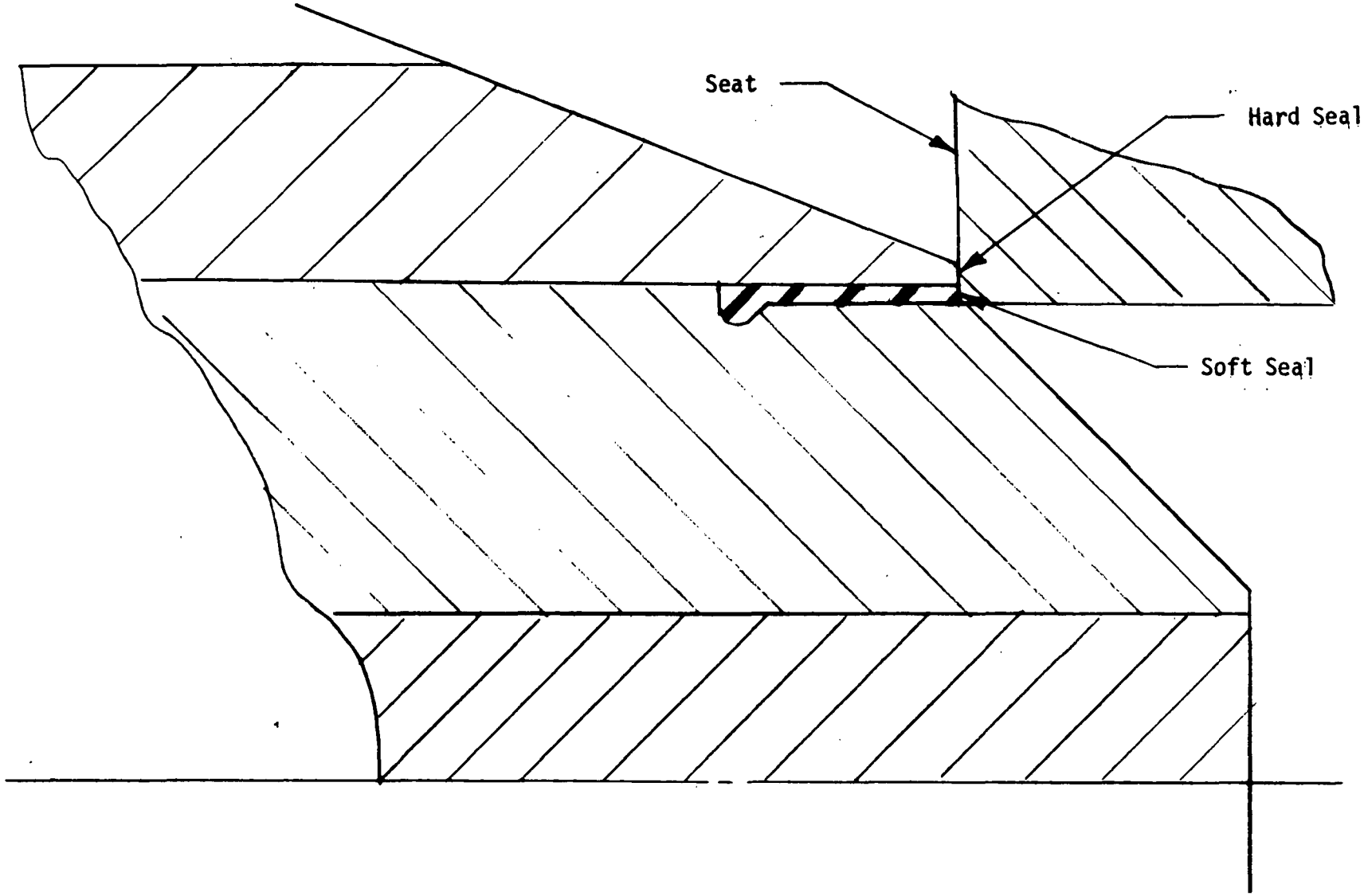

Figure 3-1. Soft-Hard, Hard-Hard Seal Scale 10/1
Original Configuration
(submitted 2-15-72)

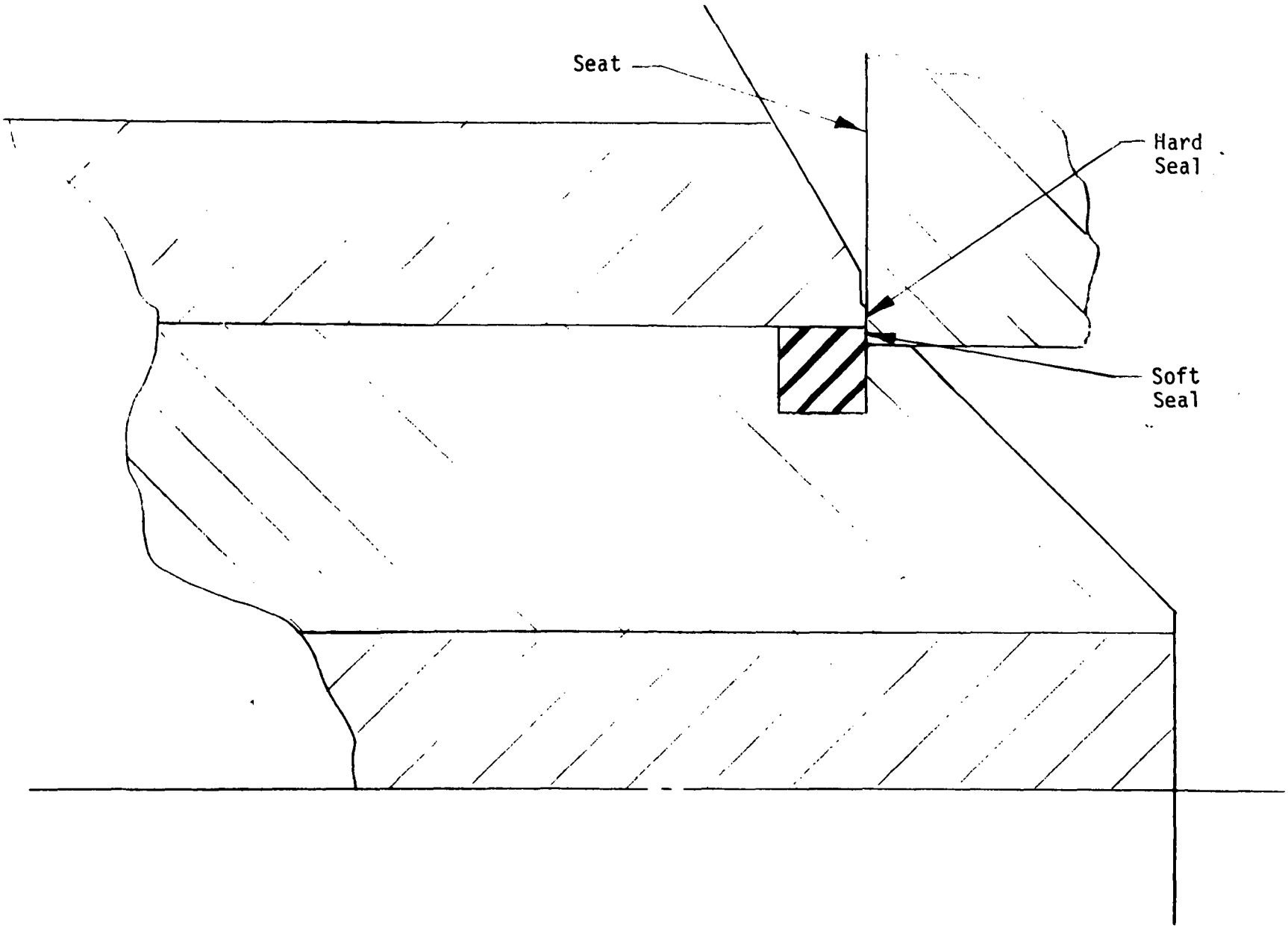

Figure 3-2. Soft-Hard, Hard-Hard Seal Revised Configuration Based on Seal Analysis

Scale 10/1

place before high forces are applied to the soft material.

3. The thickness of the outer hard seal sleeve was increased at the tip to reduce the elastic strain in the part under load. This in turn reduces the plastic flow of the insert and consequent friction loading on unsealing.

The analysis, Appendix B shows the radial fit clearance at intersecting points of hard confining walls to avoid extrusion of the soft seal to be .0027 inch for 1100 aluminum and Inconel 718. This is easily met with the original dimensions.

The effect of a modification of the seal contact shape from the original flat face was considered. Based on a single application of load a non-uniform contact stress pattern would be produced with a peak stress above average at the initial point of contact. If this action could be maintained an advantage would be apparent in that a lower actuator force would be required relative to the higher stress level. A general evaluation indicates that even though a peak stress of several times average can be achieved within the elastic range of the soft material this is not likely to be maintained with wear and corrosion effects on the surface.

3.1.2 Bulk Energized Seal

The detailed analyses of the bulk compression seal is given in Appendix C. The analysis was based on the soft metal seal housed in the outer movable cylinder. The configuration shown in the analysis has the major disadvantage of possible extrusion of soft metal into the corner radius of the flat poppet closure during actuation. Figure 3-3 is a similar design, however, the soft metal is fixed in the seat housing. The analysis is unchanged however and applies to the configuration of Figure 3-3.

The analysis of Appendix C shows friction to be the major parameter in determining actuation and loading forces. Retention of the stresses within the bulk soft metal seal will largely depend on the static friction between the soft metal and hard enclosure. Methods to improve friction would include coatings of materials having low shear strengths. At a friction factor of 0.2 the loading and unloading forces are about 500 lbs and 150 lbs, respectively. This is an optimistic value and could be higher if the coefficient of friction is higher.

In the design of Figure 3-3 an outer cylinder is required to maintain the geometry of the soft confined seal when in the open position. A spring may be used to actuate the cyclinder as the piston moves to the open position. The use of a spring would add to the actuation force to close at about 150 lbs assuming a friction coefficient of 0.2. The outer cylinder may also be actuated by the mechanism used to unseat the piston but a mechanical linkage must be provided. The optimum design would have to be determined in conjunction with the selection of the actuator. Design variations in the area exposed to sliding of the soft seal may be used to alleviate friction forces. Added complications in fabrication are likely to result however.

The bulk energized seal design offers the advantage of lower loading forces and maintenance of seal geometry independent of cycle life. Other considerations include the effects of work hardening and the build-up of hard films under exposure to the oxidizer. Aluminum is a strong

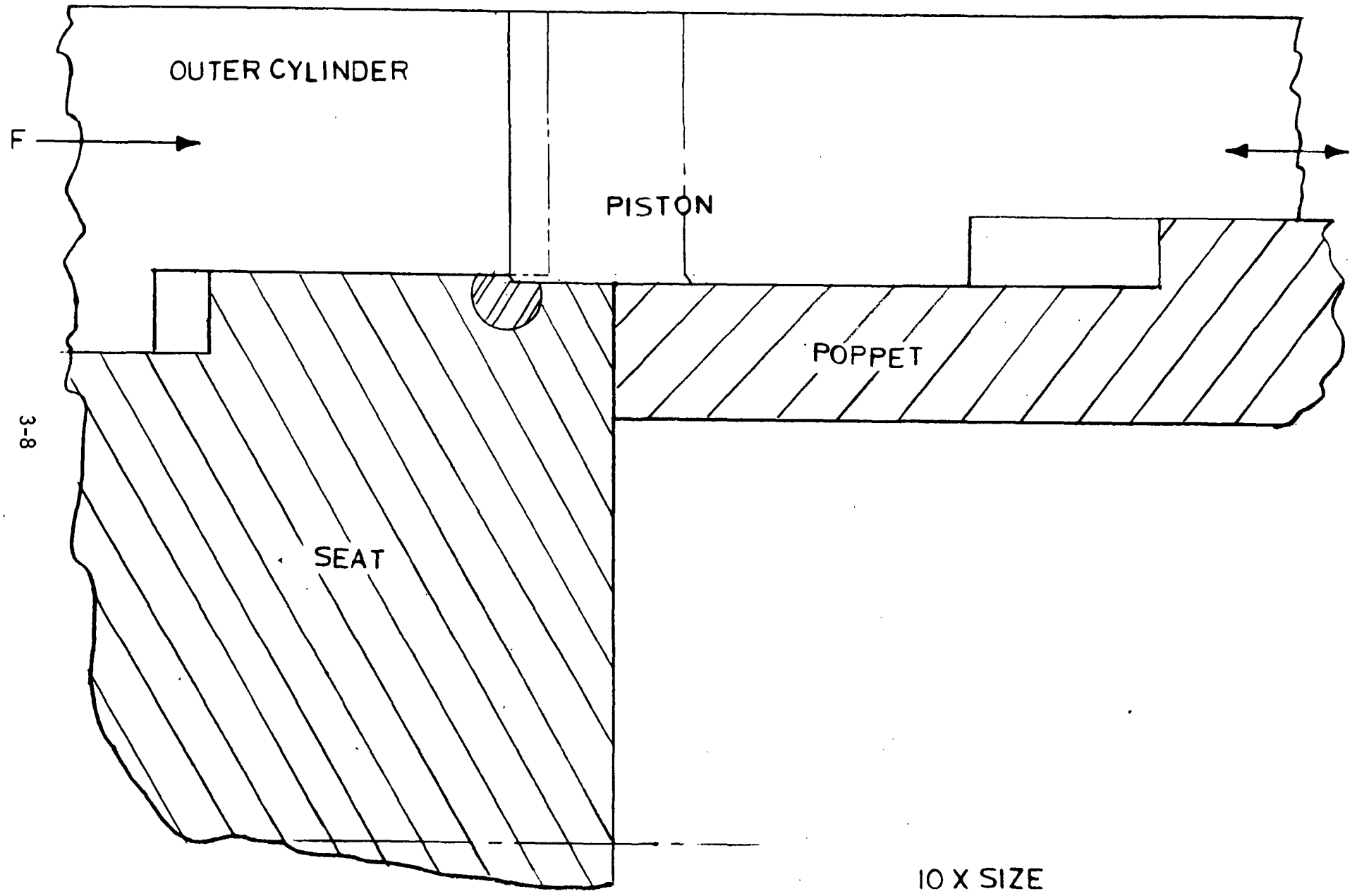

Figure 3-3. Bulk Energized Seal

candidate for the soft seal based on the lower plastic stresses to achieve the lower leakage level. However, other materials should be considered based on oxidized film properties. The properties of oxidized films after exposure to FLOX are mostly unknown. Testing of several candidate materials must be done to determine optimum sealing materials.

Contamination is always of concern in any seal mechanism. The plastic flow properties of the energized seal should be insensitive to particles equal to the surface asperity heights of the rougher surface. Foreign hard particles will require additional loads in the range given in the curves of Figure 2-6.

An additional advantage of the configuration shown in Figure 3-3 is the redundant flat seal of the poppet and seat. Flat seat design should seal better than 10^{-4} sccs He however the flat seat design is susceptible to contamination.

Figure 3-4 is a design configuration minimizing sliding motions between the piston and the soft seal. The major disadvantage of the design is the pressure load on the poppet seat area. These loads will require the poppet to be latched (fixed) after closing and prior to loading the piston. Another problem is the bulk movement of the soft metal (during the valve open position) as a result of stress retentivity.

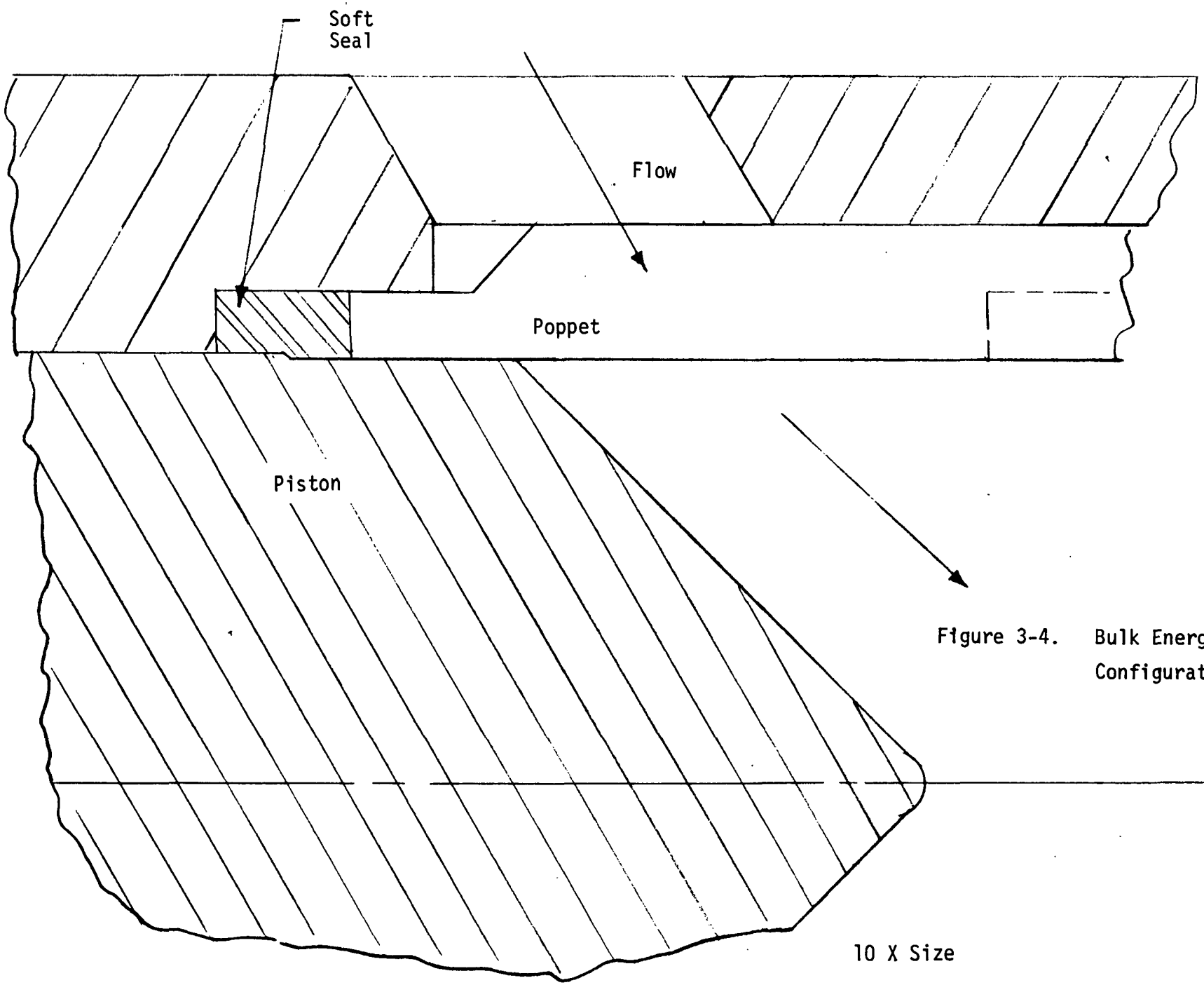

Figure 3-4. Bulk Energized Seal Configuration II

3.1.3 Summary of Comparative Design Analyses of the Soft-Hard, Hard-Hard and Bulk Compression Seals

Detailed analyses of typical designs employing both the Soft-Hard, Hard-Hard Seal and Bulk Compression sealing concepts were conducted to uncover specific problem areas in the two designs. These calculation sheets are shown in Appendices B and C. To enable a direct comparison, the valve orifice size, minimum flow cross-sectional area, soft and hard sealing material, operating temperature and seating load available from the actuator were held constant between the two designs. Final design forces will require ratioing to actual seal areas. Inconel-718 bar stock was assumed for all hard parts of the valve, while 1100-0 aluminum was used for the soft seals. Material properties were evaluated at the normal boiling-point of fluorine-oxygen mixtures ($\sim$ -300°F) except that structural stress margins were calculated at 75°F on the grounds that the valves probably would be cycled several times at room temperature during manufacturing and acceptance tests. A seating load of 493 pounds was assumed for both designs based on application of a particular pneumatic actuator. As all results are linear with actuator load, the effects of a larger or smaller actuator are easily assessed.

A yield stress of 7,000 psi was assumed to apply to the bulk aluminum soft seal material at normal temperatures but the aluminum in immediate proximity to the seal interface was assumed to have work hardened to an effective value of 15,000 psi under initial cycling. The degree to which fluoride film formation alters this value will have to be determined by test.

On this basis the design was found to produce an overall contact stress of 25,800 psi, or 1.72 times the local soft surface yield stress over a seat width of 0.012 inch in the leakage flow direction. With the same actuator load the bulk compression design generates a contact pressure of 38,000 psi, or 2.53 times the local yield stress. For the bulk compression design, the leakage flow path is 0.016 inch or one third longer than that in the extrusion design. The above results assume that by material substitutions, platings or fluoride passivation

films the coefficient of static friction between soft and hard materials can be reduced to 0.2. This value probably represents a lower limit, as the normal coefficient of friction of dry aluminum on mild steel has been reported as 0.61. The performance of both designs is sensitive to the coefficient of friction at the hard/soft interface. With high friction the seating stress of the bulk compression design is no higher than that of the Redundant Seal configuration. The actuator or opening spring load required to unseat the bulk compression configuration increases directly with coefficient of friction.

No difficulty was found in insuring adequate structural integrity of the confining hard walls for hard materials of reasonably high strength levels, such as inconel-718, for seating stresses up to four times the cryogenic yield stress of aluminum. The permanent yielding of hard walls, no matter how thick, can be expected to become a problem at seating stresses over about 70,000 psi.

A load of 328 pounds was required to slide the redundant hard/hard seat over the soft seal upon opening the initial design valve. This load could be reduced to 130 pounds by reducing the axial length of the soft seal, however. The bulk compression design required 130 pounds to overcome opening friction. This load is particularly important in designs where the actuator must energize an opening spring in addition to loading the soft/hard seal interface.

A further investigation was conducted into the effect of machining a convex radius on the hard seat of a rigidly contained soft/hard seal. Hertzian contact stresses provide an increase of 27 percent in the seal's contact stress within the 0.012 seal width as long as the soft material can be maintained elastic by side constraint. This option also offers the possibility of fabricating the soft seal of the design thicker than 0.012 inch to make it more durable and adjusting the contact radii so that the actual contact area is 0.012 inch wide.

In sum, the major advantages of the Soft-Hard, Hard-Hard Seal design are its basic simplicity and the independence of its seating stress from variations in the coefficient of friction. The design's sealing performance is less than that of the Bulk Compression Seal

with the actuator assumed. Actuator force would have to be increased by a factor of 2.53/1.72 = 1.47 to equal the sealing performance of the bulk compression design. The bulk compression design provides high seating stress at relatively low actuator load. It requires tighter control of dimensional tolerances and friction coefficients. Neither design is necessarily superior from the standpoint of unseating load, this depends on the sliding area of soft material on hard. Certain forms of the bulk compressibility design are susceptable to squeezing soft material into a radiused gap on the hard shaft.

Potentially either concept is applicable for shutoff of any of the given propellants or for the helium isolation requirement. For the cryogenic applications higher soft seal yield values must be assumed. The design must be scaled to a .625 inch diameter port for the propellant valves. A specific design is presented in Section 5.0.

3.1.4 Additional Soft-Hard Seal Concepts

Angle Contact Seal Concept

The configuration is given in Figure 3-5. This mechanism provides a method of seal loading on an angled face. It is assumed a small amount of shear motion at the seal interface is beneficial to sealing. The seal is totally confined between an outer housing, a center plug and the seal surface. The center plug is movable within the seal for a short distance and is spring loaded toward the seat.

The seat projection first enters the poppet inside diameter until the center plug is contacted. The plug is then pushed back until the seal surface contacts. The poppet force is then increased until the design seal loading is achieved.

The design assumes a contact loading at the seal interface of something above the yield strength of the soft insert. Stress flow within the soft material will be determined by the combination of the compliance of the housing and the Young's Modulus of the soft material for deflection within the elastic limit. It is possible to reach seal face unit loads above yield while still remaining within the bulk elastic range of the material in the axial direction. A pull away of the seal at the end of the housing could be assumed as shown in the drawing as opposed to extrusion to maintain a filled cavity. An analysis of friction forces is required to determine the deflection characteristics of the insert.

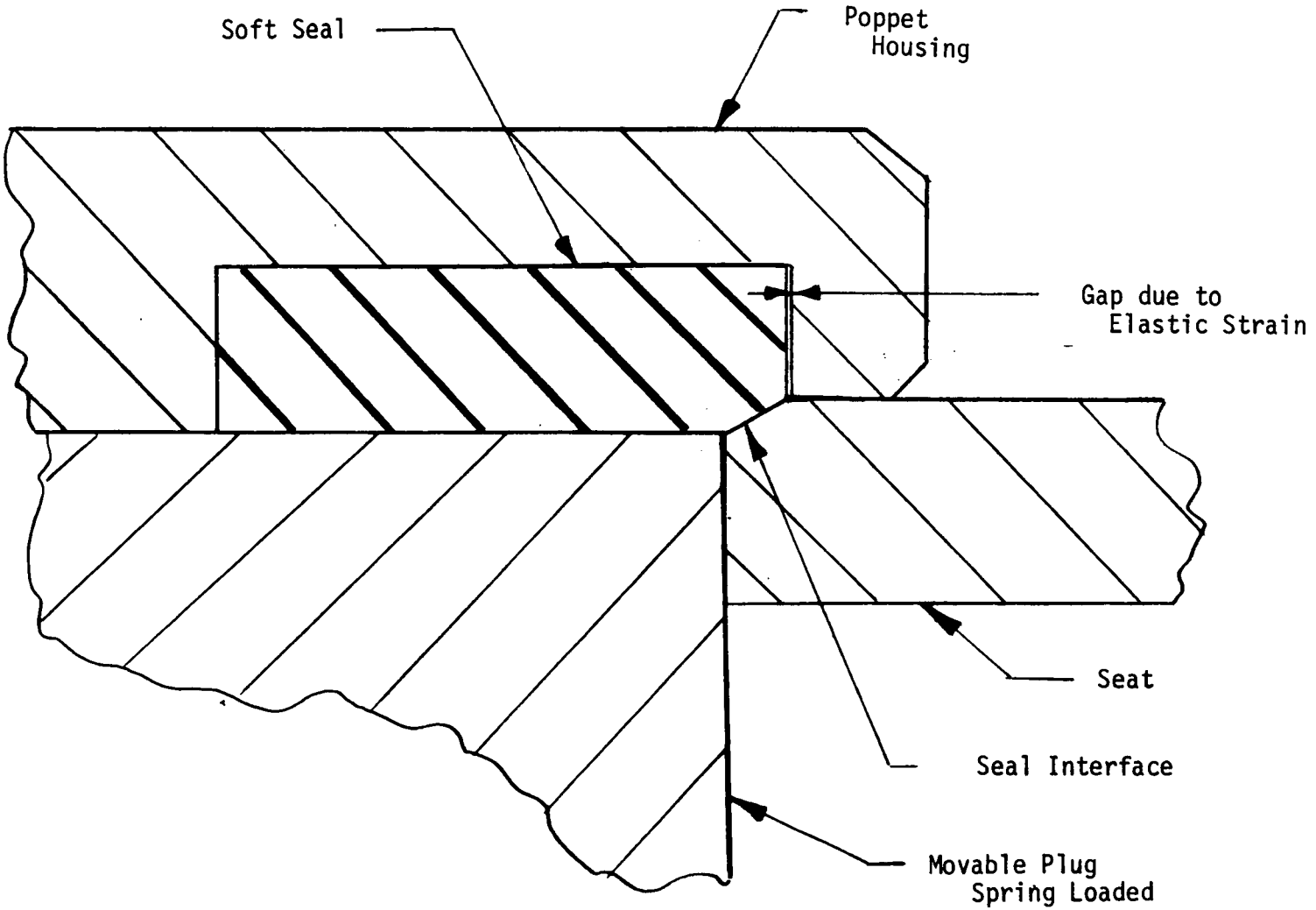

Figure 3-5. Angle Contact Seal Concept

Actuated Seal Concept

The concept is illustrated in Figure 3-6. The approach is to combine an initial shear sealing action at low seal interface unit loads with a final clamping action capable of high seal unit loads. As shown, the initial shearing action is obtained by wedging the outer poppet sleeve to load the seal and retaining lip inward. A small amount of strain in the lip and a bulk preload of the seal would be achieved. The second action is to wedge the retaining lip outward increasing the local seal loading near the outer end.

The seal release is accomplished by reversing the closing sequence. The inner wedge is withdrawn relieving the high loading of the seal. The outer sleeve is then withdrawn. The actuating mechanism could be similar to that of the Soft-Hard, Hard-Hard design using a spring linked to the actuator shaft and center plug to preload the outer sleeve. The clearance between the plug and sleeve must be sealed to avoid a by-pass leak between the plug and lip.

For the model shown a soft seal material with a 2% offset yield strength in the order of 15,000 to 25,000 psi would be a good candidate. The seal would not be totally confined with a small amount of extrusion possible at the outer tip. The use of copper, aluminum alloys, gold or nickel would be potentially possible.

This sealing mechanism assumes a degree of interface shearing action to be of advantage in promoting more intimate contact between surfaces. Based upon bearing wear characteristic data unit loads between surfaces must be kept below a given threshold value for a given material combination or a sharp increase in friction and wear is experienced. By means of controlling the outer sleeve preload, seal interface area, and the contact cone angle the seal interface loading during initial closure can be kept at the optimum level.

The inward strain imparted to the seal insert and retaining lip acts to set the loads in such a way as to make the wedging action of the center plug more effective in establishing the seal loading. The

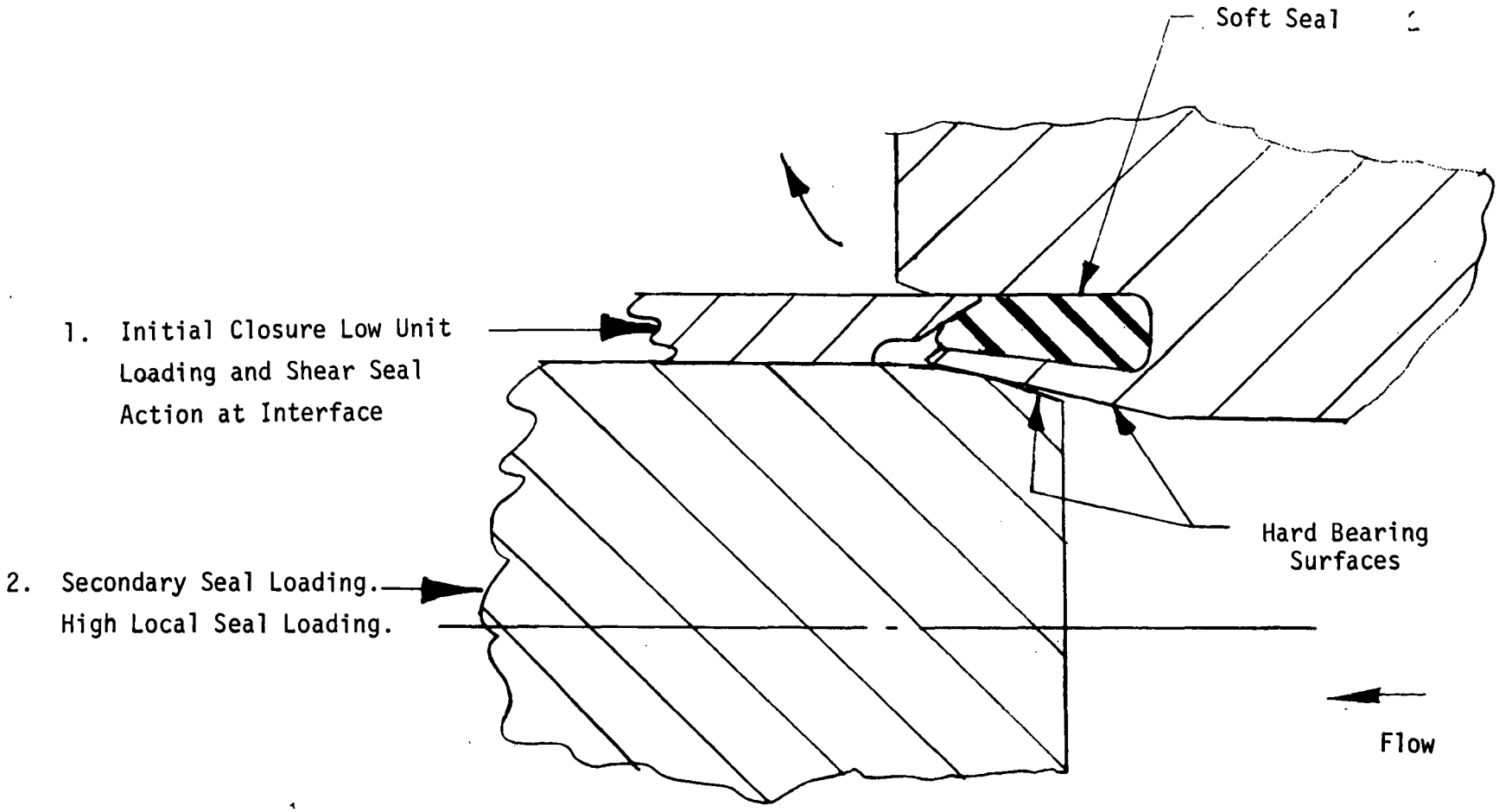

Figure 3-6. Actuated Seal Concept

9-18-72

action of the plug acts to relieve some of the radial strain in the lip and seal insert transferring this strain energy to a bulk loading of the seal with a concentrated load at the seal tip.

Knife Edge Seal Concept

A relatively simple seal concept using a knife edge or wedge poppet provides another method of providing a shearing action on sealing. The concept has some experimental basis in the gasket resealing experiment conducted by General Electric Reference 16 and described in Section 2.2.1.

The reference cites the results of a leak test of a connector using a soft copper gasket compressed and yielded between opposing knife edges. The configuration is illustrated in Figure 2-17. The knife edge diameter was approximately 1.1 inches. Leakage tests were repeated after each of six resealings, the gasket moved to a new position on each cycle. The results are summarized in Table 2-5. The results indicate a high degree of feasibility resealing a soft-hard interface. The conditions for this demonstration must be considered to be relatively severe although not involving propellant exposure.

Figure 3-7 illustrates a possible valve seal configuration. A material with a hardness like an aluminum alloy, copper or gold and with a degree of cold work would be a likely choice. The load equivalent to that used in the General Electric tests of soft copper would require a 1500 pound actuating force for the popellant isolation valve size.

The knife edge configuration could be analytically optimized by evaluation of the effects of varying the taper angle, the tip radius for a given soft insert, the elastic properties of the seal and housing and the unit loading of the angled face.

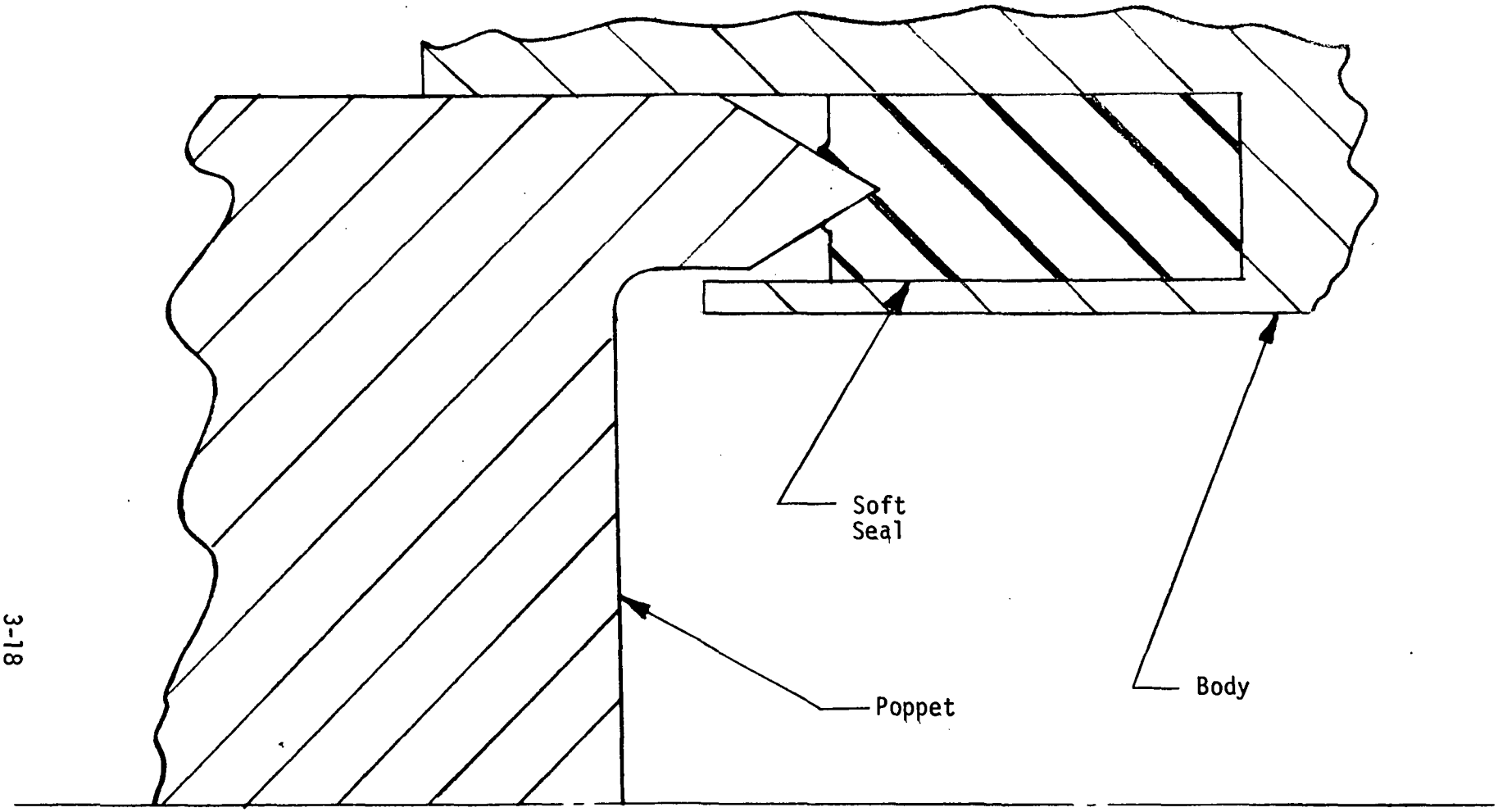

Figure 3-7
Knife Edged Seal

3.2 Combined Flat and Shear Seal Evaluation

The seat concept shown in Figure 3-8 was originally advanced for use in a propellant shutoff valve for engine application. A grooved flat face hard poppet is used in contact with a hard seat. A thin sleeve in the housing is simultaneously loaded by a spherical surface on the O.D. of the poppet to form a redundant shear seal. In principle the plunger expands the sleeve an amount within the elastic limit as it approaches the flat seat.

The evaluation indicates the configuration to be somewhat limited for the isolation valve application because of the effect of particle contamination. The optimum seal for a given combination of hard materials is determined by the geometric accuracy of the interface, the combined surface finishes, and the unit seating load within the gross elastic range of the materials. This theoretical sealing capability is affected by particulate contamination, by the reduction of average contact loading of the interface and consequent increase of leakage cross section. In addition, a degree of surface damage may occur if the particle is hard with respect to the seal material.

Effort cited in References 20 and 21 give a cross section of tests of poppet designs for both hard on hard and soft on hard combinations. Grooved flat seals and shear seal designs are evaluated with the emphasis of the work dealing with contamination tolerance. Unfortunately the test effort only reports leakage rates no less than the order of 10^{-4} SCIM GN_2 at 1000 psi. (This is near to an equivalent value in SCCS GHe.) Typical results for seat stresses in the order of 10,000 psi averages about 10^{-3} SCIM GN_2 for a variety of tests.

In principle a combination of a relatively soft material with a hardness above annealed values such as hard copper on a hard material such as 440C stainless appears to provide a good combination for absorbing hard particles if seal loading is sufficiently high.

Recommendations of Reference 21 indicate hard seal combinations are desirable where a valve can be cycled to reduce the leakage. The

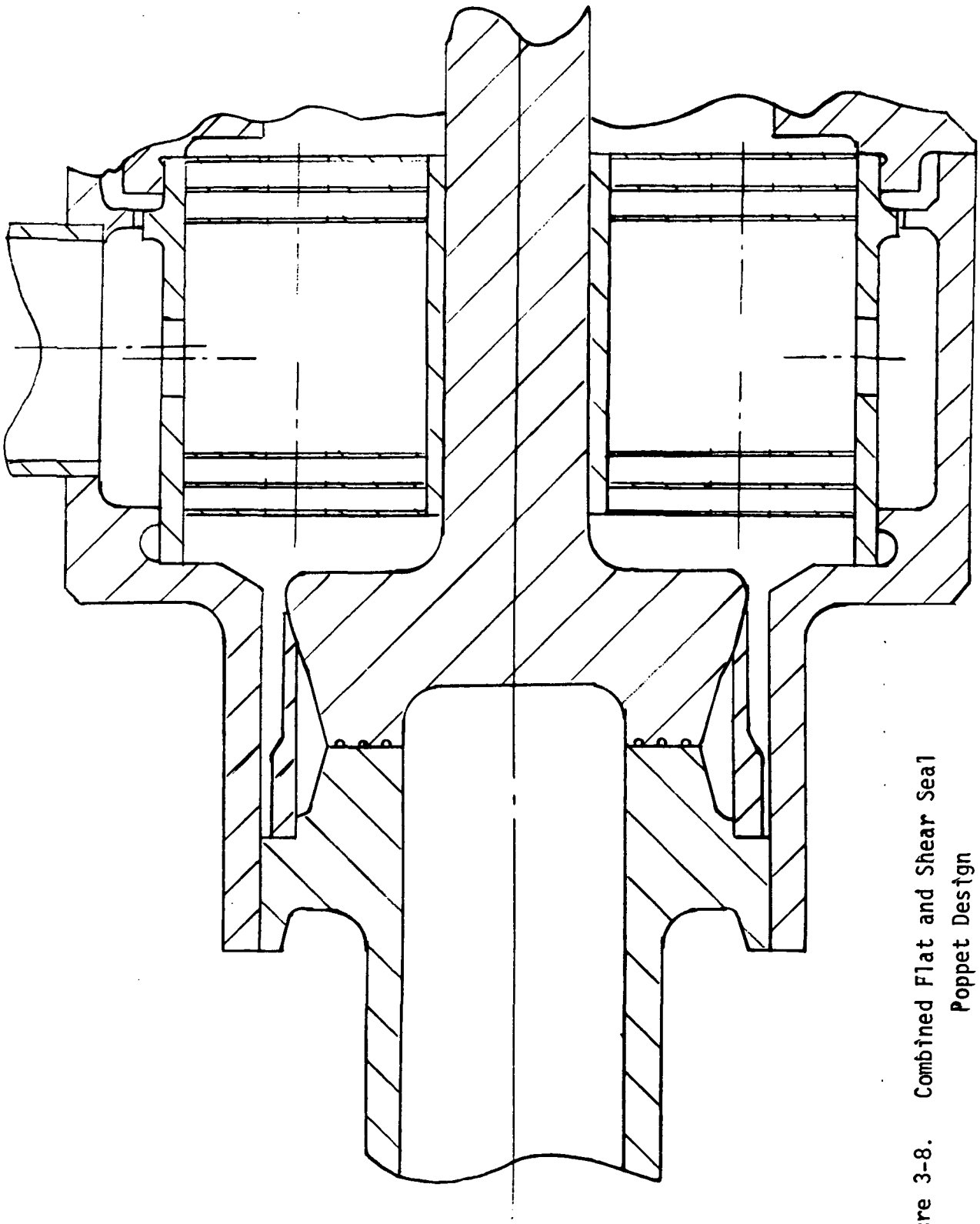

Figure 3-8. Combined Flat and Shear Seal Poppet Design

particles leave little damage and are not permanently imbedded. The particle can be flushed out with reopening of the valve. On the other hand with soft-hard combinations a single particle will not greatly affect leakage. However, with contamination present and many cycles damage due to multiple impacts it will increase the leakage. In the configuration shown the seats are considerably larger than the valve orifice. This has the disadvantage of a larger leakage perimeter as well as increasing the degree of precision required to seal. The effects of a given amount of out-of-flat or out-of-parallelism is magnified. A high degree of precision is required to align the flat seat for squareness and simultaneously center on the spherical seat. The large seat diameter also increases the thermal expansion effects within the spherical seal if different materials are used. The cavity between the flat and spherical seal must be minimized because of trapped fluid considerations.

3.3 Welded Seals

Welding or brazing the seat and poppet was considered in this study. The major problem with any fusion process is the high thermal losses due to the large temperature increase from cryogenic temperatures to the melting point of the welded metal and the associated heat loss to the propellant. A fusion type seal was therefore ruled out. Ultrasonic welding, however, was considered.

3.4 Ultrasonic Bonding

Ultrasonic welding is a solid-state bonding process. There is no large scale fusion at the interface as normally associated with welding. Since most of the energy is applied to the interface, thermal losses are low. The interface bond is characterized by a penetration of one material into the surface of the other and by breakup of the oxide or other barrier films. Almost any two metals may be bonded by this method.

Ring welds made by means of ultrasonic bonding have shown no leakage within the limits of measurement of 5×10^{-10} scc/sec helium (Reference 24). There has been no indication of preferential corrosive attack of the weld zone on tests with aluminum and 316 stainless steel. The base metal is attacked equal to the attack of the weld zone or receives the major attack when exposed to corrosive environments. No information has been found with exposure to fluorine environments.

Figure 3-9 is a conceptual schematic of an ultrasonic bonded seal. The major features of the valve seal design are the transducer-coupling system, the required damping force, the anvil and the power requirements. Since the valve requirements must be multi-cyclic the major problem to be investigated is the breaking of the bond and rebonding the same interface.

Both magnetostrictive and electrostrictive transducers are used in ultrasonic welding systems. Magnetostrictive materials change length under varying magnetic flux density. Such transducers normally consist of a laminated stack of nickel alloy and are rugged, usually used for continuous duty operation.

Electrostrictive materials are typically ceramic such as barium or lead ziconate. These materials change length when subjected to an electric field parallel to the plane of polarization. These transducers are also rugged and have conversion efficiencies more than twice that of magnetostrictive devices.

The clamping force is applied normal to the surface to be bonded. In the valve design the load may be imposed by direct actuator output or by a spring loaded mechanism. The anvil provides the support to the applied clamping force and should be acoustically designed for controlled vibration compliance with periods of out-of-phase displacement in relation to the displacement of the transducer.

If the clamping force is too low, slippage will occur at the faying surface and a poor bond is created. Too great a clamping force creates excessive damage of the surface contacted by the transducer.

Ultrasonic welding equipment is rated on the basis of the acoustical power (watts) available at the weld zone and range from less than 1 watt up to 4500 watts for spotwelding equipment to above 10,000 watts for ring-welding equipment. Ultrasonic frequencies for welding aluminum, for example, are in the range of 10,000 to 60,000 cps. The high frequencies are usually employed with the lower power welders.

An advantage of welding aluminum ultrasonically is that the metal oxides do not have to be removed prior to welding. However, large power requirements may be necessary where heavy oxides films are encountered.

Bonded joints have been known to separate inadvertently by the same ultrasonic power that originally was used in the bonding process. Separating and rebonding the seat will be required for multi-cycle operation. It is not known that this can be done but appears feasible if the selection of materials reduces or eliminates adhesive transfer of material. Candidate materials would include metal and ceramic combinations.

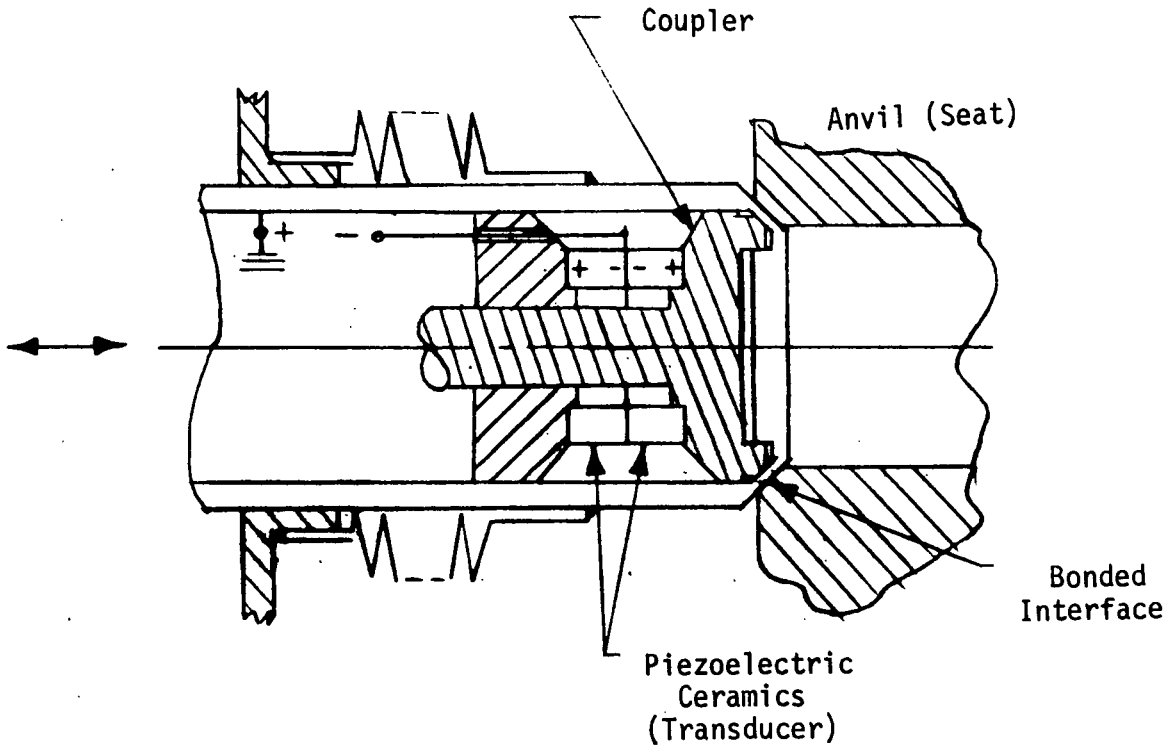

Figure 3-9. Solid State Sealed Valve - Concept

4.0 ACTUATOR TRADE-OFF STUDY

An examination of a broad range of candidate actuator concepts for the propellant and helium isolation valves was conducted to ascertain system interaction and select actuator configurations for final detail design evaluation.

The requirements for the isolation valve actuator are presented below in Table 4-1.

Table 4-1.

ISOLATION VALVE ACTUATOR REQUIREMENTS

Operating Mode	Propellant valve: Normally-open* Multi-cycle Helium valve: Normally-closed* Multi-cycle
Peak Power	10 watts D.C.
Actuation Time	Not to exceed 5 minutes
Thermal Environment	Isothermal with propellant (either cryogenic or storable)
Minimum Magnetic Disturbance to Spacecraft Instruments	
Weight	3 pounds maximum (complete valve assembly not to exceed 4 pounds)
Output	100 to 1000 lb load: .07 to .15 inch stroke

The general approach should be applicable to both propellant and helium valves except possible difference in operating mode.

*The actuation methods feasible for the isolation valves require power to be only applied for actuation or unlatching. Normally-open or normally-closed is assumed to be the direction in which the actuator is spring loaded requiring only an unlatching signal to achieve.

4.1 Actuator Characteristics to Meet System and Valve Requirements

Although the desired actuator output load and stroke are dependent upon the specific valve seat configuration, the range of interest cited in Table 4-1 permits an evaluation of energy/power requirements for the more likely candidate actuator concepts. The limited electrical power and the capability for cryogenic or essentially room temperature operation with a single design approach poses constraints on viable actuator concepts. Because of the normal position (open or closed) requirement noted in Table 4-1, the valve must be latched. Possible latching concepts examined included:

- Fusion seal
- Solenoid actuated pin or pawl
- Over-center linkage with solenoid "kicker" release
- Multiple ball detent with solenoid release
- "Negative" clutch or brake (energized open: de-energized - locked)

However, the latching mechanism selection does not greatly influence the actuator selection process. (Although the power required by the latch during the closing cycle must be considered in the design of the complete valve assembly.) Consequently, evaluation and selection of candidate actuator design concepts can be made through consideration of the relative merits of the possible different force producing approaches within the load range of interest.

Another design area common to all actuator concepts is that of assuring lubrication for sliding surfaces, bearings, gears, etc. for the desired 10 year life. With molybendum disulfide and the metal fluoride lubricants only some slight pressure above total vacuum must be maintained to preclude adhesion (References 22 and 23). As the retention of a near-atmospheric pressure hermetic seal does not appear mandatory for assured operation, the lubrication question should not be a determining factor in actuator selection.

4.2 Selection of Feasible Candidate Actuators

Figure 4-1 presents an actuator concept tree where the various design approaches are developed from consideration of the basic energy sources (electrical, pneumatic, hydraulic, and chemical). In order to evaluate the candidate actuator concepts, each approach was schematically

Figure 4-1.

ACTUATOR CONCEPT TREE

By Energy Source

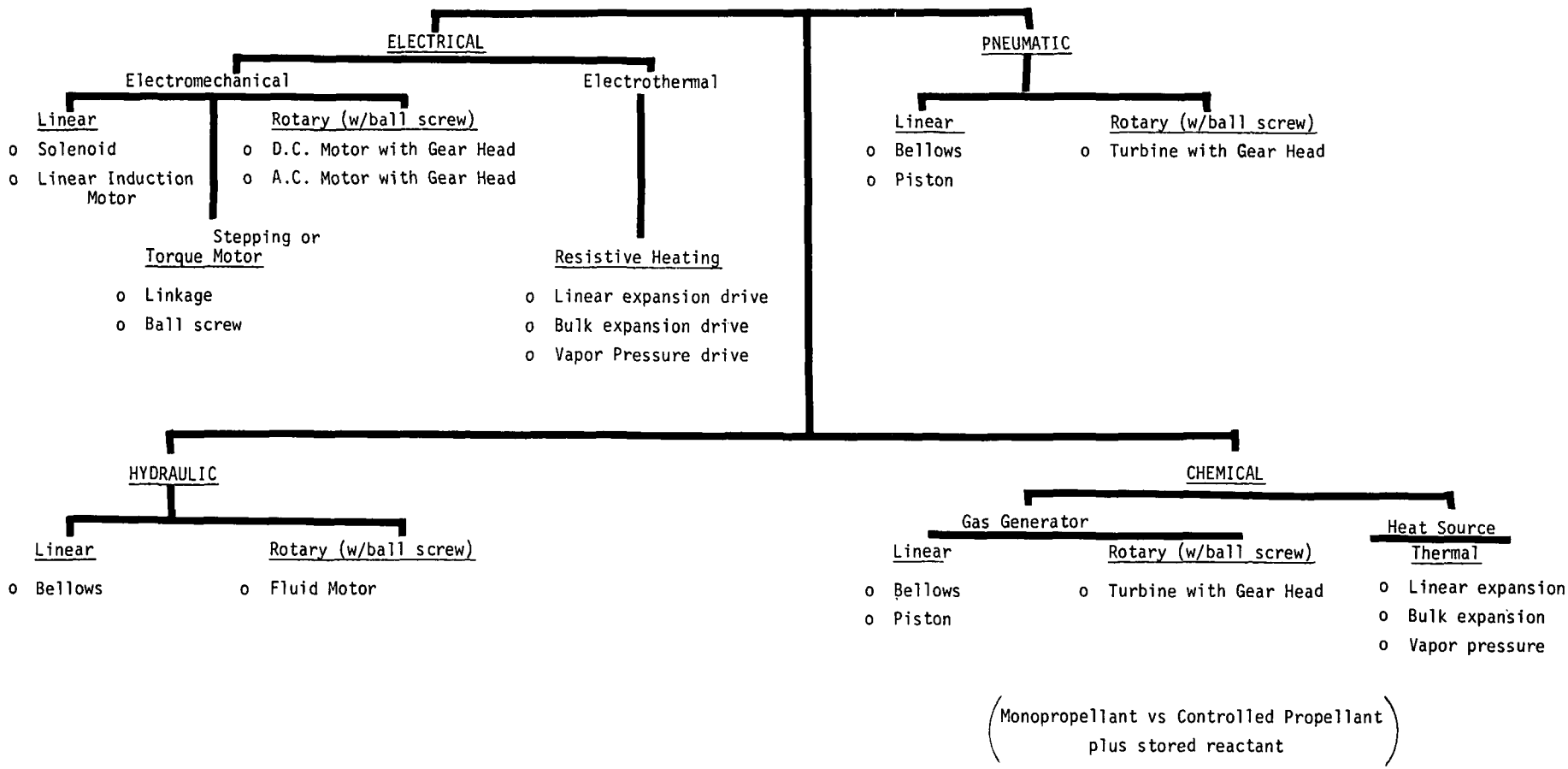

illustrated to emphasize the number (and type) of energy transfer mechanisms inherent in the design configuration, Figure 4-2. Using this schematic presentation, in combination with design calculations, the performance and system interaction considerations for the various actuator concepts were assessed relative to the following eight criteria:

- Power/energy requirements (1 watt D.C. power ≈ 1 pound system wgt.)
- Thermal and vacuum environment compatibility
- Relative weight
- State-of-the-art of concept (general practicality of approach)
- Input signal/control complexity
- Envelope
- Reliability impact on other subsystems
- Interface complexity (e.g. disposal of pneumatic vent fluids)

A scoring system was devised to rate the actuator concepts with possible scores ranging from 0 to 3 for each of the eight performance/system criteria. The meaning of each of the four score values was selected as follows:

3 - Fully compatible with requirement
2 - Better than average performance
1 - Possible incompatibility
0 - Seriously deficient

A score of 0 eliminates a concept from consideration, and this score is assigned only if it is unquestionably obvious that a given actuator concept will not meet the design requirement. A composite rating was obtained by taking the product of the individual scores and dividing by the sum of the scores. Thus, a concept which consistently scored "better than average" in all eight criteria would have a composite rating of $\frac{2^8}{2x8} = 16$.

However, before proceeding with individual ratings, a discussion of the advantages and disadvantages of the candidate actuator concepts relative to their schematics (shown in Figure 4-2) will indicate the rationale behind the ratings to be presented subsequently.

Figure 4-2 (a)

Isolation Valve Actuator Concept Schematics

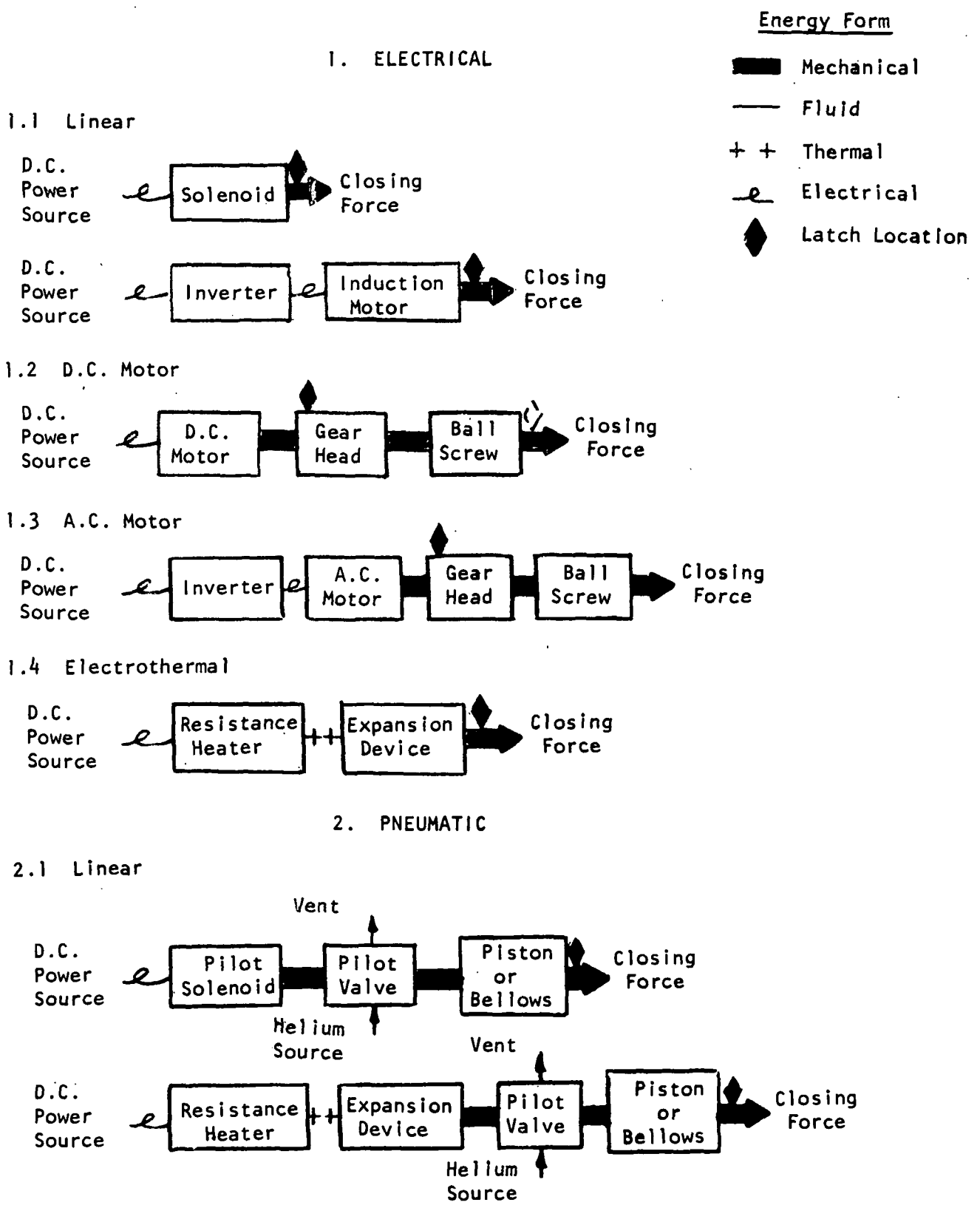

Figure 4-2 (b)

2.2 Turbine

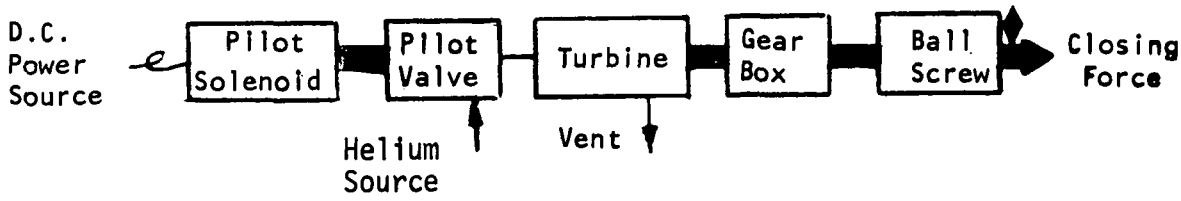

3. HYDRAULIC

3.1 Linear

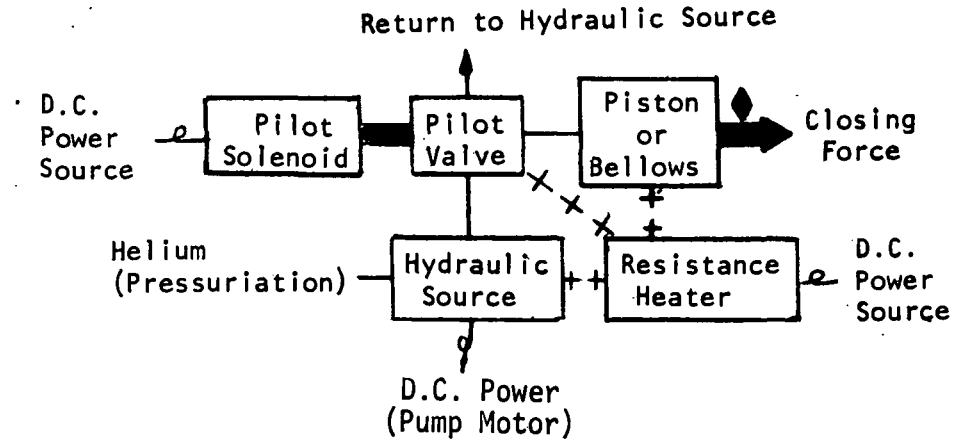

3.2 Fluid Motor

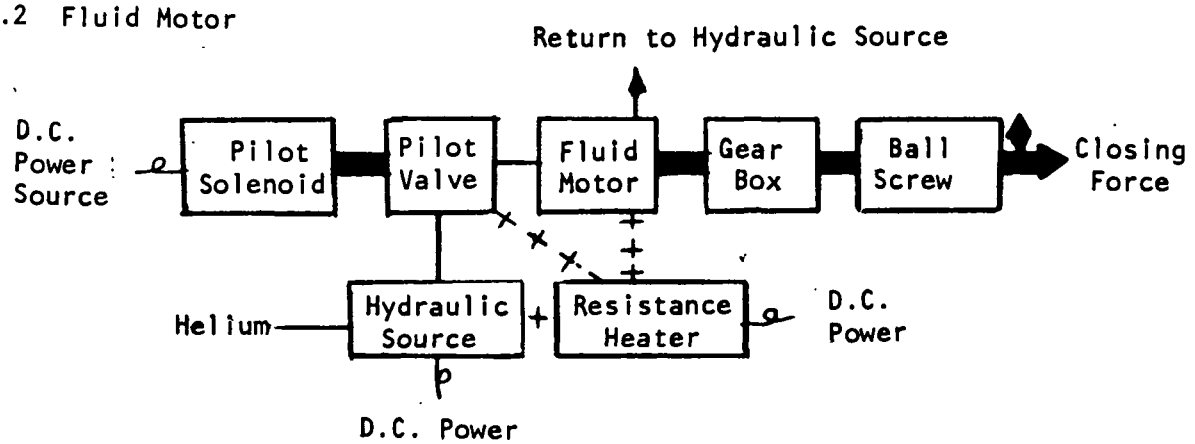

Figure 4-2 (c)

4. CHEMICAL (GAS GENERATOR AND HEAT SOURCE)

4.1 Linear (Pneumatic)

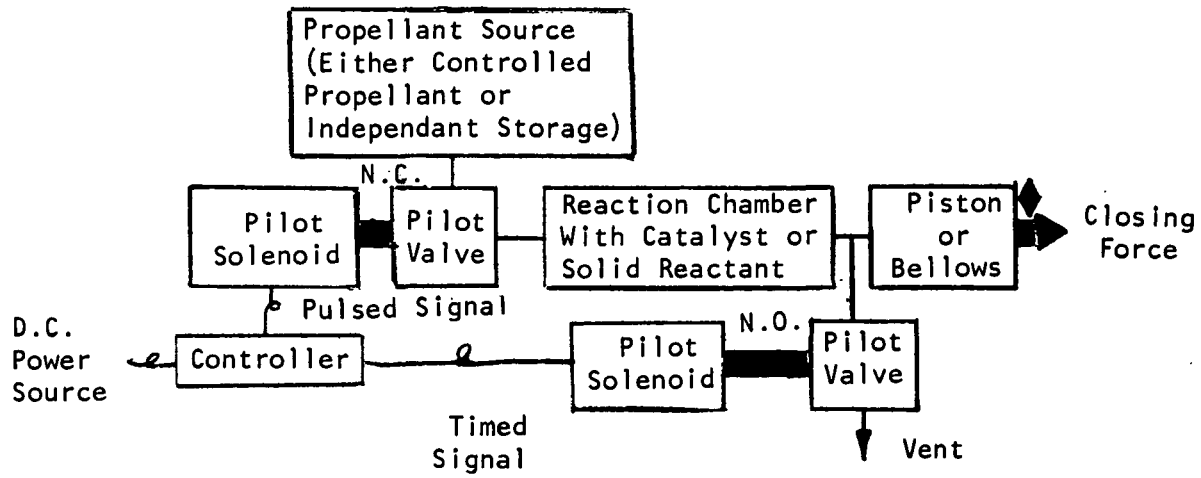

4.2 Turbine

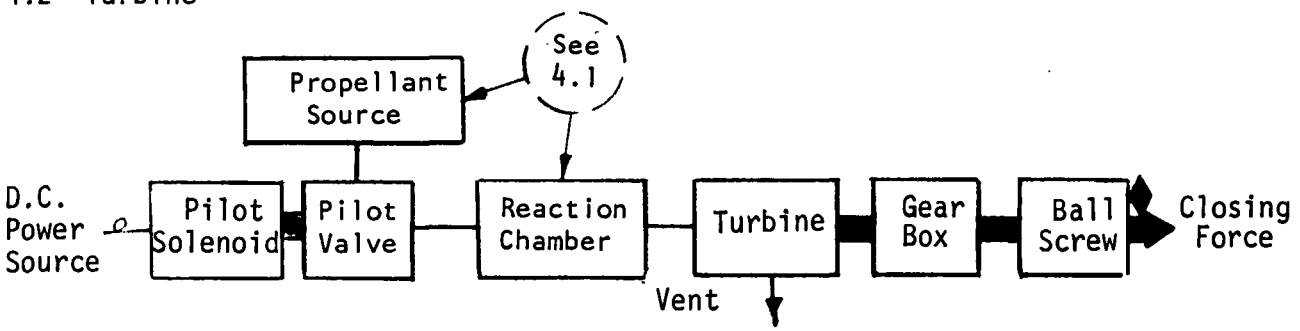

4.3 Thermal Expansion

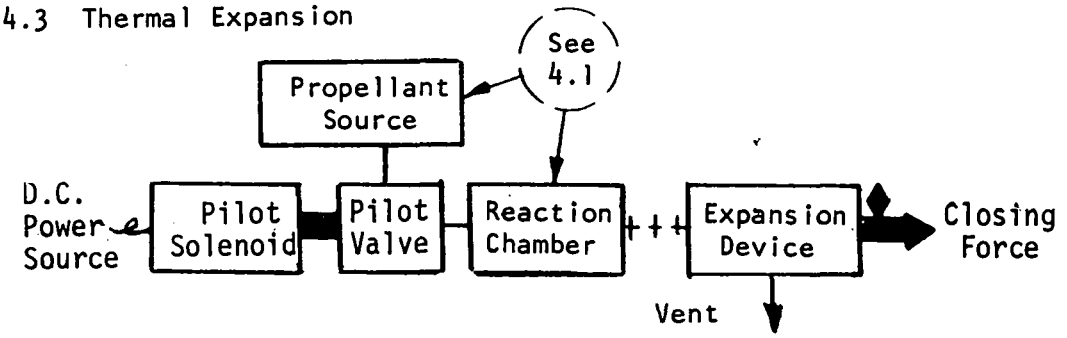

Concept 1.1 of Figure 4-2 is a direct linear electrical actuator of the solenoid or linear induction motor type. Both approaches offer simplicity and rapid response capability. However, both approaches tend to be heavy and also require greater electrical power than is available, which makes them unacceptable candidates. For example, the copper core alone for a flat-faced armature type of electromagnet designed for a 400 pound tractive force and a stroke of 0.075-inches would weigh 16.5 lb and draw in excess of 40 watts electrical power. (Reference 25)

The electric motor with planetary gear head plus a ball screw to convert the torque to linear force is a popular actuator concept. The D.C. motor version is shown as Concept 1.2 in Figure 4-2 and the A.C. motor plus inverter approach is shown as Concept 1.3. Both approaches generate high torque with low input power requirements and are straightforward designs. Figure 4-3 presents the torque-speed and torque current characteristics of both motor types. The start-up current for the permanent magnetic D.C. motor is generally 5 times (or greater) than the operating current which requires the addition of a current-limiting controller. Operation at cryogenic temperatures markedly lowers the coil resistance, which in a D.C. motor affects the start-up controllability as the coil field time constant is proportional to the ratio of the inductance to its resistance.

The utilization of a permanent magnet D.C. motor valve actuator, in either cryogenic or ambient temperature application, requires either that (1) the peak power limitation per valve be relayed to a value equal to sum of the power requirement of all the spacecraft propulsion system's isolation valves and the individual actuation commands then be sequenced to preclude power drain overlap or that (2) if the peak power limitation is considered to include start-up current drain the allowable motor size will be much smaller which, in turn, constrains the maximum force capability of the actuator. The start-up controllability of a D.C. motor at cryogenic temperatures can be markedly improved by specially fabricated higher resistance copper alloy coil windings, however, the motor now becomes functionally limited to operation only at cryogenic temperatures as checkout at room temperature will result in overheating.

Additionally, presence of the permanent magnet in the D.C. motor is undesirable because the influence on the spacecraft instruments. Further, the brush life problems inherent with this type of D.C. motor are also of concern. The use of a "Brushless" D.C. motor would eliminate the problem areas discussed above, however, a "Brushless" D.C. motor is generally less efficient than a comparable system composed of an A.C. motor and its D.C.-to-A.C. inverter. As the A.C. motor has minimal temperature sensitivity on operating characteristics it is characteristically employed in cryogenic applications and appears the more desirable approach.

The electrothermal actuator, Concept 1.4, offers high force potential in a simple design consisting of either a high expansion coefficient metal or a capsule of a high vapor pressure material. However, heat losses, which directly influence actuator efficiency, will be difficult to minimize. Also the concept appears marginal for other than pilot valve actuation. The thermally actuated pilot valve design submitted as part of Reference 2 provides a workable concept for the cryogenic application. An analysis given in Appendix D indicates at a 10-watt power level, operation can be achieved in less than 5 minutes with vacuum insulation and minimized conductive paths. Seating forces are high thereby minimizing potential leakage.

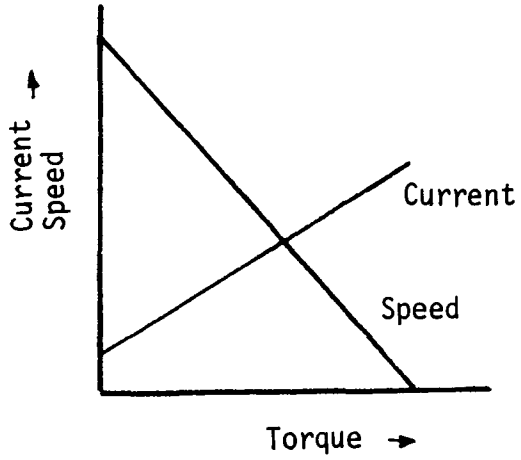

Permanent Magnet D.C. Motor

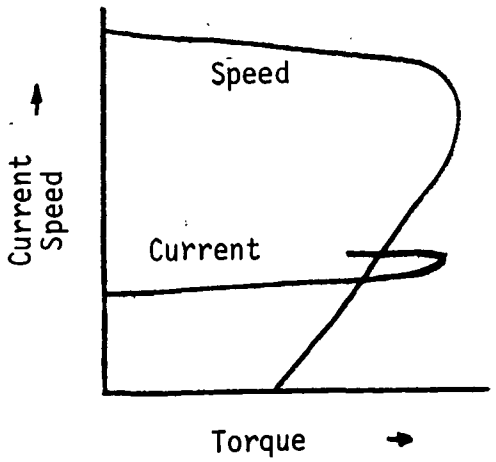

A.C. Induction Motor

Figure 4-3. Torque-speed curves for D.C. and A.C. Motors

The pilot valve pneumatic actuator configuration, Concept 2.1, offers a simple well proven design configuration with high response for a reasonable electrical power drain. However, the actuator gases must be vented overboard without generating undesirable torques on the spacecraft, which may prove difficult to achieve. More significantly, the potential for leakage through the pilot valve could result in impairing overall system operation which may require an isolation valve for the isolation valve actuator.

The pneumatic turbine, Concept 2.2, provides a high force output from a low pressure source. However, this approach is complex and introduces the problem of turbine bearing lubrication in addition to a more difficult problem in exhaust gas disposal relative to Concept 2.1 To quantify the gas disposal problem, consider the situation where a small turbine must develop a torque of 0.5 in-oz. at 120,000 rpm with an operating time of 2 minutes. The specific propellant consumption (SPC) for an infinite pressure ratio can be calculated from

$$\text{SPC}, \frac{\text{lb}}{\text{hp-hr}} = 1282 \left(\frac{\text{Molecular Weight}}{\text{T, °R}} \right) \left(1 - \frac{1}{\gamma} \right) \frac{1}{\eta_M \eta_{AD}}$$

Using a mechanical efficiency (η_M) of 20% and an adiabatic efficiency (η_{AD}) of 25%, the following SPC and required gas flows were obtained:

	SPC, lb/hp-hr	Quantity of Gas in 2 Minutes, lb.
Hydrazine Decomposition Products	30.8	.062
Helium Gas at 160°R	25.6	.052
Helium Gas at 530°R	77.4	.156

As can be seen, the quantity of gas to be dumped overboard without introducing spacecraft torque disturbances is considerable.

The hydraulic actuator approaches (Concepts 3.1 and 3.2) are analogous to the two pneumatic concepts discussed above. One advantage of the hydraulic approach is the possible capability for positive open and closed actuation. However, the disadvantages are quite severe: (1) extremely complex, (2) requires hydraulic source, (3) may require constant heater power to preclude freezing, and (4) requires a common hydraulic source for all isolation valves if the electrical power limit is to be met (with possible reliability compromise through this interdependency). Therefore, the hydraulic actuator approaches are unacceptable.

The chemical energy approaches (chemically generated gases for a pneumatic actuator, turbine drive, or a thermal expansion device) are shown as Concepts 4.1 through 4.3. All three approaches offer the potential for high force output with a reasonable electrical power consumption. However, as can be seen in the schematics of Figure 4-2, these concepts are extremely complex and add another potential propellant leakage situation. Because of the reduced chemical reaction rates at cryogenic temperatures, the concepts may be impractical. Further, if the chemical reactions do occur at cryogenic temperatures, the reaction products may freeze within the actuator mechanisms. Additionally, the disposal of the exhaust products poses a problem. In summary, the chemical energy approaches are very poor candidates.

4.3 Comparison of Electromechanical and Pneumatic Actuation

Table 4-2 presents the individual and composite scores for each of the eight performance/system interaction criteria discussed above, and Figure 4-4 presents the composite rating in a bar graph form. The length of the bar above the zero baseline gives the relative rating of each method. As can be seen in Figure 4-4 (or Table 4-2), there are two outstanding candidate approaches:

- A.C. Motor with gearhead and ball screw
- Pilot-operated pneumatic actuator

Because of the leakage potential of the pilot valve pneumatic configuration the electric motor approach is preferable as is shown by the ratings. However, the pneumatic actuator approach is more readily scalable to higher loads.

Figure 4-5 presents the system weight change per actuation in terms of actuator load and stroke for a helium pneumatic actuator. Also shown is the effective piston diameter versus load. For a given load and stroke combination, an energy value can be read from the figure which directly corresponds to a system weight change. The system weight includes the helium in the actuator, the helium required in the storage bottle required to permit withdrawal ($\sim$ 1.5 pounds stored per pound withdrawn), and the change in helium storage bottle weight. It should be noted that the system weight change between -300°F and +65°F conditions is quite small because the greater density of helium at -300°F is counterbalanced by the greater storable bottle weight at ambient temperature as shown below.

Temperature	Helium Density at 300 psia	Ratio Titanium Bottle + Contents per pound of helium at 4000 psia	Composite
-300°F	.68 lb/ft^3	4.0	
+ 65°F	.21 lb/ft^3	9.6	
Ratio: $\frac{\text{cold}}{\text{ambient}}$	3.24	.416	1.35

Table 4-2. Isolation Valve Actuator Ratings

Schematic Reference Numbers		Power Energy Reqmts	Thermal & Environmental Compatibility	Weight	State-of-the Art	Envelope	Input Signal & Complexity	Reliability Impact On Other Subsystems	Interface Complexity	Composite Rating
1.0	ELECTRICAL									
1.1	Linear (Solenoid or Induction Motor)	0	2	1	3	3	2	3	3	0
1.2	D.C. Motor) with ball screw and	2	1	2	3	2	1	3	3	12.7
1.3	A.C. Motor) gear head	2	2	2	3	2	2	3	3	45.5
	Torque or Stepping Motor	2	2	2	2	2	1	3	3	17.0
1.4	Thermal - Linear Expansion	1	2	2	1	2	2	3	3	9.0
	Thermal - Bulk Exp. or Vapor Press.	2	1	2	1	2	2	3	3	9.0
2.0	PNEUMATIC									
2.1	Linear (Bellows or Piston)	3	3	2	3	2	3	1	2	34.0
2.2	Turbine with Ball Screw & Gear Head	2	2	2	1	2	1	1	1	1.3
3.0	HYDRAULIC									
3.1	Linear (Bellows or Piston)	1	0	0	1	0	1	2	1	0
3.2	Fluid Motor	1	0	0	1	0	1	2	1	0
4.0	CHEMICAL (Gas Generator)									
4.1	Linear (Bellows or Piston)	3	1	2	1	2	3	2	1	4.8
4.2	Turbine	3	1	2	1	2	1	2	1	1.9
	CHEMICAL (Heat Source)									
4.3	Linear Expansion	3	1	2	1	2	2	2	1	3.4
	Bulk Expansion or Vapor Press.	3	1	2	1	2	2	2	1	3.4

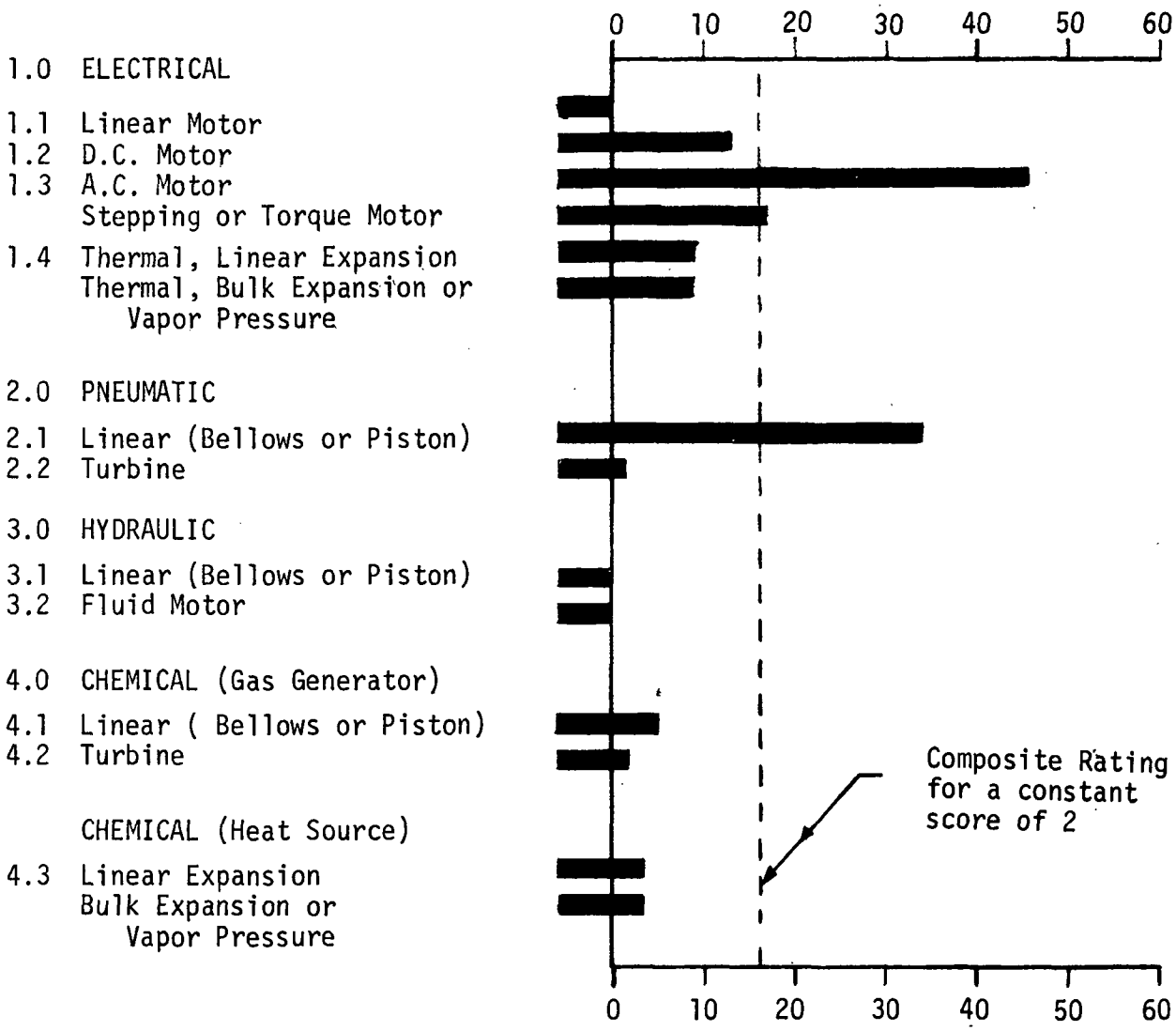

Figure 4-4. Isolation Valve Actuator
Composite Applicability Rating

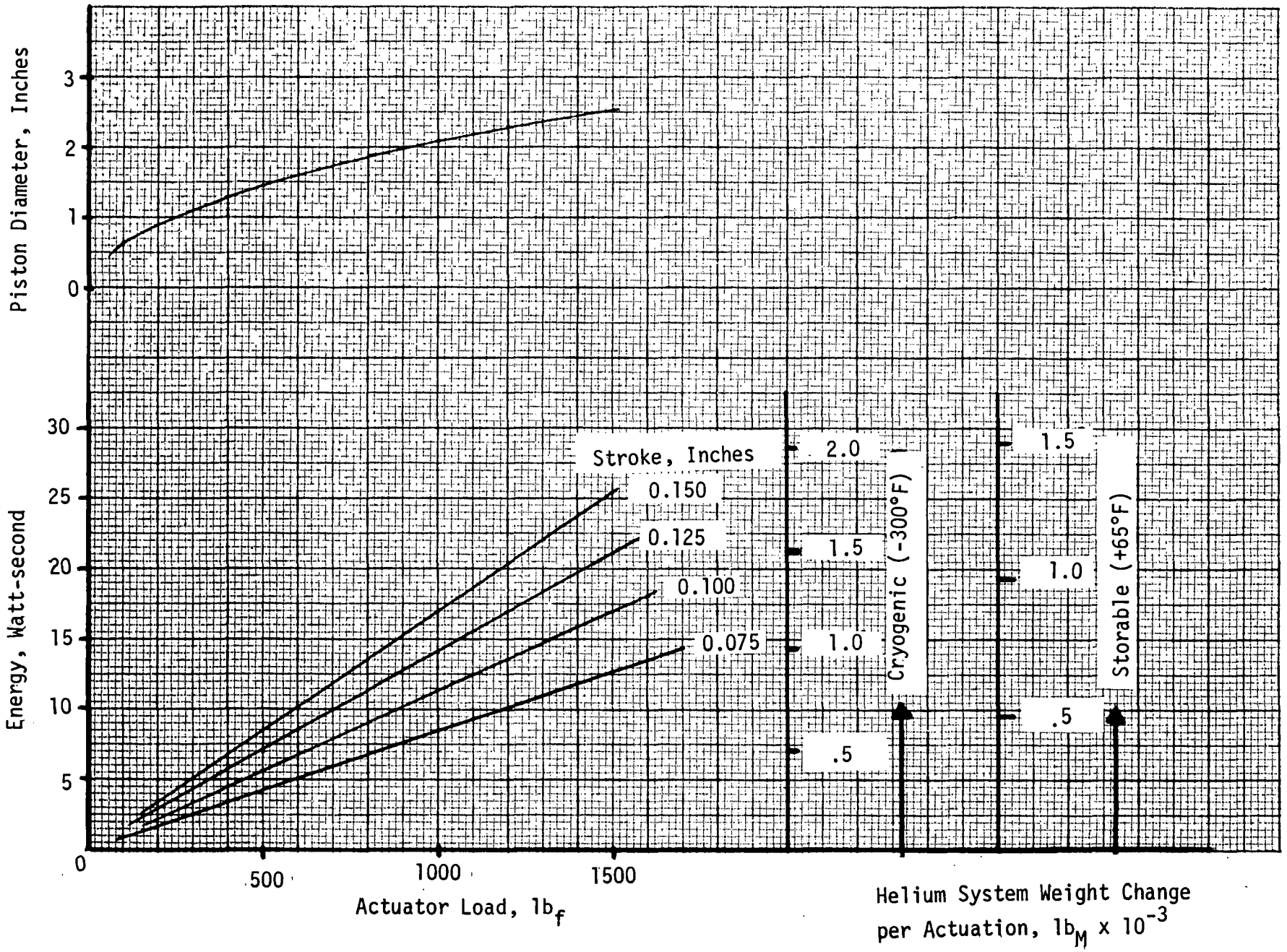

Figure 4-5. System Weight/Energy Requirements Helium Actuator at 300 psia

As shown in Figure 4-5, the change in actuator size and helium requirements with increasing load and/or stroke is readily scalable.

Figure 4-6 presents the ball screw input rpm in terms of A.C. motor power and actuator load and stroke. The A.C. motor is a 27 volt, 400 Hertz, one-phase induction motor turning at 21,000 rpm. The voltage-frequency selection provides the capability for high motor speed, high efficiency in the inverter, and minimizes RFI as low voltages are maintained. The inverter is a solid-state device consisting of power transistors excited by an oscillator circuit which fires alternately to develop a controlled cyclic current output from a direct current input. The approximate 90 percent efficiency of the ball screw is reflected in the ordinate torque values shown in Figure 4-6. The efficiency of the planetary gear head is a variable as the input speed to the ball screw is reduced to increase torque capability. The change of speed and torque shown in the right-hand side of Figure 4-6 represents the effects of gear head efficiency variation for commercially available gear heads for motors of this power level (see Table 4-3). Provided the ball screw input torque is 300 inch-ounces or less, satisfactory operation is obtainable at less than 10 watts. For higher torque values a larger (higher power) motor would be required to avoid the extreme torque-speed sensitivity shown in Figure 4-6 for torque values greater than 300 inch-ounces.

In summary, both an A.C. motor with gear head and ball screw and a pilot-operated pneumatic actuator appear as outstanding candidate actuator approaches. The electric motor approach is preferable because of the leakage potential of the pilot valve in the pneumatic actuator configuration.

Table 4-3.

Gear Head Characteristics

Used for A.C. Motor Actuator Parameter Study

(21,000 RPM Input)

Output Speed RPM	Torque Multiplier	Approximate Efficiency %
65	166	52
43	250	52
28	382	52
19	580	52
11	817	44
7.5	1,230	44
4.9	1,860	44
3.3	2,710	42
1.9	3,950	37
1.3	6,000	37
.86	9,000	37
.57	13,600	37

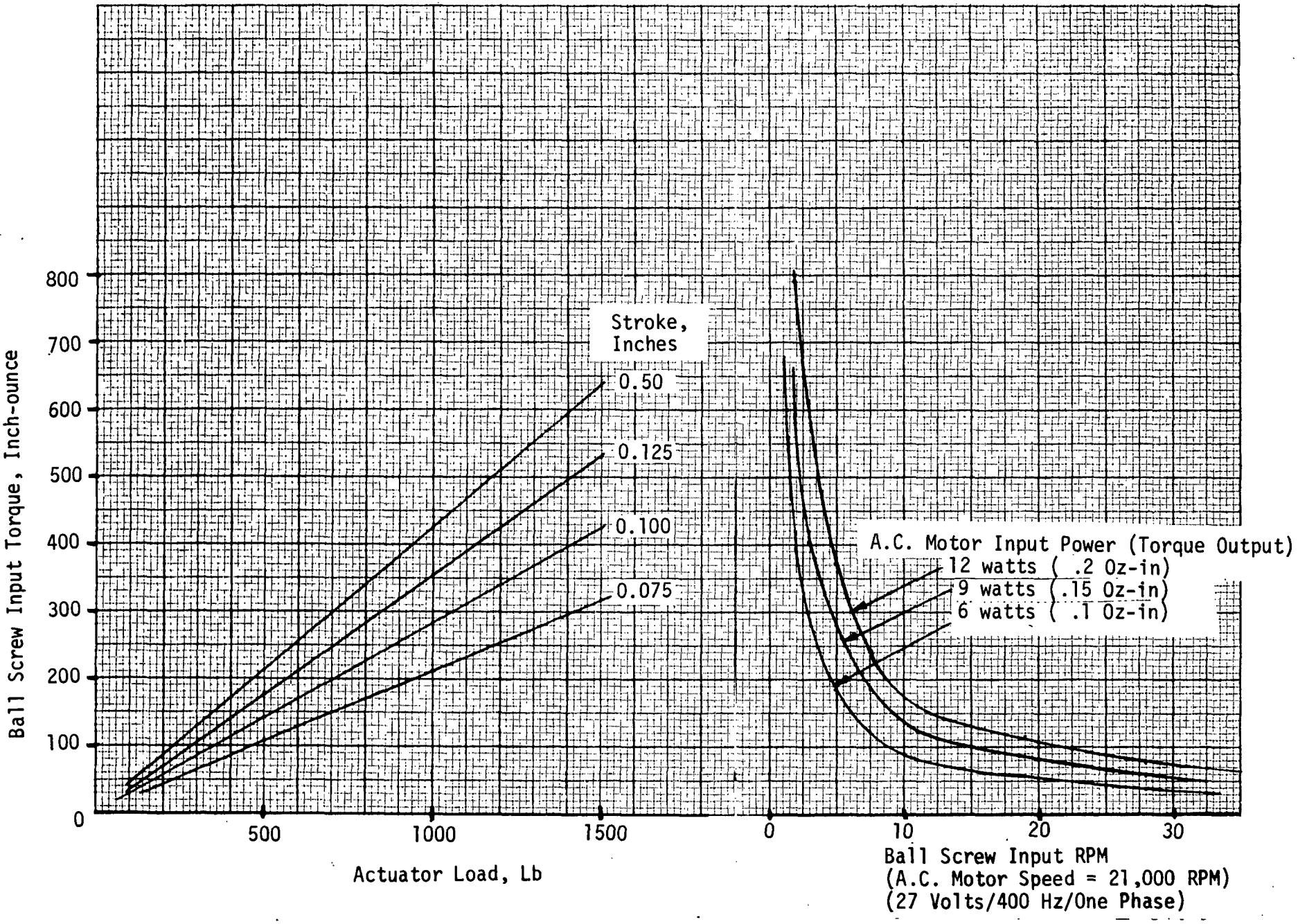

Figure 4-6. A.C. Motor, Gear Train, and Ball Screw Actuator Energy Requirements

5.0 SOFT-HARD, HARD-HARD POPPET SEAL ISOLATION VALVE DESIGN

5.1 Requirements

The propellant isolation valve described in this section was designed on the basis of application of a soft seal poppet mechanism utilizing a soft-hard and hard-hard redundant seating. A cross section of the design is provided in Figure 5-1. The design includes a pneumatic actuator featuring a thermally actuated pilot valve and a thermal latch functioning by fusion of a solder alloy.

The poppet seal design given in Figure 5-1 has been revised from the original configuration in response to recommendation of analysis subsequently conducted (Section 2.0) As a result of the analysis higher required actuating forces are estimated than were designed into the actuator shown. An increase in unit loading of the soft seal from 25,800 psi to 56,000 psi at cryogenic temperature was indicated. The design is described however to document the concepts involved. The design could potentially be scaled up to provide the necessary higher forces. An analysis of the actuating force predicated for the valve design given is provided in Appendix D.

The requirements for the Space Storable Propulsion Module demanding the greatest increase in the state-of-the-art for an isolation valve involves long term zero liquid leakage sealing of the reactive propellants primarily liquid fluorine or Flox. Usable materials are limited to metals or ceramets for propellant exposure. The basic requirements established for the valve design include:

Table 5-1. Design Requirements

Flowrate (LF_2)	1.039 lbm/sec
(Hydrazine)	0.561 "
(Flox)	1.187 "
(MMH)	0.456 "
Pressure drop (LF_2)	11.0 psid (including filter)
Connecting line size	.750 dia. tube
Inlet pressure (max)	400 psia
Propellant temperature range	-300 to 85°F
Internal leakage	zero as defined by JPL Technical Report 32-926

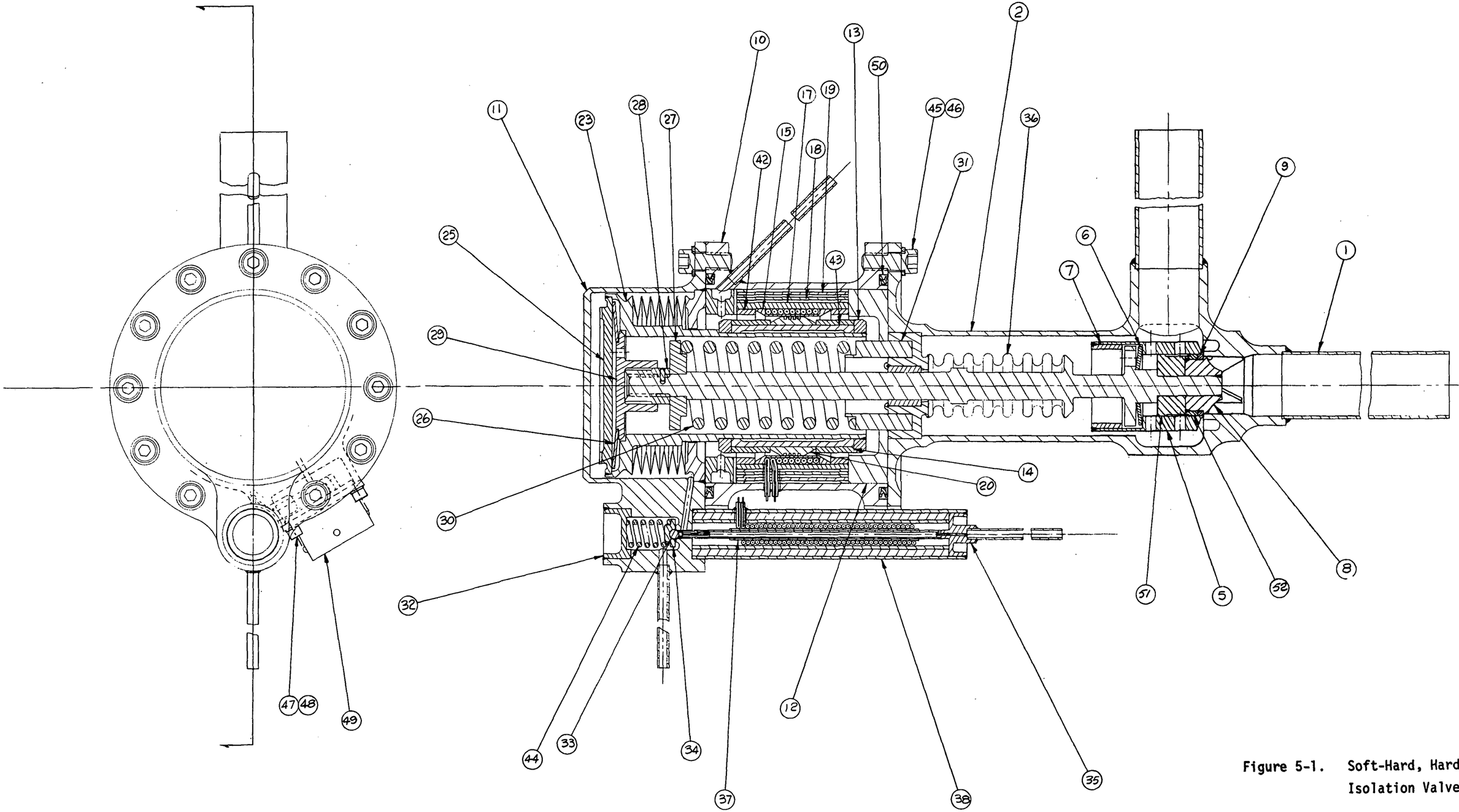

Figure 5-1. Soft-Hard, Hard-Hard Isolation Valve Design

Sterilization temperature	275°F
Flight actuations	30 approx. for 360 hours
Time in space	10 years
Actuation power limit	10 watts

These requirements as per the JPL Space Storable Module Feed System Design Requirements Document Ref. 26.

5.2 Design Approach

The valve seal concept utilized in the design Figure 5-1 applies a hard on hard metal seal with a soft on hard seal in series with it. Investigations conducted applying the hard on hard approach indicate the seal ability is limited by the finishes that can be maintained on the closing surfaces and to some extent the contact load imposed. At best, the requirement established for the isolation valve can barely be met by a hard seal interface. The surface degradation with reactive propellants plus the potential for particle contamination leaves little possibility of success for hard seats alone. A soft metal sealing material loaded above the compressive yield stress against a hard surface does offer the sealing ability required. Wear is the primary problem to be faced with the soft material. Larger wear particles are generated by both adhesive and rubbing wear with soft materials. The study cited by Reference 1 and further investigation documented in Section 2 of this report verifies the soft metal seal approach as having the greatest potential of achieving the low leakage desired.

A conventional poppet valve configuration was selected for the design. The use of a bellows shaft seal was established as the only feasible approach for the fluorine oxidizer application. A formed metal bellows is indicated for the valve shaft seal. The formed bellows offers a better choice over welded designs because of ease of cleaning the surfaces between convolutions and the greater inherent metallurgical integrity offered by a one piece design. These factors are especially important with use of fluorine propellant. The bellows has been sized to limit the hydraulic unbalance of the poppet.

The poppet shaft guidance is distributed between a finned support in the downstream seat bore and a plain sleeve bearing outside of the propellant environment. The maximum spacing of the guides with the poppet guiding immediately adjacent to the seat offers a maximum locating accuracy. A small amount of squareness error at the seat can be compensated by flexure bending of the shaft under seat loading. The narrow axial contact line of the finned guide provides an advantage over a sleeve design in the propellant environment in that a small amount of corrosion can be tolerated between surfaces without binding and can easily be sheared out and dissipated on actuation.

The Soft-Hard, Hard-Hard poppet seal concept was originated early in the effort in the configuration shown in Figure 3-1. As a result of the analysis discussed in Section 3.1.1 the configuration was revised to the form shown in Figure 3-2. This design is reflected in Figure 5-1.

5.3 Design Description

5.3.1 Poppet Assembly

The primary element of the overall valve design is the poppet seal mechanism. With reference to Figure 5-1, the assembly is made-up of a number of details designed to transmit the shaft load from the actuator to the hard-hard and then the soft-hard seating elements. The seat is an integral part of the housing (1). The outer sleeve (5) contacts the seat to form the hard-hard seal. The soft seal (9) confined between the outer sleeve and the inner plug (8) contacts the inner edge of the seat to provide the soft-hard seal. The Bellville spring (6) transmits a part of the shaft load (governed by the spring force) into the outer sleeve to load the hard surfaces. The remainder of the force is directly transmitted into the soft seal. The design characteristics of the valve are best described by Table 5-2. The sleeves (51) and (52) are provided for assembly of the soft seal onto the plug. The sleeve (52) acts as a retainer for the soft seal ring. The piece is welded to provide a seal at the inside diametral clearance. The potential leakage path at the inside diameter of the

Table 5-2. Valve Design Data

Port diameter (Equiv. orifice)	.6250 $\pm$ .0002 - Area .306 in^2
Soft seal interface width	.012 $\pm$ .0004
Soft seal perimeter (nominal)	2.000
Soft seal area	.024 in^2
Hard seal width	.015 $^{+\ .000}_{-\ .001}$
Hard seal area	.0311 in^2
Soft seal material	1060-0 Al
Hard seal material	Inconel 718 RC38-40
Seat material	Inconel 718 RC32-36
Soft seal finish	RMS 8
Hard seal finish	RMS 2
Seat finish	RMS 2
Soft seal load	1344 lbs
Soft seal unit load	56,000 psi
Hard seal load	50 lbs
Hard seal unit load	1600 psi
Stroke	.176 design - .156 min. opening
Pressure drop	Less than 1.0 psid at LF_2 flowrate of 1.039 lb/sec
Seal Bellows	
Material	Inconel 718
Outside diameter	.750
Effective area	.301 in^2
Wall	.0065 in^2
Max. rated pressure	492 psi
Spring rate	112 lbs/inch
Allowable travel	.192
Poppet Loading Belleville Spring	
Force at .020 deflection	51.5 lbs

soft seal is blocked. The sleeve (51) transmits the load from the seal retainer sleeve to the shaft.

The level of friction between the soft seal and the hard-hard seal element may exceed the 50 pound nominal Belleville spring force as shown by the Analysis, Appendix B. This is not a problem in that it is only necessary to force the outer sleeve back over the soft seal on the closing stroke. The actuating force must exceed that to break the static friction between them. On opening it is not necessary or desirable that the outer sleeve move on the soft seal. This mechanism allows the hard poppet seal to adjust to wear of the soft seal without unnecessary wear of the radial surface of the soft seal.

Materials usable in the fluorine stream must provide maximum compatibility with regard to surface corrosion. Prior evaluation in reference 1 established the range of potential materials. Inconel 718 has been selected for the structural parts of the assembly. Aluminum 1060 or 1100 is recommended for the seal combining excellent compatibility with both the oxidizers and fuels and favorable yield characteristics at cryogenic temperatures and normal temperatures. With the all-welded construction of the valve which is much to be favored for the fluorine application a common alloy is desirable to avoid inter-alloy welds. To achieve a favorable bearing at the finned poppet guide a different heat treat is assumed for each part. If necessary, a hard nickel plate can be used on the bearing portion of the valve bore. Rigid control of plating processes must be maintained however to obtain consistently good results in contact with the oxidizers.

5.3.2 Pneumatic Actuator

The valve actuator is a simple bellows seal single acting piston type designed for pressure closing of the valve and spring opening. The design shown will provide a net force output of 468 pounds utilizing a closing spring (30) of 100 pounds force in the closed position. Design characteristics are provided in Table 5-3.

Table 5-3. Actuator Design Data

Pneumatic Piston and Spring

Bellows effective area	2.27 in^2
Piston output force at 250 psi	568 lbs
Opening spring load (closed position)	100 lbs
Net actuator closing force	468 lbs
Preload Belleville spring Load at .020 deflection	550 lbs

Thermal Latch

Latched Lock Strength

Fused area	1.43 in^2
Solder shear yield strength	2000 psi
Allowable load	2860 lbs

Thermal Latch Power Requirement

Estimated on basis of 300°F temperature rise to fuse solder:

At 30% effeciency	2.0 watt hours are required
At a 5 watt input	24 minutes time required

Thermal Pilot Valve

Pilot Valve Poppet Loading

Load to raise seat unit loading to yield strength level of stainless steel (35,000 psi)	26 lbs

Pilot Actuator Stroke

For a temperature rise of 400°F, the actuator stroke	=	.008 inch

Pilot Actuator Power Requirement

Estimated on the basis of a 400°F temperature rise at 30°F efficiency .5 watt hours are required at a 5 watt input	=	5 minutes time required

A Belleville preload spring (26) has been incorporated in the design to assure a sustained load on the poppet. The spring acts in the load path between the latch and poppet. The small dimensional effects due to thermal changes over a period of time will be compensated with only a minor force change.

Pilot Valve

A thermally actuated three-way pilot valve incorporating a ball poppet is used to operate the actuator. The design is based upon expansion of a tubular element with an electrically applied temperature rise. The primary advantage of the design is that a high poppet seating force in the order of 35,000 psi can be achieved providing a high sealing capability within an electrical load limit of 10 watts.

The device consists of the expansion tube fastened to a jacket assembly at the right hand end. Expansion of the center tube with respect to the outer jacket causes motion of the left hand end of the tube to operate the valve. The expansion tube is surrounded by a close fitting tube which forms the inner wall of a vacuum jacket. This tube is surrounded by a metal sheathed heating element brazed to it. A radiation shield and multilayer vacuum insulation surround the heater assembly. The expansion tube incorporates a vent seat assembly at the tip with vent flow passing through the tube. The ball poppet is normally seated blocking the pressure supply to the actuator.

On expansion of the tube, the seat contacts the ball closing the vent port. As the tube continues to expand, the ball is raised off of the pressure seat and pressure is applied to the actuator. Upon cooling of the expansion tube the reverse process occurs. Design analysis is provided in Appendix E.

Thermal Latch

The fusion and solidification of a solder alloy is utilized for unlocking and locking of the latch. The inner latch sleeve (20) moves within a heated platten ring (15). The parts are tinned together. The sleeve is made of a brass alloy. Capillary action of the diametral clearances and circumferential grooves in the sleeve will keep the alloy in place when melted.

Ceramic insulation thermally isolates the heated elements to limit heat conduction into the surrounding metal. The outer housing jacket is evacuated to increase insulating qualities. A metal jacketed tubular heater is wrapped around the platten. Application of heat fuses the solder releasing the parts. Analysis indicates fusion can potentially be obtained for 60-40 solder (374°F liquidus) with 5 to 10 watts by limiting the material to be heated and by care in insulation selection and placement.

6.0 CONCLUSION

As a result of the Phase I effort a broad evaluation of sealing methods with potential for meeting the zero liquid leakage requirement was completed. Actuation methods capable of meeting valve operating requirements and compatible with the system configuration and mission environmental conditions have been established.

Results of the poppet seal study reveals the soft-hard metal sealing approach to provide the greatest potential for long term low leakage sealing with high reliability for limited closing cycles. The analysis has provided a guideline upon which to base design selection. The analysis indicates the desired zero-liquid leakage can be met with the soft metal approach providing unit seal loading is sufficiently high (2 to 3 times yield) and the propellant chemical effects on the seal surface do not adversely alter the soft seal function. A modified configuration of the Soft-Hard, Hard-Hard seal configuration conceived early in the program has been carried to a detailed prototype design stage.

Testing is ultimately required to verify seal performance in the propellants. It is recommended oxidizer testing of the valve poppet seal be initiated as early as possible. Due to the character of the mission the severest part of the propellant exposure (open time and cycling) can be demonstrated in a short time. Open time is likely not to exceed 200 hours in ten years with total mission cycles less than 30. Meaningful tests can be conducted in real times of that order. Static samples could be continuously exposed to determine effects of the closed configuration.

Ultimate selection of the soft and hard materials of the seal interface must be based on test. At the outset, aluminum offers an advantage in being relatively soft, compatible in all the propellants, and providing favorable cryogenic and cold work characteristics. Gold or copper could be used and may ultimately prove to be preferable.

Although a pneumatic actuator is provided as part of the prototype design, results of the actuator-trade-off study show the electromechanical approach to be ultimately the most favorable from both the component and system standpoint. The method is equally workable for both the propellants and for the helium isolation requirement. From the system standpoint electromechanical actuation requires only an electrical connection to the actuator. Both pneumatic lines and potential pilot valve leakage inherent with the pneumatic design are eliminated.

The electric motor and gearing are both feasible for long term exposure to the cryogenic and vacuum environment. An A.C. motor with an inverter or a brushless D.C. motor with attendant electronics are the primary candidates. Gear-motor combinations providing actuation forces in the order of 500 to 1500 pounds with input under 10 watts and actuating times of minutes are feasible.

For interim testing an inexpensive pneumatic actuator could be utilized capable of the design poppet forces. It is recommended the electromechanical actuating method be adopted for the ultimate flight system.

7.0 NEW TECHNOLOGY

1. Redundant Valve Poppet Seal Concept, Francis L. Merritt
   Included in Status Report No. 5, 22 February to 21 March 1971, reported 30 March 1971.

2. Thermally Actuated Valve, Francis L. Merritt
   Included in Status Report No. 13, 23 October to 22 November 1971, reported 31 October 1971. Concept first presented in assembly drawing submittal 19 March 1971.

3. Solid State Bonded Seal Multi-Cycle Valve, Richard J. Salvinski
   Concept noted in Status Report No. 25, 28 October to 24 November 1972. Concept described in Alternate Poppet Seal and Actuator Trade-off Study, TRW Report 72.4781.6-251, submitted 16 November 1972.

4. Bulk Energized Metal Seal, Richard J. Salvinski and Francis L. Merritt.
   Concept described in Alternate Poppet Seal and Actuator Trade-off Study, TRW Report 72.4781.6-251, submitted 16 November 1972.

5. Actuated Poppet Seal Concept, Francis L. Merritt and Richard J. Salvinski.
   Concept described in Alternate Poppet Seal and Actuator Trade-off Study, TRW Report 72.4781.6-251, submitted 16 November 1972.

8.0 REFERENCES

1. Detailed Evaluation Report-Development of a Space Storable Propellant Isolation Valve. JPL Contract 953029, TRW Report No. 71-4781.6-180, 4 October 1971.

2. Pneumothermal Actuated Propellant Isolation Valve Design Package JPL Contract 953029, 15 February 1972.

3. Study of Advanced Techniques for Determining the Long Term Performance of Components. NASA Contract NAS 7-782 TRW Report No. 168-68-6014-R000, March 1972.

4. Fluorine System Handbook. Douglas Missile and Space Systems Division, Contract NAS W-1351, Report NASA CR 72064, 1 July 1967.

5. E. Rabinowicz, Compatibility Criteria for Sliding Materials, presented at the 1966 ASME Spring Lubrication Symposium, June 6-8, New Orleans, La.

6. E. Rabinowicz, Friction and Wear of Materials, John Wiley and Son, New York, New York, 1965.

7. Advanced Spacecraft Valve Technology Compilation, Volume I Mechanical Controls, Report No. 12411-6012-R000, TRW Systems. Contract NAS 7-717, July 1970.

8. F. Merritt, L. Dumont, et. al., Wide Range Flow Control Program. TRW Systems Technical Report AFRPL-TR-68-32, December 1968.

9. H. D. Samuel, Liquid Fluorine Shutoff Valve Development Program. McDonnell Douglas Astronautic Co., TR No. AFRPL-TR-69-41, April 1969.

10. R. L. Crozier, Space Storable Oxidizer Valve. Aerojet Liquid Rocket Co., NASA CR-72691, 31 August 1971.

11. G. R. Pfeifer, Advanced ACS Valve Sealing Surface Compatibility Investigation. The Marquardt Co., AFRPL-TR-71-84, September 1971.

12. P. Bauer, Investigation of Leakage and Sealing Parameters, ITT Research Institute, Technical Report AFRPL-TR-65-153, August 1965.

13. F. O. Rathbun, Jr., Design Criteria for Zero-Leakage Connectors for Launch Vehicles. Volume 3 Sealing Action at the Seal Interface, General Electric Co., Contract NAS 8-4012, March 15, 1963.

14. J. P. Laniewski, Design Criteria for Zero-Leakage Connectors for Launch Vehicles, General Electric Co., Contract NAS 8-4012, 20 July 1967.

15. Paul Bauer, et. al., Analytical Techniques for Design of Seals for Use in Rocket Propulsion Systems, Volume I Static Seals. IITRI, Technical Report AFRPL-TR-65-61, May 1965.

16. F. O. Rathbun, Jr., Design Criteria for Zero-Leakage Connectors for Launch Vehicles. Fundamental Seal Interface Studies and Design Testing of Tube and Duct Separable Connectors. General Electric Co., Contract NAS 8-4012, June 1, 1964.

17. AD809182, Aerospace Fluid Component Designers Handbook, Volume I, March 1967.

18. Thomsen, et. al., Mechanics of Plastic Deformation in Metal Processing, MacMillan, 1965.

19. Faupel, J. H., Engineering Design, Wiley, New York, 1964.

20 G. F. Tellier, J. W. Lewellen; Poppet and Seat Design Criteria for Contaminant Particle Resistance. Rocketdyne Division of North American Rockwell, Report AFRPL-TR-70-1, April 1970.

21. G. F. Tellier, T. R. Spring; Contaminant Particles in Metal-to-Metal Closures. Rocketdyne Division of North American Rockwell, Report AFRPL-TR=71-112, December 1971.

22. D. H. Buckley, Friction Wear and Lubrication in Vacuum, NASA SP-277

23. M. E. Campbell, Solid Lubricants - A Survey. NASA SP-5057 (01)

24. H. J. McCracken, Welding Handbook, CH ed Section 38, American Welding Society.

25. C. Rotens, Electromagnetic Devices.

26. Space Storable Propulsion Module Feed System Design Requirements, JPL Document 71X09500 dated 9-71.

27. Alternate Poppet Seal and Actuator Trade-off Study, TRW Report No. 72.4781.6-251 dated 16 November 1972.

28. Cryogenic Material Data Handbook, Volume I, Air Force Materials Lab, Report No. ML-TDR-64-260, August 1964.

9.0 APPENDICES

Appendix A
Leakage Test Data for Cycled Soft Gasket
(From General Electric Report, Reference 13)

5.3 Design Testing

The purpose of the tests was to determine whether the welded knife-edge connector met the design requirements. It was therefore necessary to duplicate the environmental conditions, pressurize the connector and measure the leakage. The design requirements are described in Sec. 5.1, the test equipment is described in Sec. 5.4.2 and the test procedure and results are described in this section.

5.3.1 Preliminary Tests

The performance of the connector depends upon the preload put in at assembly. Because the calculation of the preload from the torque applied to the nut is inaccurate the nut was calibrated. A set of strain gages was mounted on opposite flats of the nut and wired to read only pure axial strain. Then the nut was loaded in a universal testing machine in a manner that duplicates the nut loading in the connector. The strain versus load reading gave a straight line calibration curve. Then with the use of this curve it was possible to accurately set the preload during assembly by measuring the strain in the nut.

Another test which should have been performed before the other connector tests, but was not, was an assembly test to determine if the flanged-section actually seats on the union. Because of the low yield stress of annealed copper and the high preload it was assumed that the flanged-section would seat on the union during assembly. However, the annealed copper raw material was not as soft as expected and during the sequence of tests run it became questionable whether the flanged-section did seat on the union. Therefore, the flanged-section was coated with a bluing compound and the connector was assembled with an increasing sequence of preloads. The results showed that the flanged-section did not seat on the union at assembly and probably not at anytime during the tests.

Therefore, the tests did not take full advantage of the independent load path built into the connector. If the flanged-section had seated on the union and created the independent load path the seal would have been less sensitive to externally applied loads. This would have meant a lower level of leakage, but as there was no measurable leakage in most of the tests the improved sealing could not have been measured. Therefore, the results of the leakage testing would have changed very little.

The results of the test to determine seating does indicate a need for a softer gasket, smaller included angle on the knife-edge, less depth of cut of the knife-edge prior to seating of the flanged-section on the union, and a containment of the gasket that does not interfere with the seating of the flanged-section. These changes to the sealing area of the connector should be made and tested before the connector design is considered final.

5.3.2 Room Temperature Test

5.3.2.1 Test Procedure

This test was performed at room temperature. The connector was assembled with a preload of 2300 lb. Leakage readings were taken at each of a sequence of internal pressure and external moment settings.

5.3.2.2 Test Results

The test pressure, moment settings, and leakage readings are tabulated below:

Helium Pressure Psig	Transverse Moment Inch lb	Helium Leakage atm cc/sec
0	0	n.m.*
300	0	n.m.
600	0	n.m.
910	0	n.m.
1190	0	n.m.
1500	0	n.m.
475	0	n.m.
475	150	n.m.
475	300	n.m.
475	450	n.m.
1000	0	n.m.
1000	150	n.m.
1000	300	n.m.
1000	450	n.m.
1500	0	n.m.
1500	150	n.m.
1500	300	n.m.
1500	450	n.m.

*n.m. - none measurable.

The sensitivity of the mass spectrometer leak detector varied due to the cleanliness of the vacuum system and other factors. Therefore, it is only possible to say that there was no measurable leakage and to state the level of leakage which was measurable. It can then be concluded that if there was any leakage

it was below this measurable level. The level of leakage measurable was determined by placing a sequence of known leaks in the system and measuring the leakage.

n.m. for this test was below 9×10^{-7} atm cc/sec.

5.3.3 Reassembly Test

5.3.3.1 Test Procedure

This sequence of tests was run at room temperature. A new gasket was installed in the connector and tested for leakage at internal pressure to 1500 psig and external moments to 450 inch lb. The connector was then disassembled, the gasket was removed and remounted on the connector, the connector was reassembled, and the connector was tested for leakage as before. In this way a total of six tests were run using the same gasket.

5.3.3.2 Test Results

For each test the gasket orientation, preload, test points and leakage are tabulated.

5.3.3.2.1 First Test - New Gasket

Preload = 2300 lb

Helium Pressure Psig	Transverse Moment Inch lb	Helium Leakage atm cc/sec
0	0	n.m.
310	0	n.m.
600	0	n.m.
900	0	n.m.
1200	0	n.m.
1500	0	n.m.
1500	150	n.m.
1500	300	n.m.
1500	450	n.m.

n.m. $< 3 \times 10^{-6}$ atm cc/sec.

5.3.3.2.2 First Reassembly

Gasket removed and remounted backwards and rotated 90°.

Preload = 2200 lb.

Helium Pressure Psig	Transverse Moment Inch lb	Helium Leakage atm cc/sec
0	0	n.m.
300	0	n.m.
600	0	n.m.
900	0	n.m.
1210	0	n.m.
1500	0	n.m.
1500	150	n.m.
1500	300	n.m.
1500	450	n.m.

n.m. $< 9 \times 10^{-7}$ atm cc/sec

5.3.3.2.3 Second Reassembly

Gasket rotated 90° clockwise.

Preload = 2200 lb.

Helium Pressure Psig	Transverse Moment Inch lb	Helium Leakage atm cc/sec
0	0	n.m.
310	0	n.m.
600	0	n.m.
900	0	n.m.
1200	0	n.m.
1500	0	n.m.
1500	150	n.m.
1500	300	n.m.
1500	450	3×10^{-4}

n.m. $< 3 \times 10^{-6}$ atm cc/sec

5.3.3.2.4 Third Reassembly

Gasket rotated 90° clockwise.

Preload = 2200 lb.

Helium Pressure Psig	Transverse Moment Inch lb	Helium Leakage atm cc/sec
0	0	n.m.
310	0	n.m.
610	0	n.m.
900	0	n.m.
1200	0	n.m.
1500	0	2×10^{-5}
1500	150	5×10^{-4}
1500	300	$> 1 \times 10^{-2}$
1500	450	not attempted

n.m. $< 3 \times 10^{-6}$ atm cc/sec

5.3.3.2.5 Fourth Reassembly

Gasket removed and remounted backwards.

Preload = 2200 lb.

Helium Pressure Psig	Transverse Moment Inch lb	Helium Leakage atm cc/sec
0	0	n.m.
300	0	n.m.
600	0	n.m.
900	0	n.m.
1200	0	n.m.
1500	0	n.m.
1500	150	n.m.
1500	300	n.m.
1500	450	n.m.

n.m. $< 3 \times 10^{-6}$ atm cc/sec

5.3.3.2.6 Fifth Reassembly

Gasket rotated 180°.

Preload = 2200 lb.

Helium Pressure Psig	Transverse Moment Inch lb	Helium Leakage atm cc/sec
0	0	n.m.
300	0	n.m.
610	0	n.m.
900	0	n.m.
1200	0	n.m.
1500	0	2×10^{-4}
1500	150	6×10^{-4}
1500	300	4×10^{-3}
1500	450	$>8 \times 10^{-3}$

n.m. $< 3 \times 10^{-6}$ atm cc/sec

5.3.4 Extended Time Test

5.3.4.1 Test Procedure

This test was run at room temperature. The connector was assembled with a preload of 2200 lb. The connector was pressurized to 1500 psig of helium and loaded with an external moment of 450 inch lb. Then leakage readings were taken periodically for 72 hours.

5.3.4.2 Test Results

Time Since First Reading Hours	Helium Leakage atm cc/sec
0:00	n.m. ($< 3 \times 10^{-6}$)
0:15	"
0:30	"
1:00	"
1:30	"
2:30	"
3:30	"
4:30	"

(continued on following page)

Time Since First Reading Hours	Helium Leakage atm cc/sec
(continued)	
5:30	n.m.
6:30	"
9:50	n.m. ($< 4 \times 10^{-5}$)
25:05	n.m. ($< 4 \times 10^{-5}$)
35:35	n.m. ($< 1 \times 10^{-5}$)
51:15	n.m. ($< 4 \times 10^{-5}$)
72:00	n.m. ($< 1 \times 10^{-5}$)

5.3.5 High Temperature Test

5.3.5.1 Test Procedure

The connector was assembled with a preload of 2200 lb. The connector was then heated to 500°F with no internal pressure or external moment applied. When the connector was at temperature the leakage was measured at a sequence of internal pressures and external moment settings.

5.3.5.2 Test Results

Helium Pressure Psig	Transverse Moment Inch lb	Connector Temperature °F	Helium Leakage atm cc/sec
0	0	510	n.m.
300	0	510	n.m.
600	0	510	n.m.
900	0	500	n.m.
1200	0	500	n.m.
1500	0	500	n.m.
500	0	500	n.m
500	150	490	n.m.
500	300	490	n.m.
500	450	490	n.m.
1000	0	490	n.m.
1000	150	490	n.m.
1000	300	500	n.m.
1000	450	500	n.m.
1500	0	500	n.m.
1500	150	500	n.m.
1500	300	500	n.m.
1500	450	500	n.m.*
1500	500	490	8×10^{-5}

n.m. $< 2 \times 10^{-6}$ atm cc/sec

* At this point there was a momentary leak which closed-up before it could be read. Therefore, the moment was increased above the design requirement and the next test point was taken.

5.3.6 Low Temperature Test

5.3.6.1 Test Procedure

The connector was assembled with a preload of 2300 lb. The connector was then cooled to -300°F with no internal pressure or external moment applied. When the connector was at temperature the leakage was measured at a sequence of internal pressures and external moment settings.

5.3.6.2 Test Results

Helium Pressure Psig	Transverse Moment Inch lb	Connector Temperature °F	Helium Leakage atm cc/sec
0	0	-300	n.m.
300	0	-300	n.m.
600	0	-300	n.m.
900	0	-300	n.m.
1220	0	-300	n.m.
1500	0	-300	n.m.
500	0	-300	n.m.
490	150	-300	n.m.
1020	150	-300	n.m.
1500	150	-300	n.m.
500	300	-300	n.m.
1000	300	-300	n.m.
1500	300	-300	n.m.
520	450	-300	n.m.
1000	450	-300	n.m.
1500	450	-300	n.m.

n.m. $< 6 \times 10^{-6}$ atm cc/sec

APPENDIX B

SOFT-HARD, HARD-HARD REDUNDANT SEAL DESIGN ANALYSIS

EXTRUSION CONCEPT POINT DESIGN STRESS ANALYSIS

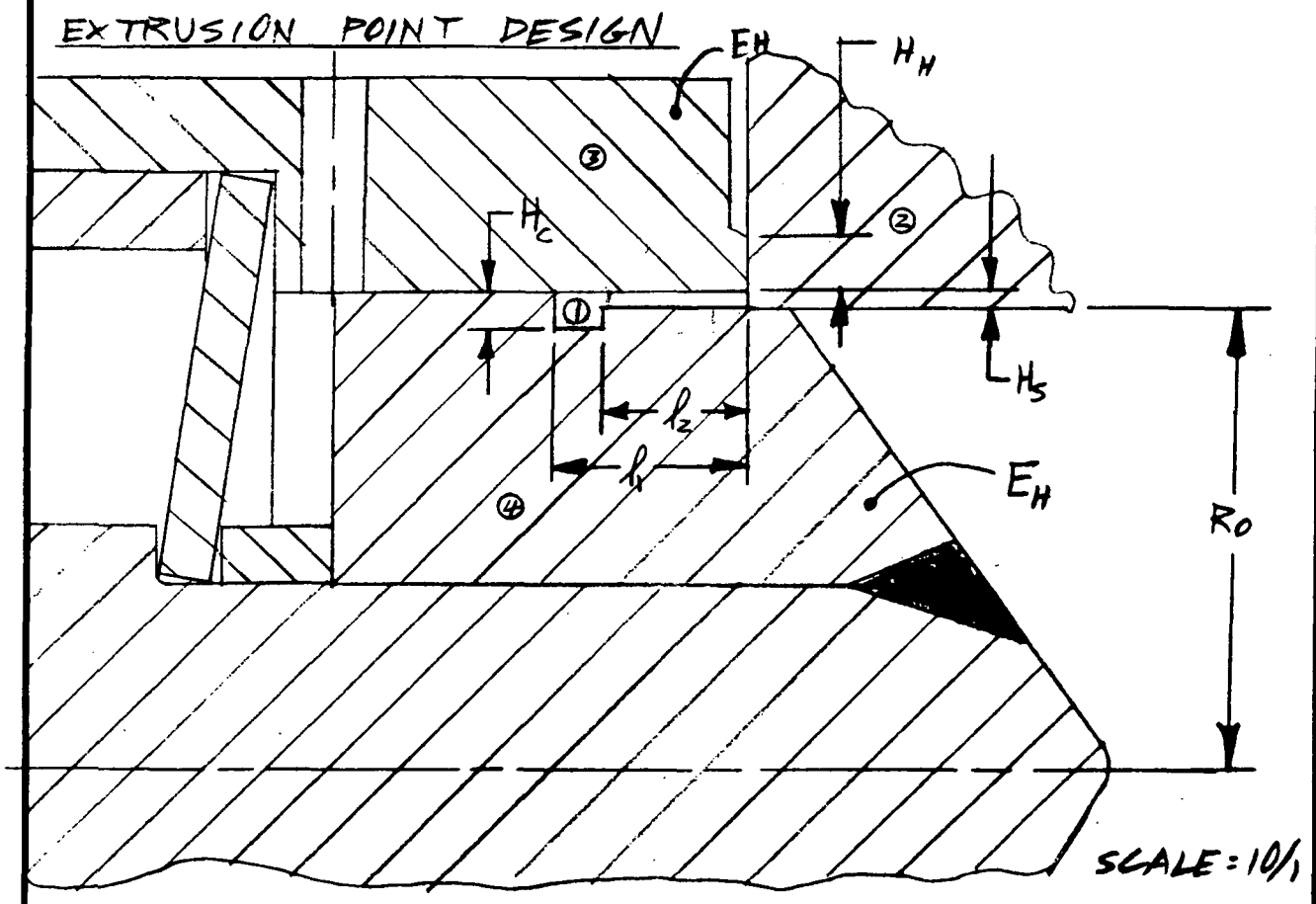

AT THIS POINT OF THE DESIGN, MANY DIMENSIONS COULD BE CHANGED IF ADVANTAGE IS FOUND IN DOING SO, BUT AS STARTING POINTS, ASSUME:

SOFT MATERIAL = 1100-0 ALUM.

HARD MATERIAL = INCO-718 (AMS 5664, BAR STOCK)

R_O = 0.250 IN

H_S = 0.012 IN

H_G = 0.030 IN

H_H = 0.015 IN

ℓ_1 = 0.156 IN

EXTRUSION CONCEPT

EXTRUSION POINT DESIGN

ACTUATOR FORCE BUDGET

TOTAL ACTUATOR FORCE = $(3.06\ IN^2)(250\ PSI)$
= 765 LB.

LET FORCE TO DEFLECT BELLOWS =	122 LB
" " " OPENING SPRING =	100 LB
" " SEAT HARD/HARD SEAL =	50 LB
" " " SOFT/HARD SEAL =	493 LB
TOTAL =	765 LB.

SOFT SEAT AREA
$= 3.14(.262^2 - .250^2) = 0.01915\ IN^2$

HARD SEAT AREA
$= 3.14(.277^2 - .262^2) = 0.0254\ IN^2$

SOFT SEAT CONTACT STRESS
$= \frac{493\ LB}{0.01915\ IN^2} = 25,800\ PSI.$

HARD SEAT CONTACT STRESS
$= \frac{50\ LB}{0.0254\ IN^2} = 1,970\ PSI.$

MECHANICAL PROPERTIES OF 1100 ALUM. @ FLOX STORAGE TEMP: (-300°F)

F_{CY} = 6,000 TO 8,000 PSI (ANNEALED)

F_{CY} = 15,000 TO 20,000 PSI (WORK HARDENED)

$E = 12.3 \times 10^6$ PSI $\qquad \nu = 0.33$

$F_{TU} = 18,200$ PSI. $\qquad F_{SU} \cong 10,900$ PSI.

EXTRUSION CONCEPT

EXTRUSION POINT DESIGN

THE DESIGN WILL BE EVALUATED FIRST WITH THE GENERAL DESIGN CURVES:

ASSUMING THE WORK HARDENED $F_{cy} \cong 15{,}000$ psi.

$$\frac{f}{F_{cy}} = \frac{25{,}800 \text{ psi}}{15{,}000 \text{ psi}} = 1.72$$

FROM FIGURE 1, REDUCTION OF SURFACE ASPERITY HEIGHT = 46% OF $h_{NO\ LOAD}$ (COINING) A LEAKAGE ANALYSIS WOULD INDICATE IF THIS IS ACCEPTABLE. A HIGHER CONTACT STRESS WOULD SEEM DESIREABLE, BUT H_s IS ALREADY TINY.

WITH REGARD TO THE GAP BETWEEN ① & ② FROM FIGURE 6 at $f/F_y = 1.72$: $H_G/H_s = 0.225$

$$H_{GAP} = 0.225\,(0.012 \text{ IN}) = 0.0027 \text{ IN.}$$

THEREFORE THE SHARPNESS OF THE EDGE RADIUS ON BODY ② MUST BE CONTROLED CAREFULLY.

FROM FIGURE 3, THIS DESIGN COULD ONLY INDENT WEAR PARTICLES A SHORT DISTANCE INTO SOFT SEALING INTERFACE.

EXTRUSION CONCEPT

FLEXIBILITY AND STRESS IN HARD WALLS

MECHANICAL PROPERTIES OF INCONEL-718:

(REF. MIL-HDBK-5B, SECTION 6.3.5)

ROOM TEMPERATURE (70°F)

$\alpha = 6.4 \times 10^{-6}$ IN/IN/°F

$F_{TU} = 180,000$

$F_{TY} = 150,000$

$e = 10\%$

$E = 29.0 \times 10^6$ psi.

$\nu \cong 0.30$

CRYOGENIC TEMPERATURE (-300°F) (AERO. STRUCTURAL METALS HANDBOOK)

$F_{TU} = 180,000 (1.16) = 209,000$ psi

$F_{TY} = 150,000 (1.17) = 175,500$ psi.

$E = 29.0 (1.10) = 32.0 \times 10^6$ psi.

FLEXIBILITY AND STRESS IN HARD WALLS

INSIDE WALL:

NEGLECTING THE RESTRAINT OF THE UNLOADED PORTION OF BODY (3), LAMÉS FORMULAS FOR THICK WALLED CYLINDERS CAN BE USED:

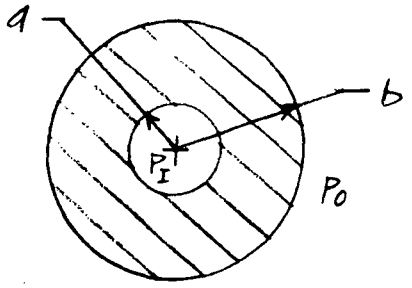

(SEE TIMOSHENKO, STRENGTH OF MATERIALS, SEC. 40)

$P_o = 25{,}800$ psi, $P_I = 0$ psi.

$a = 0$ IN, $b = 0.250$ IN., $\nu = 0.3$

$$(\delta_R)_b = -\frac{b P_o}{E_H}\left(\frac{a^2+b^2}{b^2-a^2} - \nu_H\right) = \frac{-(.25)(25{,}800)}{32\times10^6}\left[1-0.3\right]$$

$$= -0.141\times10^{-3} = -0.000141 \text{ IN (INWARD)}$$

$$\text{FLEXIBILITY} = C_3 = \frac{141\times10^{-6}\text{ IN}}{25{,}800\text{ psi}} = 5.46\times10^{-9}\ \frac{\text{IN}}{\text{psi.}}$$

ELASTIC STRESSES at $r=b$:

$$f_r = \frac{-P_o b^2}{b^2-a^2}\left(1-\frac{a^2}{r^2}\right) = -P_o = -25{,}800 \text{ psi.}$$

$$f_T = \frac{-P_o b^2}{b^2-a^2}\left(1+\frac{a^2}{r^2}\right) = -P_o = -25{,}800 \text{ psi.}$$

MARGINS AT 75°F:

$$(M.S.)_Y = \frac{150{,}000}{1.0\,(25{,}800)} - 1 = \underline{+4.81}$$

$$(M.S.)_{ULT} = \frac{180{,}000}{1.5\,(25{,}800)} - 1 = \underline{+3.65}$$

EXTRUSION CONCEPT

FLEXIBILITY AND STRESS IN HARD WALLS

OUTSIDE WALL:

$P_o = 0$ psi, $P_I = 25{,}800$ psi.

$a = .250 + .012 = 0.262$, $b = .262 + .115 = .377$ in.

$$(\delta_R)_{r=a} = \frac{+aP_I}{E_H}\left(\frac{a^2+b^2}{b^2-a^2} + \gamma_H\right) = \frac{(.262)(25{,}800)}{32\times10^6}\left[\frac{.142+.0686}{.142-.0686} + .3\right]$$

$$= 0.670\times10^{-3} = 0.000670 \text{ in (outward)}$$

$$\text{FLEXIBILITY} = C_4 = \frac{670\times10^{-6} \text{ in}}{25{,}800 \text{ psi}} = 25.9\times10^{-9}\ \frac{\text{in}}{\text{psi}}$$

STRESSES AT $r = a$: (HIGHEST STRESS UNTIL YIELD)

$$f_r = \frac{a^2P_I}{b^2-a^2}\left(1-\frac{b^2}{r^2}\right) = \frac{.0686(25{,}800)}{.142-.0686}\left[1-\frac{.142}{.0686}\right]$$

$$= 24{,}200(-1.07) = -25{,}900 \text{ psi.}$$

$$f_T = \frac{a^2P_I}{b^2-a^2}\left(1+\frac{b^2}{r^2}\right) = 24{,}200(+3.07) = +74{,}300 \text{ psi.}$$

SINCE COMBINED TENSION - COMPRESSION, FIND DISTORSION ENERGY EQUIVALENT STRESS:

$$f_E = \frac{1}{\sqrt{2}}\sqrt{f_r^2 + (f_T - f_r)^2 + f_T^2}$$

$$= \frac{1}{1.414}\left[670 + 10{,}040 + 5{,}510\right]^{1/2} = \frac{127{,}500}{1.414}$$

$$= 90{,}100 \text{ psi.}$$

EXTRUSION CONCEPT

FLEXIBILITY AND STRESS IN HARD WALLS

MARGINS AT 75°F:

$$(M.S.)_Y = \frac{150{,}000}{1.0\,(90{,}100)} - 1 = \underline{+0.66}$$

$$(M.S.)_U = \frac{180{,}000}{1.5\,(90{,}100)} - 1 = \underline{+0.33}$$

CHECK HOW MUCH OUTER WALL DEFLECTION COULD BE REDUCED IF MADE MUCH THICKER:

$$(\delta_R) = \frac{9PI}{E_H}\left[\frac{1+\frac{a^2}{b^2}}{1-\frac{a^2}{b^2}} + \nu_H\right] = \frac{.262\,(25{,}800)}{32\times10^6}(1.3)$$

$$= 0.274\times10^{-3} = 0.000274$$

$$\text{FLEXIBILITY} = \frac{274\times10^{-6}}{25{,}800} = 10.6\times10^{-9}\ \frac{IN}{PSI}$$

∴ FACTOR OF 2.5 IMPROVEMENT IS POSSIBLE.

EXTRUSION CONCEPT

FLEXIBILITY AND STRESS IN SOFT SEAL

NEGLECTING INITIAL GAPS, THE SOFT MATERIAL WILL PLASTICALLY FLOW ONLY TO THE EXTENT THAT THE HARD CONFINING WALLS DEFLECT. CONSIDER AN ELEMENT OF THE SOFT MATERIAL ORIENTED TO THE AXIAL, TANGENTIAL & RADIAL DIRECTIONS:

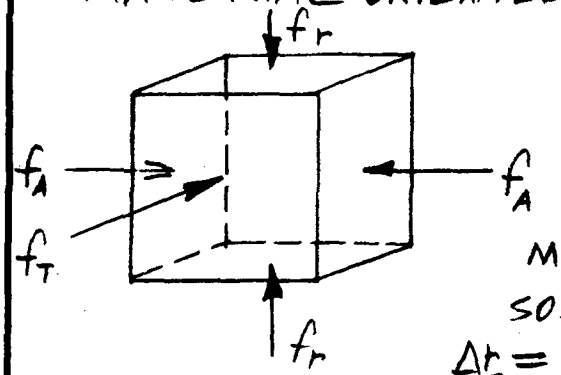

(FIRST ASSUME HYDROSTATIC BEHAVIOR & USE DEFLECTIONS TO FIND PLASTIC FLOW)

MEAN DEFLECTION OF THE SOFT MATERIAL @

$$\Delta r_s = \frac{1}{2} f_r (C_3 - C_4)$$

$$\epsilon_T = \frac{2\pi \Delta r_s}{2\pi \bar{r}_s} = \frac{1}{2} \frac{f_r}{\bar{r}_s} (C_3 - C_4) = -39.8 \times 10^{-9} f_r \left(\frac{IN}{IN}\right)$$

$$\epsilon_r = \frac{\Delta H_s}{H_s} = \frac{f_r (C_3 + C_4)}{H_s} = -2620 \times 10^{-9} f_r \left(\frac{IN}{IN}\right)$$

ALSO, THE VALUE OF $f_A = -25{,}800$ PSI IS KNOWN

IF THE SOFT MATERIAL STAYS ELASTIC THE SYSTEM IS SOLVABLE EASILY:

$$\epsilon_A = \frac{1}{E}\left[f_A - \nu (f_r + f_T)\right] \quad (1)$$

$$\epsilon_r = \frac{1}{E}\left[f_r - \nu (f_T + f_A)\right] = C_r f_r \quad (2)$$

$$\epsilon_T = \frac{1}{E}\left[f_T - \nu (f_A + f_r)\right] = C_T f_T \quad (3)$$

EXTRUSION CONCEPT

FLEXIBILITY AND STRESS IN SOFT SEAL

BY (2): $f_T = (EC_T + \nu) f_r + \nu f_A$ (1)

$EC_r f_r = f_r - \nu(EC_T f_r + \nu f_r + \nu f_A) - \nu f_A$ (2)

$$f_r = \frac{\nu^2 + \nu}{(1 - EC_r - \nu EC_T - \nu^2)} f_A \quad (3)$$

$$= \frac{(.109 + .33)}{(1 + 32.2 + 0.33(0.490) - .109)} (-25{,}800 \text{ psi})$$

$$= \frac{0.39}{+33.25} (-25{,}800) = -302 \text{ psi. (ELASTIC SOLN)}$$

$$f_T = (-.490 + .33)(-302) + 0.33(-25{,}800)$$

$$= +48 - 8500 = -8452 \text{ (ELASTIC SOLN)}$$

THE QUESTION IS THEN: IS THE ELASTIC SOLUTION VALID, OR DO THE APPLIED STRESSES PRODUCE PLASTIC YIELDING DUE TO FLEXIBILITY OF THE WALLS? FIND UNIAXIAL STRESS EQUIVALENT TO THIS TRIAXIAL STRESS COMBINATION:

$$f_E = \frac{1}{\sqrt{2}} \left[(f_A - f_r)^2 + (f_r - f_T)^2 + (f_T - f_A)^2 \right]^{1/2}$$

$$= 0.707 \left[(-25.8 + 0.302)^2 + (-0.302 + 8.45)^2 + (8.45 + 25.8)^2 \right]^{1/2}$$

$$= 0.707 \left[1018 \right]^{1/2} = -22{,}700 \text{ psi.}$$

PREPARED
CHECKED
MODEL

EXTRUSION CONCEPT.

FLEXIBILITY AND STRESS IN SOFT SEAL

THUS ELASTIC SOLUTION RESULTS SHOW PLASTIC YIELDING WILL TAKE PLACE WITH WALLS FLEXIBLE. A CLOSER APPROXIMATION TO THE PLASTIC SOLUTION CAN BE OBTAINED BY USING A SECANT MODULUS INSTEAD OF AN ELASTIC MODULUS IN THE ELASTIC EQUATIONS.

FROM A STRESS-STRAIN CURVE FOR 1100 ALUM @ -320°F AT $f = 22{,}700$ PSI. :

$$\epsilon = 0.075 \text{ IN/IN}$$

$$\text{SECANT MODULUS} = E_s = \frac{f}{\epsilon} = \frac{22{,}700}{.075} = 303{,}000 \text{ psi.}$$

SUBSTITUTING INTO ELASTIC EQUATIONS:

$$E_s C_r = 0.303 \times 10^6 (-2620 \times 10^{-9}) = 0.794$$

$$E_s C_T = 0.303 \times 10^6 (-39.8 \times 10^{-9}) = 0.012$$

$$f_r = \frac{\nu^2 + \nu \quad (f_A)}{(1 - E_{Cr} - \nu E_{CT} - \nu^2)} = \frac{0.439(-25{,}800)}{(1 + 0.794 + .33(.012) - .109)}$$

$1 + 0.794 + .33(.012) - .109 = 1.689$

$$= -6700 \text{ psi.}$$

$$f_T = (-0.012 + 0.33)(-6700) + 0.33(-25{,}800)$$

$$= -2130 - 8500 = -10{,}630 \text{ psi.}$$

$$\epsilon_A = \frac{1}{E_s}[f_A - \nu(f_r + f_T)] = \frac{-25{,}800 - 0.33(-17{,}330)}{0.303 \times 10^6} = \frac{-20{,}090}{.303 \times 10^{+6}}$$

$$= 66{,}300 \mu \frac{IN}{IN} = 0.066 \frac{IN}{IN}.$$

EXTRUSION CONCEPT.

FLEXIBILITY AND STRESS IN SOFT SEAL RIGID WALLS

FOR REFERENCE, SOLVE ELASTIC CASE WHERE CONFINING WALLS ARE TOTALLY RIGID (ZERO LATERAL STRAINS), CONSIDER f_A KNOWN

$$E\epsilon_A = f_A - \nu f_r - \nu f_T$$

$$E\epsilon_r = f_r - \nu f_T - \nu f_A = 0$$

$$E\epsilon_T = f_T - \nu f_r - \nu f_A = 0$$

$$f_T = \nu f_r + \nu f_A$$

$$f_r - \nu(\nu f_r + \nu f_A) - \nu f_A = 0$$

$$(1-\nu^2) f_r - (\nu+\nu^2) f_A = 0$$

$$f_r = \frac{\nu(1+\nu)}{(1+\nu)(1-\nu)} f_A = \frac{\nu}{1-\nu} f_A$$

$$f_T = \frac{\nu^2}{1-\nu} f_A - \nu f_A = \left[\frac{\nu^2}{1-\nu} - \nu\right] f_A = \frac{\nu}{1-\nu} f_A$$

$$\epsilon_A = \left[1 - \frac{2\nu^2}{1-\nu}\right] \frac{f_A}{E}$$

IF $\nu = 0.33$

$$f_r = f_T = \frac{.33}{0.67} f_A = 0.493\, f_A$$

$$\epsilon_A = \left[1 - \frac{2(.109)}{0.67}\right] \frac{f_A}{E} = 0.674\, \frac{f_A}{E}$$

EQUIVALENT COMPRESSIBILITY

$$\beta_E = \frac{f_A V_0}{\Delta V} = \frac{f_A \ell^3}{\ell^2 \cdot \ell \epsilon_A} = \frac{E}{\left(1 - \frac{2\nu^2}{1-\nu}\right)} = 1.485\, E \quad \text{FOR } \nu = 0.33$$

FLEXIBILITY AND STRESS IN SOFT SEAL RIGID WALLS

AT DESIGN POINT STRESS:

$$f_r = f_T = 0.493\,(-25{,}800\ \text{psi}) = -12{,}700\ \text{psi}.$$

$$\epsilon_A = 0.674\,\frac{(-25{,}800)}{12.3\times10^{-6}} = -1412\times10^{-6}\ \frac{\text{IN}}{\text{IN}}.$$

AXIAL DEFLECTION DURING SEATING

$$\delta_A = \epsilon_A\, \ell_1 = 0.156\,(-0.001412) = -0.00022\ \text{IN}.$$

COMPARING THE MORE REALISTIC PLASTIC FLEXIBLE WALL STRESSES WITH THE IDEALIZED ELASTIC RIGID WALL STRESSES, ONE FINDS LITTLE DIFFERENCE, I.E. WITH PLASTIC ACTION THE STRESSES APPROACH RIGID WALL STRESSES AS A LIMIT.

EXTRUSION CONCEPT

LOAD REQUIRED TO UNSEAT SEAL FROM OUTER SLEEVE

WHEN THE SEATING LOAD IS REDUCED TO ZERO, $f_A = 0$ BUT THE PLASTIC PARTS OF f_r & f_T CANNOT RELIEVE UNLESS THE HARD WALLS CAN RETURN TO THEIR UNDEFLECTED POSITIONS. IN PARTICULAR THE RELAXED VALUE OF f_r WILL CONTROL THE FRICTIONAL FORCE REQUIRED TO BACK OFF THE SEAL. THE ELASTIC PARTS OF f_r & f_T WILL RELIEVE, LEAVING THE PLASTIC PARTS:

$$f_A = 0$$

$$f_r = -6700\,psi + 302\,psi = -6400\,psi$$

$$f_T = -10,630 + 8452\,psi = -2180\,psi.$$

FURTHER RELIEF WOULD OCCUR IF f_E UNDER THESE STRESSES IS SEVERAL TIMES YIELD, IN WHICH CASE THEY WILL YIELD THE SOFT MATERIAL IN THE AXIAL DIRECTION. IN THIS CASE THE LATERAL STRESSES ARE AT, NOT ABOVE, YIELD SO FURTHER RELIEF IS UNLIKELY.

EXTRUSION CONCEPT

LOAD REQUIRED TO UNSEAT SEAL FROM OUTER SLEEVE

FRICTIONAL LOAD TO UNSEAT = COEFFICIENT OF FRICTION OF ALUMINUM ON MILD STEEL ≅ 0.60
μ FOR ALUMINUM ON INCO-718 MUST BE MEASURED.
∴ SOLVE FOR $\mu = 0.2$ AND $\mu = 1.0$ (NORMAL RANGE)

L_U (COULOMB FRICTION) $= \mu f_t \cdot 2\pi (R_O + H_S) \ell_1$
$= (0.2)(6400\ PSI)(6.28)(.262)(.156)$

$= (0.2)(400)(.256\ IN^2) = 328\ LB.$

IF THE COEFFICIENT OF FRICTION IS FOUND TO BE HIGHER, L_U COULD EXCEED L_S.
FOR EXAMPLE IF $\mu = 1.0$, $L_U = 1640\ LB.$

THIS SITUATION CAN BE REMEDIED BY REDUCING THE LATERAL CONTACT AREA (ℓ_1)

FOR EXAMPLE IF $\mu = 1.0$, TO REDUCE L_U TO $L_S = 493\ LB$:

$$\ell_1 = \frac{0.156}{3.33} = 0.047\ IN., \quad L_U = 493\ LB.$$

TO PREVENT TENSILE YIELDING WHEN L_U IS APPLIED, ℓ_2 HAS A MAXIMUM VALUE:

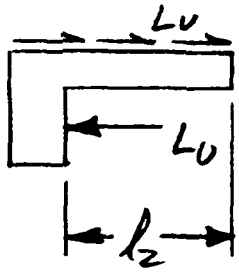

$$\frac{(\ell_2)_{MAX}}{\ell_1} L_U = F_{TY}\, \pi \left[(R_O + H_S)^2 - R_O^2 \right]$$

EXTRUSION CONCEPT.

LOAD REQUIRED TO UNSEAT SEAL FROM OUTER SLEEVE

$$(\ell_2)_{MAX} = \frac{0.047\,(6000\ psi)\,(0.01915\ in^2)}{493\ LB}$$

$$= 0.011\ IN.$$

MIGHT AS WELL MAKE $\ell_2 = 0$, THEN WOULD LOOK LIKE:

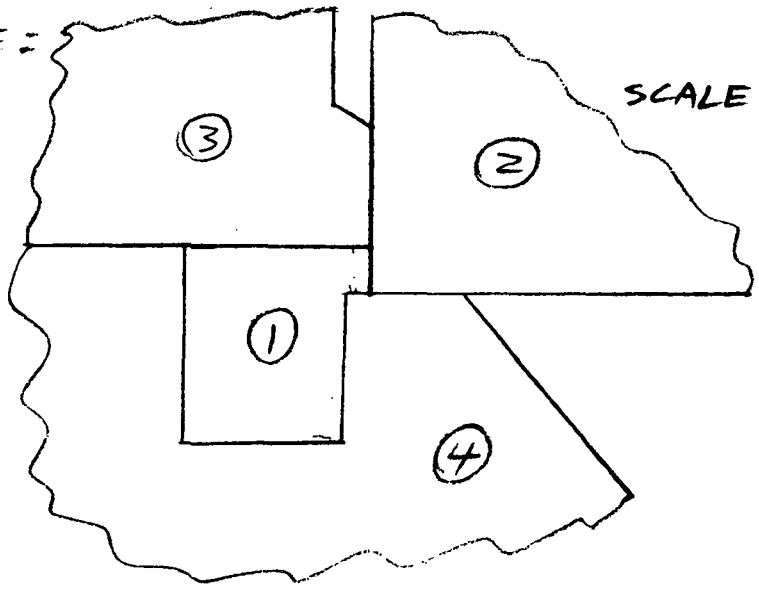

SCALE = 20/1

EXTRUSION CONCEPT

EFFECT OF SEALING INTERFACE SHAPE ON LOCAL CONTACT PRESSURE PROFILE

IT HAS BEEN SUGGESTED THAT AN INCREASE IN LOCAL CONTACT PRESSURE MIGHT BE OBTAINED BY VARYING THE SHAPE OF THE SOFT/HARD CONTACT SURFACE, SUCH AS:

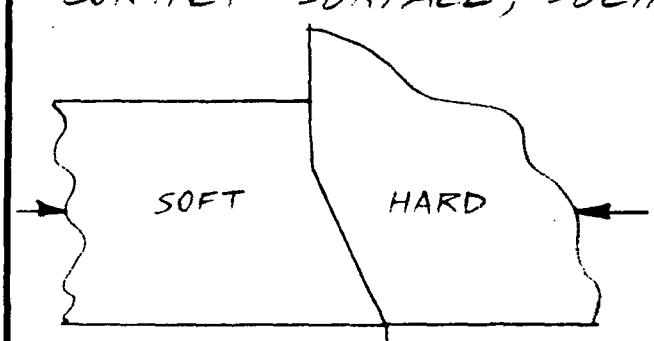

ANGLED

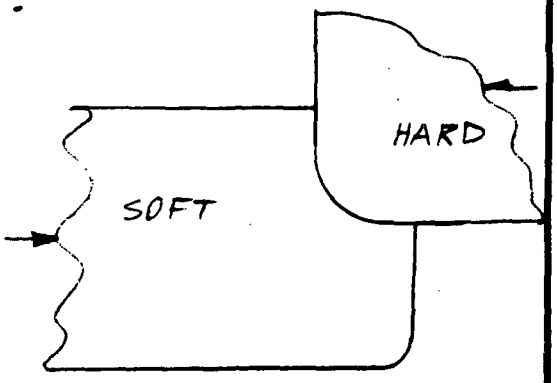

RADIUSED

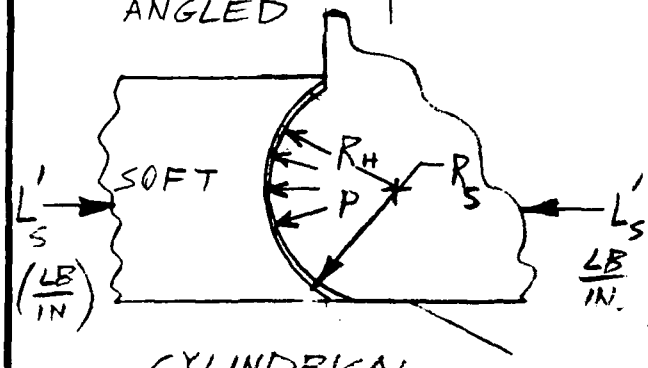

CYLINDRICAL

AS AN EXAMPLE, THE CYLINDRICAL CONCEPT WILL BE EVALUATED AS A FUNCTION OF LOCAL BULK ELASTIC PROPERTIES AFTER SEVERAL INITIAL RUN IN CYCLES IN WHICH YIELDING TAKES PLACE, HERTZ CONTACT STRESS FORMULAS WILL BE USED FROM ROARK, TABLE XIV, CASE 6:

$$P_{MAX} = 0.798 \sqrt{\frac{2(R_S - R_H)L'_S}{R_S R_H \left[\frac{1-\nu_S^2}{E_S} + \frac{1-\nu_H^2}{E_H}\right]}}$$

PREPARED
CHECKED
MODEL

EXTRUSION CONCEPT.

EFFECT OF INTERFACE SHAPE ON CONTACT PRESSURE

UNFORTUNATELY, IF R_S IS SET EQUAL TO R_H IN THE UNSTRESSED STATE $P_{MAX} = 0$ WHICH MEANS THE SOLUTION BREAKS DOWN UNDER THESE CONDITIONS AS $P_{AVERAGE} = \frac{L'_S}{H_S}$ THE RANGE OF POTENTIAL PRESSURE INCREASES SHOULD BE COVERED, HOWEVER, BY STARTING WITH THE SOFT SEALING SURFACE FLAT ($R_S \Rightarrow \infty$) AND VARYING R_H. FROM ROARK, TABLE ~~XIV~~, CASE 4:

$$P_{MAX} = 0.798 \sqrt{\frac{L_S'}{2R_H\left[\frac{1-\nu_S^2}{E_S} + \frac{1-\nu_H^2}{E_H}\right]}}$$

$$= 0.798 \sqrt{\frac{493\ LB/1.605\ IN}{2\left[\frac{1-0.109}{12.3\times10^6} + \frac{1-.09}{32\times10^6}\right]R_H}} = \frac{0.798}{\sqrt{R_H}}\left[1521\times10^6\right]^{1/2}$$

$$= \frac{31,100}{\sqrt{R_H}} \quad Psi.$$

IF $R_H = \frac{1}{2} H_S = \frac{1}{2}(.012) = 0.006$ IN (FULL RADIUS)

$$P_{MAX} = \frac{31,100}{0.0775} = 401,000 \text{ psi.}$$

$$\frac{P_{MAX}}{P_{AVE}} = \frac{401,000}{25,800} = 15.55$$

PREPARED
CHECKED
MODEL

EXTRUSION CONCEPT

EFFECT OF INTERFACE SHAPE ON CONTACT PRESSURE

OF COURSE ONE MIGHT HAVE TO USE LESS THAN A FULL RADIUS IF THE CONSTRAINING WALLS CANNOT BE MADE STIFF ENOUGH TO RETURN THE SOFT MATERIAL TO A FLAT SURFACE AGAIN.

THE WIDTH OF THE CONTACT AREA IS GIVEN BY:

$$b = 1.6\sqrt{2R_H L_s' \left[\frac{1-\nu_s^2}{E_s} + \frac{1-\nu_H}{E_H}\right]}$$

$$= 1.6\sqrt{2\left(\frac{307\ LB}{IN}\right)\left(0.1009\times10^{-6}\ \frac{IN^2}{LB}\right)R_H}$$

$$= 12.6\times10^{-3}\sqrt{R_H}$$

FOR $R_H = 0.006$ (FULL RADIUS)

$$b = 0.975\times10^{-3}, \quad \frac{H_s}{b} = \frac{.012}{.000975} = 12.3$$

SIMILARLY, FOR OTHER R_H:

R_H/H_s	R_H (IN)	$\sqrt{R_H}$ ($IN^{0.5}$)	P_{MAX} (PSI)	b (IN)	P_{MAX}/P_{AVE}	H_s/b
0.5	.006	.0775	401,000	.000975	15.55	12.3
1.0	.012	.1097	284,000	.00138	11.00	8.70
2.0	.024	.155	201,000	.00195	7.80	6.15
4.0	.048	.219	142,000	.00276	5.50	4.35
8.0	.096	.310	100,200	.00390	3.89	3.08
10.0	.120	.346	90,000	.00436	3.49	2.75

WHICH IS PLOTTED ON THE NEXT PAGE.

INFLUENCE OF HARD SEAT RADIUS ON PEAK CONTACT PRESSURE AND WIDTH, EXTRUSION CONCEPT DESIGN POINT

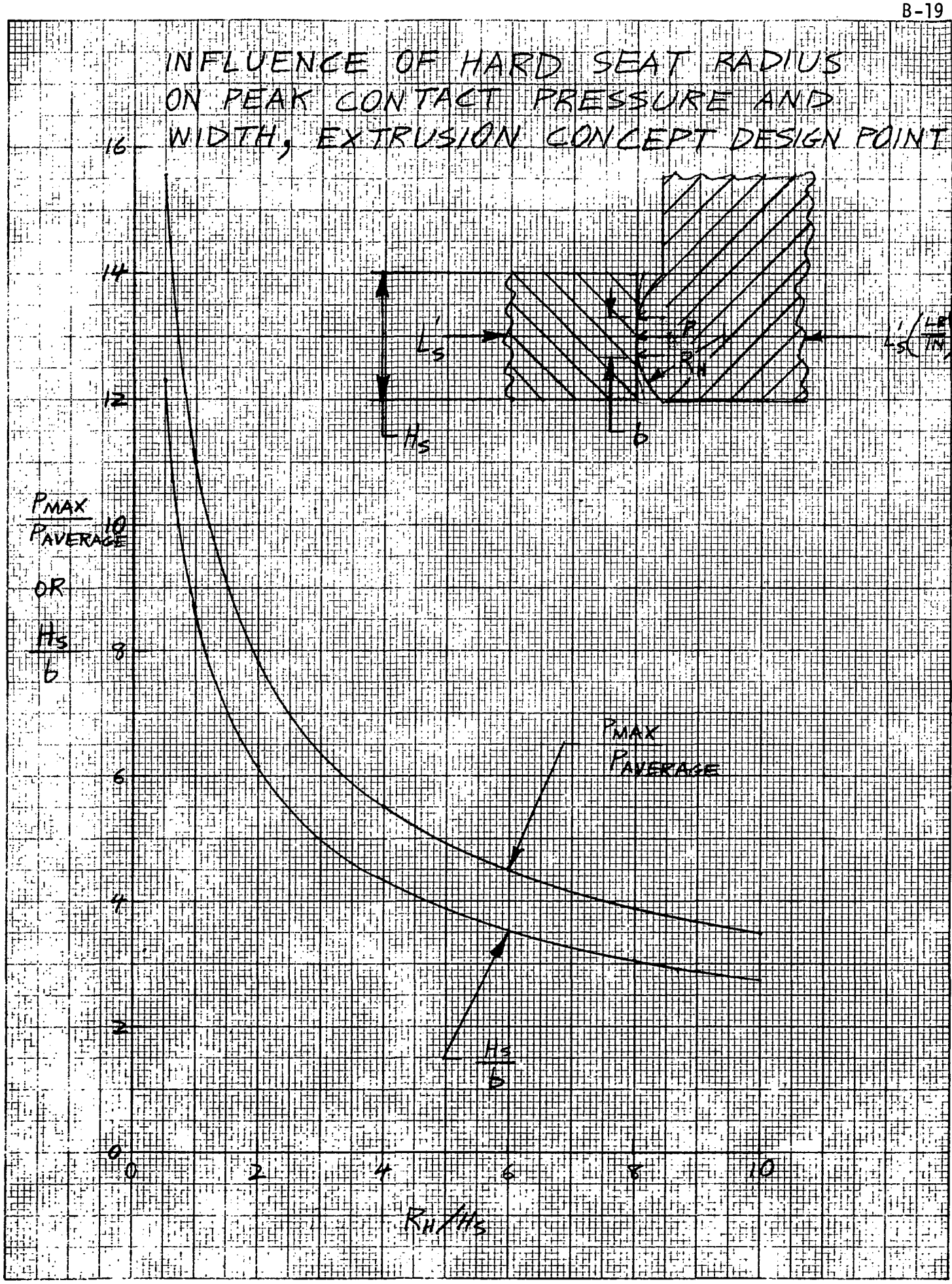

APPENDIX C

BULK COMPRESSION SEAL

DESIGN ANALYSIS

BULK COMPRESSION POINT DESIGN STRESS ANALYSIS

BULK COMPRESSION POINT DESIGN

SCALE = 10/1

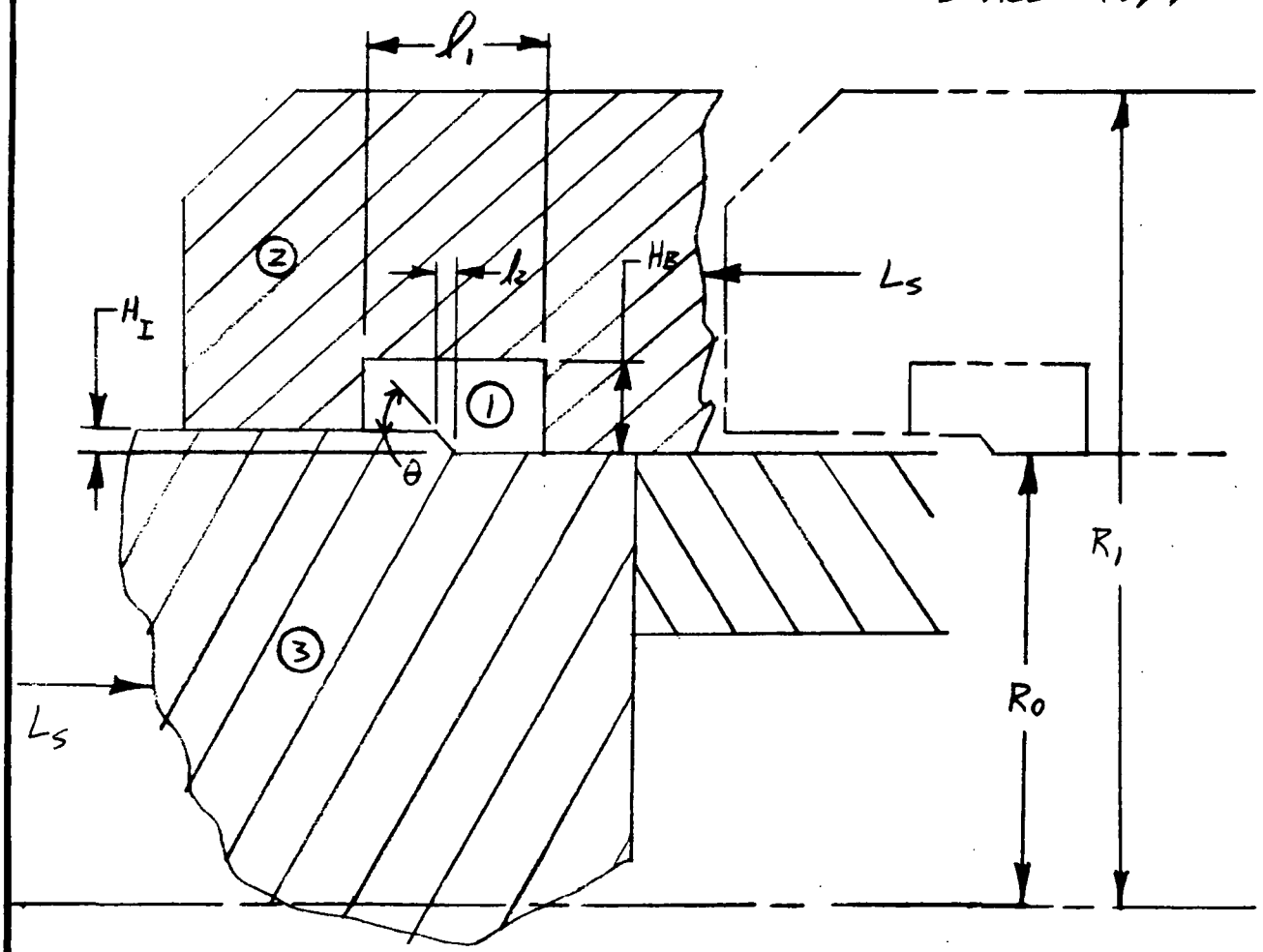

ASSUME AS TENTATIVE STARTING DIMENSIONS:

SOFT MATERIAL = 1100-0 ALUMINUM

HARD MATERIAL = INCO-718 (AMS 5664)

$R_0 = 0.250$ IN

$H_B = 0.050$ IN

$H_I = 0.003$ IN

$l_1 = 0.100$ IN

$L_s = 493$ LB

$\theta = 1.544° = 0.03$ RADIANS

PREPARED
CHECKED
MODEL

BULK COMPRESSION CONCEPT

BULK COMPRESSION POINT DESIGN

SOFT MATERIAL VOLUME $= \ell_1 \pi\left[(R_O + H_B)^2 - R_O^2\right]$

$= 0.100\,(3.14)\left[(.3)^2 - (.25)^2\right] = (.1)(.0863)$

$= 0.00863\ IN^3$

SEALING SURFACE AREA $= 2\pi(R_O + H_B)\,\ell_1$

$= 6.28\,(.2515)(.1) = 0.158\ IN^2$

CONSIDER AXIAL EQUILIBRIUM:

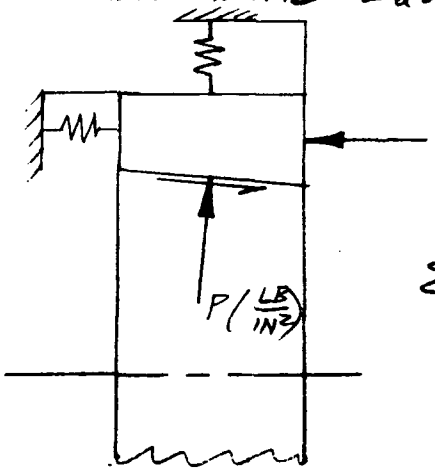

ASSUME CONTACT ONLY L_s OVER ℓ_2:

$$\Sigma F_A = +P_r(\sin\theta)(2\pi R_M)\left(\frac{\ell_2}{\cos\theta}\right) + \mu P_r(\cos\theta)(2\pi R_M)\left(\frac{\ell_2}{\cos\theta}\right) - L_s = 0$$

$$= 2\pi R_M P_r \ell_2\left[\tan\theta + \mu\right] - L_s = 0$$

ASSUME $\mu = 0.6$, $\ell_2 = \ell_1$, $\theta = 0.3$ RADIANS

$$P_r = \frac{L_s}{2\pi R_M \ell_2\left[\tan\theta + \mu\right]} = \frac{493\ LB}{0.158\left[.03 + 0.6\right]} = 4950\ psi.$$

NOT $> F_{cy}$

NEXT LOOK AT ORIGINAL SHAPE:

PREPARED
CHECKED
MODEL

BULK COMPRESSION CONCEPT.

BULK COMPRESSION POINT DESIGN

ASSUME HYDROSTATIC ASSUMPTION IS LOCALLY VALID IN RADIAL DIRECTION:

(RIGOROUS SOLUTION COULD BE FOUND WITH FINITE ELEMENT ELASTICITY PROGRAM SUCH AS TRW'S AS171B PROGRAM, BUT TIME DOES NOT PERMIT.)

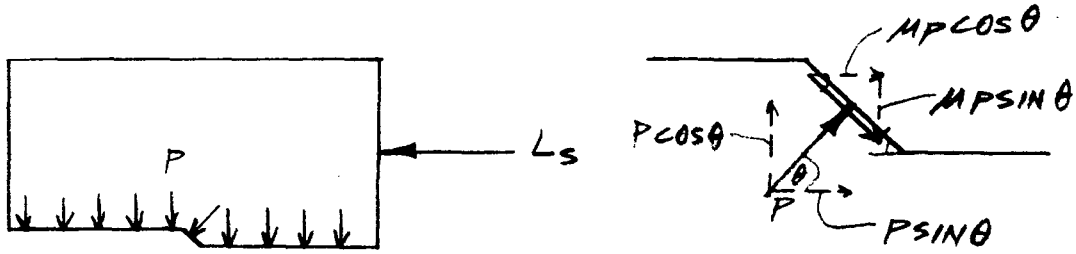

$$L_s = (\ell_1 - \ell_2)(2\pi R_M)\mu P + \mu P\cos\theta\,(2\pi R_M)\frac{\ell_2}{\cos\theta} + P\sin\theta\,(2\pi R_M)\left(\frac{\ell_2}{\cos\theta}\right) = 2\pi R_M P\left[\mu\ell_1 + \tan\theta\,\ell_2\right]$$

ASSUME $\mu \tilde{=} 0.6$ (LIKE ALUM ON MILD STEEL)

$$P = \frac{L_s}{2\pi R_M\left[\mu\ell_1 + \tan\theta\,\ell_2\right]}$$

LET $L_s = 493$ LB
$\ell_1 = 0.100$ IN
$\ell_2 = .003$ IN
$\theta = 45°$

$$= \frac{493}{1.58\left[0.6(.1) + (1)(.003)\right]} = 4950 \text{ psi.}$$ SAME RESULT.

TWO AVENUES OF IMPROVEMENT ARE APPEARENT:

(a) WITH COATINGS, PLATINGS AND DIFFERENT MATERIAL SELECTIONS ONE CAN REDUCE μ TO PERHAPS 0.1 – 0.2

(b) BY BURYING MOST OF SOFT MATERIAL IN HARD, ℓ_1 CAN BE REDUCED.

BULK COMPRESSION CONCEPT.

BULK COMPRESSION POINT DESIGN

THIS REVISED CONFIGURATION MIGHT LOOK LIKE:

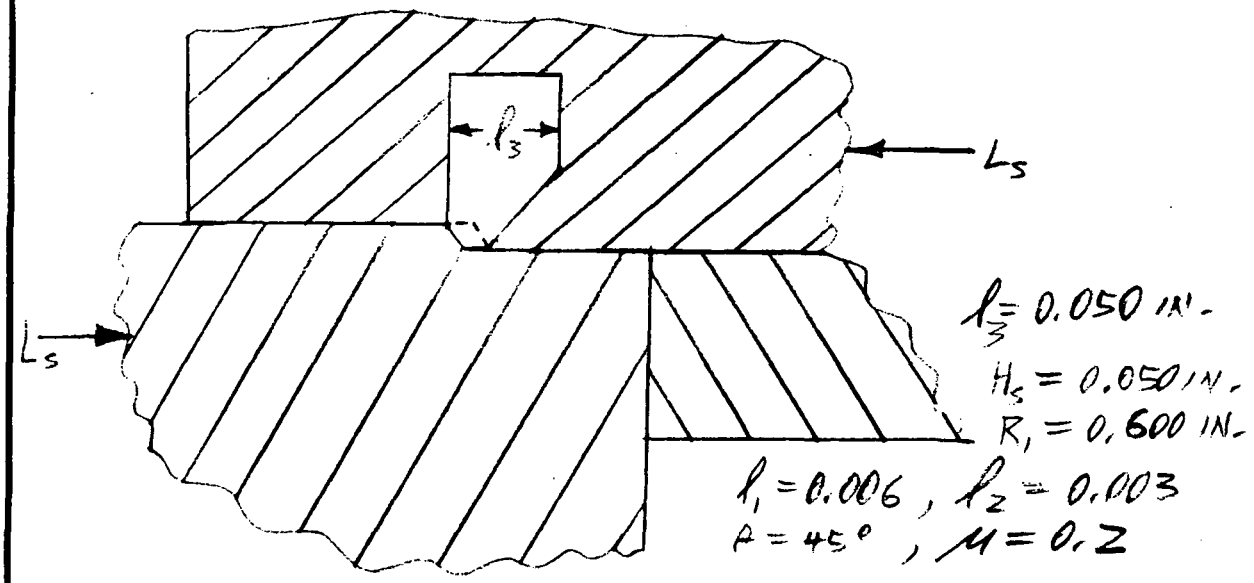

$$P = \frac{493}{(1.58)[0.2(.006)+(1)(.003)]} = 74{,}300 \text{ PSI.}$$

$$\frac{P}{F_{CY}} = \frac{74{,}300 \text{ psi}}{15{,}000 \text{ psi}} = 4.95 \sim 5\times \text{ YIELD.}$$

FROM GENERAL DESIGN CURVES:

FIGURE 1, REDUCTION OF SURFACE ASPERITY

$$\text{HEIGHT} = \frac{h}{h_{\text{NO LOAD}}} = 10.2\%$$

FIGURE 3, INDENTATION OF WEAR PARTICLES
> THEIR DIAMETER

FIGURE 6, GAPS REQUIRED: $\frac{H_G}{H_S} = 0.014$

$H_G = 0.014(.003)$
≤ 0.000042 HARD TO MAINTAIN, BUT
A SMALL HARD TAB LOADED AGAINST (3) BY P WOULD HELP.

FLEXIBILITY AND STRESS IN HARD WALLS

INSIDE WALL, RADIAL

BY SAME FORMULAS AS USED FOR EXTRUSION DESIGN.

$P_o = 74{,}300$ PSI., $a = 0$, $b = 0.250$

$$(\delta_R)_{r=b} = \frac{b P_o}{E_H}\left(\frac{a^2+b^2}{b^2-a^2} - \nu_H\right)$$

$$= -0.000406 \text{ (INWARD)}$$

FLEXIBILITY $= C_o = 5.46 \times 10^{-9} \frac{IN}{PSI.}$

ELASTIC STRESSES, $r = b$

$$f_r = \frac{-P_o b^2}{b^2-a^2}\left(1 - \frac{a^2}{r^2}\right) = -74{,}300 \text{ PSI.}$$

$$f_T = \frac{-P_o b^2}{b^2-a^2}\left(1 + \frac{a^2}{r^2}\right) = -74{,}300 \text{ PSI.}$$

MARGINS @ 70°F

$$M.S._y = \frac{150{,}000}{1.0(74{,}300)} - 1 = \underline{\underline{+1.02}}$$

$$M.S._{ULT.} = \frac{160{,}000}{1.5(-74{,}300)} - 1 = \underline{\underline{+0.61}}$$

OUTSIDE WALL, RADIAL

$r_o = 0$, $P_I = 74{,}300$ PSI., $a = .300$, $b = .600$

$$(\delta_R)_{r=a} = \frac{+a P_I}{E_H}\left(\frac{a^2+b^2}{b^2-a^2} + \nu\right) = \frac{.350(74300)}{32\times10^6}\left[\frac{.360+.090}{.360-.090} + .3\right]$$

(1.9)

$$= 1600\times10^{-7} = 0.00160 \text{ IN.}$$

$$\text{FLEXIBILITY} = \frac{1600 \cdot 10^{-7}}{74{,}300} = 21.5\times10^{-9} \frac{IN}{PSI.}$$

FLEXIBILITY AND STRESS IN HARD WALLS

STRESSES AT $r = a$:

$$f_r = \frac{a^2 P_I}{b^2 - a^2}\left(1 - \frac{b^2}{a^2}\right) = \frac{.09(74,300)}{.36 - .09}\left(1 - \frac{.36}{.09}\right)$$

$$= -74,300 \text{ PSI.}$$

$$f_T = \frac{a^2 P_I}{b^2 - a^2}\left(1 + \frac{b^2}{a^2}\right) = \frac{.09(74,300)}{.36 - .09}\left(1 + 4\right)$$

$$= +124,000 \text{ PSI.}$$

IN THIS CASE THERE WILL ALSO BE A SUPERIMPOSED AXIAL STRESS. ASSUME THE THEORETICAL RIGID WALL SOLUTION, THEN PRESSURE AGAINST H_B IS:

$$P_{LATERAL} = 0.493\ f_r = 0.493(74,300 \text{ PSI})$$

$$= 36,600 \text{ PSI.}$$

$$\text{AXIAL CAVITY AREA} = \pi\left[(R_0 + H_B)^2 - R_0^2\right]$$

$$= 3.14\left[.090 - .0625\right] = 0.0865 \text{ IN}^2$$

$$\text{AXIAL AREA, MEMBER } ② = \pi\left[R_1^2 - (R_0 + H_B)^2\right]$$

$$= 3.14\left[.360 - .090\right] = 0.847 \text{ IN}^2$$

$$f_A = \frac{L_{AXIAL}}{A_H} = \frac{(36,600 \text{ PSI})(0.0865 \text{ IN}^2)}{0.847 \text{ IN}^2}$$

$$= +3,740 \text{ PSI.}$$

FLEXIBILITY AND STRESSES IN HARD WALLS

UNIAXIAL EQUIVALENT STRESS:

$$f_E = \frac{1}{\sqrt{2}}\left[(f_A - f_L)^2 + (f_L - f_T)^2 + (f_T - f_A)^2\right]^{1/2}$$

$$= 0.707\left[(3.74 + 74.3)^2 + (-74.3 - 124)^2 + (124 - 3.74)^2\right]^{1/2}$$

$$= 0.707\left[6090 + 39{,}400 + 4{,}500\right]^{1/2} = 173{,}000 \text{ psi.}$$

WHICH WILL YIELD INCO-718 @ 75°F IF VALVE IS TO BE ACCEPTANCE TESTED AT ROOM TEMPERATURE (F_{TY} = 150,800 psi.)

AT CRYOGENIC TEMPERATURE, STRESS IS VERY CLOSE TO YIELD (F_{TY} = 175,500 psi.)

HARD WALL SHOULD BE MADE THICKER AND/OR HIGHER STRENGTH MATERIAL SUBSTITUTED AND CALCULATIONS REPEATED.

AXIAL CAVITY FLEXIBILITY:

$$\delta_A = \frac{P l^2}{EA} = \frac{(36{,}600 \text{ psi})(.05)^2}{32\times10^6\,(.847)} = 3.38\times10^{-6} \text{ IN.}$$

$$\text{AXIAL FLEXIBILITY} = \frac{3.38\times10^{-6}}{74{,}300 \text{ psi.}} = 0.0455\times10^{-9}\ \frac{\text{IN}}{\text{PSI.}}$$

FLEXIBILITY AND STRESS IN SOFT SEAL

REVISED CAVITY VOLUME, $V_0 = 2\pi R_c \cdot \frac{1}{2} H_s \ell_3$

$= 6.28(.250 + .0334)(.5)(.050)(.050) = 1.779(.00125)$

$= 0.00222\ IN^3$

FIND CHANGE IN SOFT MAT'L VOLUME @ $P = 74{,}300$ PSI

$$B_E = \frac{E}{1 - \frac{2\nu^2}{1-\nu}} = 1.485E = 1.485(12.3 \times 10^6)$$ FOR $\nu = 0.33$

$= 18.25 \times 10^6$ PSI.

$$\Delta V_S = \frac{P V_0}{B_E} = \frac{(74{,}300\ PSI)(.00222\ IN^3)}{18.25 \times 10^6\ PSI.} = 9.05 \times 10^{-6}\ IN^3$$

FIND CHANGE IN HARD CAVITY VOLUME @ $P = 74{,}300$ PSI

$V_0 = \pi R_c H_s \ell_3$

$\ln V_0 = \ln \pi + \ln R_c + \ln H_s + \ln \ell_3$

$$\frac{dV_H}{V_0} = \frac{dR_c}{R_c} + \frac{dH_s}{H_s} + \frac{d\ell_3}{\ell_3}$$

USING DEFLECTIONS AS APPROXIMATIONS TO DIFFERENTIALS:

$dH_s = .000406 + .00160 = +2006 \times 10^{-6}$ IN.

$d\ell_3 = +3.38 \times 10^{-6}$ IN.

$dR_c = \frac{1}{2}[+1600 - 406] \times 10^{-6} = +597 \times 10^{-6}$

$$\frac{\Delta V_H}{V_0} = \frac{597 \times 10^{-6}}{.2834} + \frac{2006 \times 10^{-6}}{.05} + \frac{3.38 \times 10^{-6}}{.05} = 0.0423$$

$\Delta V_H = .0423(.00222) = 94.0 \times 10^{-6}\ IN^3$

FLEXIBILITY AND STRESS IN SOFT SEAL

A ONE INCH STROKE OF THE 0.003 IN. INTERFERENCE STEP CREATES A VOLUME CHANGE OF: $\Delta V_I = (1\ IN)(.003\ IN)(6.28)(.2515\ IN)$

$= 0.00474\ IN.^3/IN.$

∴ STROKE OF SHAFT TO PRODUCE $p = 74{,}300$ PSI:

$$\text{STROKE} = \frac{\Delta V_S + \Delta V_H}{\Delta V_I} = \frac{(94.0+9.05)\times 10^{-6}}{4.74\times 10^{-3}} = 21.8\times 10^{-3}\ IN.$$

$= 0.022\ IN.$

WHICH INDICATES THAT THE ALLOWANCE FOR STROKE OF $(\ell_1 - \ell_2) = 0.003$ IN THAT WAS MADE ON P. 4 IS INSUFFICIENT, AND ℓ_1 MUST BE INCREASED, LOWERING THE SEAL PRESSURE

$$(\ell_1 - \ell_2) = (0.022\ IN)\left(\frac{P}{74{,}300}\right) = 0.296\times 10^{-6}\ P$$

$$P = \frac{L_S}{2\pi R_M\left[(\ell_1-\ell_2)\mu + (1+\tan\theta)\ell_2\right]} = \frac{493}{1.58\left[0.2(\ell_1-\ell_2)+2(.003)\right]}$$

$$= \frac{312}{0.2(0.296\times 10^{-6}P)+0.006} \Rightarrow P^2 + 101.4\times 10^3 P - 5.28\times 10^9 = 0$$

$P = 38{,}000$ PSI.

$(\ell_2 - \ell_1) = 0.296\times 10^{-6}(38\times 10^3) = 0.01125\ IN.$

FLEXIBILITY AND STRESS IN SOFT SEAL

SO $\frac{f_r}{F_{cy}} = \frac{38,000}{15,000} = 2.53$ TIMES WITH FRICTION

WHEN ACTUATOR LOAD IS RELEASED, HARD WALLS WILL RELAX, "EXTRUDING" SOFT MAT'L BACK OUT OF CAVITY. AREA RATIO =

$$\text{AREA RATIO} = \frac{.012\ \text{IN} + .003\ \text{IN}}{0.050\ \text{IN}} = 0.30$$

AT THIS RATIO, EXTRUSION WILL TAKE PLACE UNTIL $\frac{f_r}{F_{cy}} \simeq 1.4$ WITHOUT FRICTION

≈ 1.9 WITH FRICTION

THEN LOAD TO OVERCOME FRICTION AND OPEN VALVE:

$f_{r\,\text{UNLOADED}} \approx 1.9(15,000) = 27,500$ psi.

AREA $= 6.28(.25\text{IN})(.015\text{IN}) = 0.0236\ \text{IN}^2$

$L_{\text{UNSEAT}} = 27,500\,(.0236)(0.2) = 130\ \text{LB}$

WITH FRICTION FACTOR OF 0.2

< 493 LB SEATING LOAD ... O.K.

APPENDIX D

PROPELLANT ISOLATION VALVE

STRESS ANALYSIS

PREPARED J. L. REEVE 1/11/73 REPORT NO. PAGE D-1

CHECKED

MODEL

PROPELLANT ISOLATION VALVE STRESS ANALYSIS

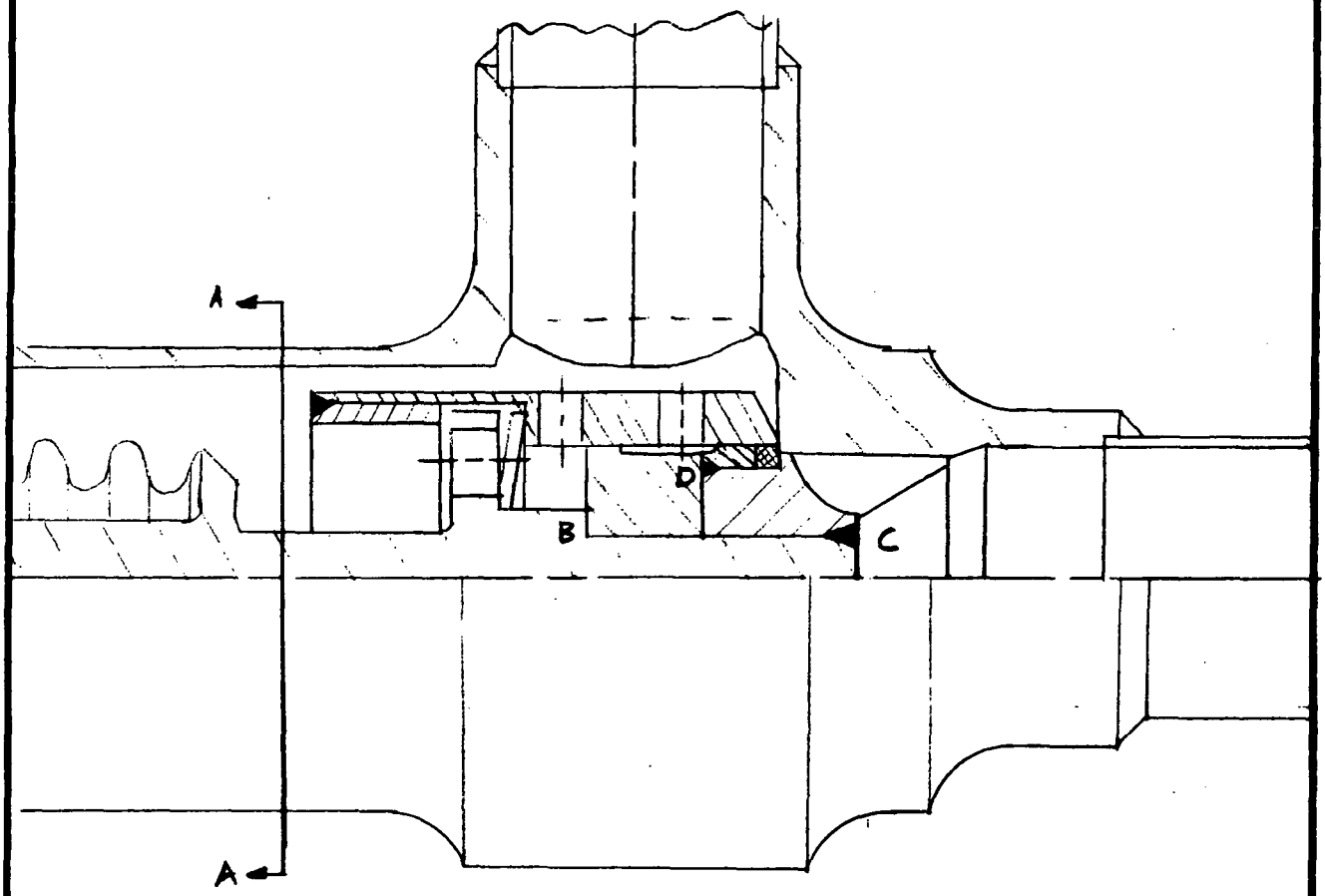

MATERIALS:

SOFT SEAL MATL = 1060-0ALUM (PURER THAN 1100, ~ SAME MECHANICAL PROPERTIES)

HARD SEAL MATL = INCONEL 718 (R_c 38-40)

SEAT MAT'L = INCONEL-718 (R_c 32-36)

MATERIAL PROPERTIES

INCO-718 (MIL-HDBK-5B, SECTION 6.3.5)

70°F

$\alpha = 6.4 \times 10^{-6}$ IN/IN °F

$F_{TU} = 180{,}000$ $\quad e = 10\%$

$F_{TY} = 150{,}000$

$E = 29.0 \times 10^6$

$\nu = 0.30$

-300°F (AERO. STRUCTURAL METALS HANDBOOK)

$F_{TU} = 1.16\ (180{,}000) = 209{,}000$ psi.

$F_{TY} = 1.17\ (150{,}000) = 175{,}500$ PSI.

$E = 1.10\ (29.0 \times 10^6) = 32.0 \times 10^6$

SEATING STRESSES

THE PRELIMINARY VALVE ANALYSIS NOTED THAT THE SEATING STRESS OF THE SOFT-HARD SEAL THEN UNDER CONSIDERATION WAS ON THE LOW SIDE OF THE RANGE INDICATED BY THE PLASTIC SEATING THEORY THAT HAD BEEN DEVELOPED (REF. TRW 72.4781.6-251, P. 55). THE SEATING STRESS OF 25,800 PSI IN USE AT THAT TIME WAS DICTATED MAINLY BY THE 493 POUNDS AVAILABLE FROM THE COMPANION ACTUATOR. IF THE VALVE DESIGN IS DECOUPLED FROM A SPECIFIC ACTUATOR, A SEATING STRESS CAN BE SELECTED ENTIRELY ON THE BASIS OF SEATING CONSIDERATIONS.

A TEST SERIES UNDER ANOTHER PROGRAM WILL SOON MEASURE THE SEATING STRESS NECESSARY TO REACH VARIOUS LEAKAGE LEVELS. IN ADVANCE OF THESE RESULTS, THE PLASTIC SEATING THEORY OF THE REFERENCE INDICATES THAT BULK STRESSES OF 2-3 TIMES THE YIELD STRESS ARE REQUIRED FOR GOOD SURFACE CONFORMANCE.

ANOTHER REASON TO INCREASE THE SEATING STRESS IS ILLUSTRATED ON THE NEXT PAGE. CONVENTIONALLY THE YIELD STRESS IS DEFINED AS THAT NECESSARY TO PRODUCE A PLASTIC STRAIN

SEATING STRESSES

OF 0.2%. FOR MOST 'HARD' MATERIALS THIS STRESS IS NEAR THE POINT ON THE STRESS-STRAIN CURVE WHERE A MARKED INCREASE IN STRAIN OCCURS WITH A SMALL INCREASE IN STRESS. THE METAL WORKING TYPE OF PLASTIC SEATING THEORIES ARE BASED ON AN IDEALIZED ELASTO-PLASTIC STRESS STRAIN CURVE COMPOSED OF TWO STRAIGHT LINES. IN THE CASE OF 'SOFT' MATERIALS SUCH AS ANNEALED ALUMINUM THE 0.2% YIELD STRESS IS OFTEN MUCH LOWER THAN THE STRESS AT WHICH AN ELASTO-PLASTIC CURVE WOULD GIVE A GOOD APPROXIMATION. IN PARTICULAR ACCORDING TO THE CURVE BELOW, WHILE THE 0.2 YIELD STRESS OF 1100-0 ALUM MAY BE 7-15 KSI, THE CURVE IS NOT FLAT UNTIL ~28 KSI.

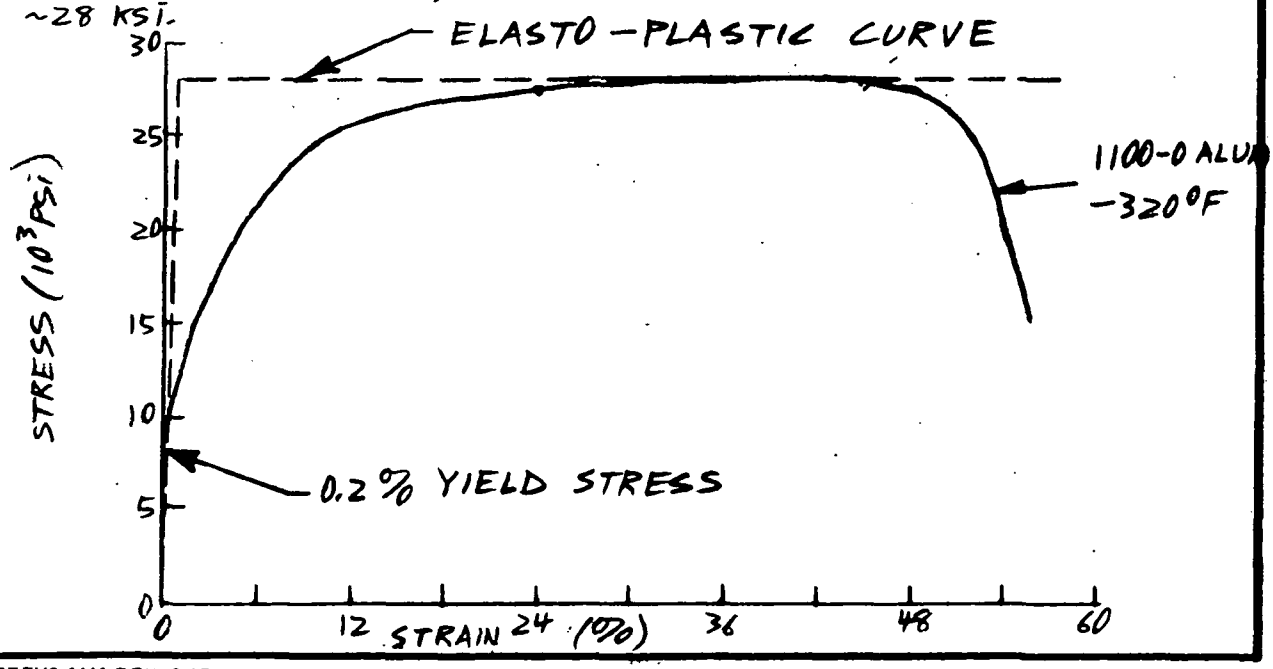

SEATING STRESSES

THE VALVE WILL BE STRESSED FOR AN ACTUATOR LOAD PRODUCING 2 TIMES "YIELD STRESS" IN THE SOFT SEAL, YIELD STRESS BEING DEFINED AS THE ELASTO-PLASTIC VALUE OF 28 KSI. IF LEAKAGE TESTS INDICATE THAT 3 TIMES YIELD IS NECESSARY TO ACHIEVE ZERO LEAKAGE, ANY MARGINAL SECTIONS OF THE DESIGN CAN BE REINFORCED BEFORE FABRICATION.

$$f_{\substack{SEATING, \\ SOFT}} = 2 \times (-28{,}000\ PSI) = -56{,}000\ PSI.$$

$$A_{\substack{SOFT \\ SEAL}} = (2\ IN)(0.012\ IN) = 0.024\ IN^2$$

$$L_S = 56{,}000 / .024 = 1344\ LB.$$

AS IN THE PRELIMINARY ANALYSIS, 50 LB IS ALLOWED TO SEAT THE HARD SEAL:

$$A_{\substack{HARD \\ SEAL}} = (0.015\ WIDTH)(2.07\ IN\ PERIMETER)$$
$$= 0.0311\ IN^2$$

$$f_{\substack{SEATING, \\ HARD}} = \frac{50\ LB}{0.0311\ IN^2} = 1{,}610\ PSI.$$

ACTUATOR LOAD BUDGET (CLOSING)

OPENING → +
CLOSING → −

	LOAD (LB)
SOFT SEAL LOAD	+ 1344
HARD SEAL LOAD	+ 50
WORST CASE HYDRAULIC IMBALANCE (BELLOWS DOWNSTREAM WITH DOWNSTREAM VENTED)	+ 82.5
SEAL BELLOWS FORCE (CLOSED)	+ 0
OPENING SPRING LOAD (CLOSED)	100
ACTUATOR FORCE (CLOSED)	+ 1577 LB.

MAIN SHAFT

CROSS SECTION AT A (MINIMUM DIAMETER)

LOAD = -1344 LB -50 LB = -1394 LB.

$A_{SECTION} = 0.7854(.500\ IN)^2 = 0.196\ IN^2$

$f_{CLOSED} = \frac{-1394\ LB}{0.196\ LB} = -7120$

$(M.S.)_{YIELD} = \frac{150{,}000}{(1.0)(7120)} - 1 = \underline{\underline{+20.0}}$

$(M.S.)_{ULT.} = \frac{180{,}000}{(1.5)(7120)} - 1 = \underline{\underline{+15.8}}$

STEP IN CROSS SECTION AT B

WHEN IN COMPRESSION ON CLOSING, THE SHAFT LOAD WILL SPLIT BETWEEN STEP AT B & WELD AT C. ASSUME 100% OF LOAD ON EACH.

$A_{STEP} = 0.7854(.750^2 - .440^2) = 0.289\ IN^2$

$f_{CLOSED} = \frac{-1394\ LB}{0.289\ IN^2} = -4820\ psi.$

... LESS CRITICAL THAN SECTION A.

MAIN SHAFT

WELD AT C BECAUSE OF ASSEMBLY CONSIDERATIONS, THIS INCO-718 WELD CANNOT BE HEAT TREATED TO THE SOLUTION TREATED AND AGED CONDISION (THE 1060-0 ALUM WOULD MELT). USE ANNEALED WELD ALLOWABLES, ASSUME MINIMUM 0.095 PENETRATION:

AT 70°F, 0.7 WELD FACTOR

$F_{TY} = 30{,}000$ PSI, $F_{TU} = 75{,}000$ PSI.

$F_{SU} = 0.6(75) = 45{,}000$ PSI.

CLOSING LOAD = -1344 LB. (CONSERVATIVE)

SHEAR AREA = $3.14(0.220\ IN)(0.095\ IN) = 0.0656\ IN^2$.

$$f_{SHEAR\ CLOSING} = \frac{1344\ LB}{0.0656\ IN^2} = 20{,}500\ PSI.$$

$$(M.S.)_{ULT,\ CLOSING} = \frac{45{,}000\ PSI(0.7)}{(1.5)(20{,}500\ PSI)} - 1 = \underline{\underline{+0.02}}$$

WELD AT D

COULD BE HEAT TREATED AFTER WELD TO NEAR PARENT METAL STRENGTH. IF THE TWO WELDED SURFACES AT D ARE GROUND FLUSH, WELD IS NOT PLACED IN SHEAR. IF TOLERANCE MISMATCH CAUSES FULL 1344 LB LOAD TRANSMISSION THROUGH WELD, MARGIN STILL POSITIVE IF

$$\text{PENETRATION} \geq (.095\ IN)\left(\frac{.22\ IN}{.281\ IN}\right) = 0.075\ IN.$$

MAIN SHAFT

EULER BUCKLING OF SHAFT SEGMENTS: A MID-SPAN BEARING AREA IS PROVIDED TO PREVENT THIS.
LONGEST SPAN = 6.7 INCH., PINNED ENDS
MIN. DIA. = 0.50 INCH., $A = 0.196\ IN^2$

$$I = \frac{\pi}{4} R^4 = 0.7854(0.25)^4 = 30.7 \times 10^{-4}\ IN^4$$

$$\rho = \sqrt{\frac{I}{A}} = \left[\frac{30.7 \times 10^{-4}}{19.6 \times 10^{-2}}\right]^{1/2} = 0.125\ IN.$$

$$\frac{L}{\rho} = \frac{6.7}{0.125} = 53.6$$

$$P_{CR} = \frac{\pi^2 EI}{L^2} = \frac{9.85(29 \times 10^6)(.307 \times 10^{-3} IN^4)}{44.9}$$

$$= 19{,}500\ LB$$

$$(M.S.) = \frac{19{,}500}{1.5(1394)} - 1 = \underline{\underline{+8.32}}$$

FLEXIBILITY AND STRESS IN SOFT SEAL

CONSIDER A UNIT WIDTH OF SEAL PERIMETER:

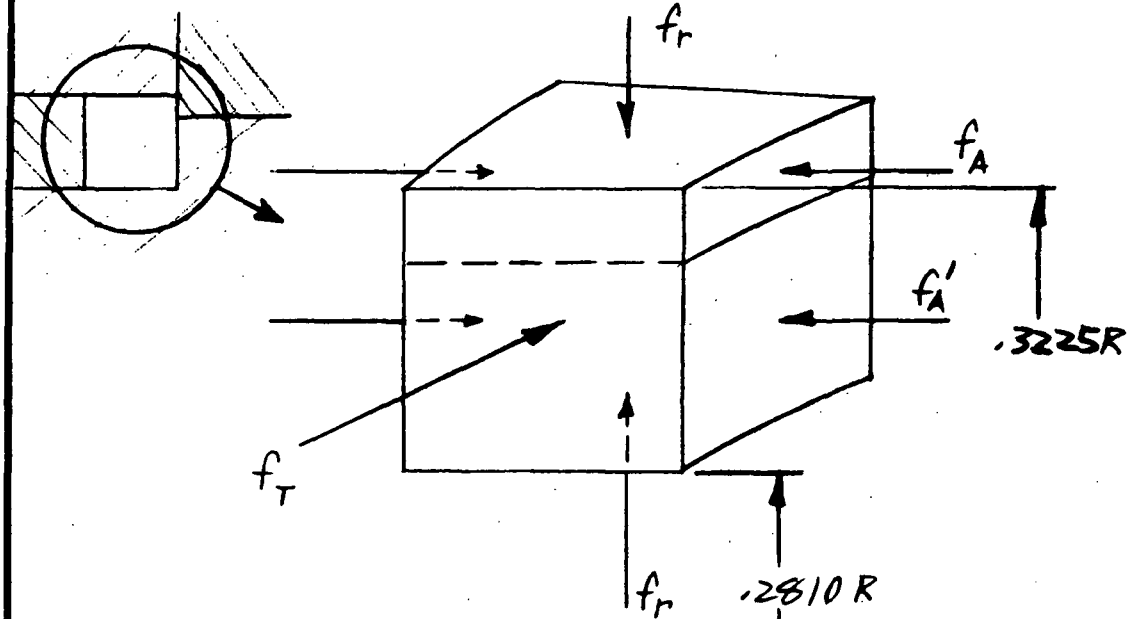

FOR NON RIGID WALLS, ONE CANNOT A PRIOR ASSUME THAT THE HYDROSTATIC ASSUMPTION WILL HOLD FOR LOW SEALING LOADS. FOR A 56,000 PSI SEALING STRESS, THE ASSUMPTION SHOULD BE CLOSE.
THEN $f_A = f_A'$

FIND LOADED DEFLECTIONS IN CONFINING WALLS FOR $f_A = f_r = f_T = 56{,}000$ psi.

INNER WALL THICK WALLED CYL. EQ.
(TIMOSHENKO, STRENGTH OF MATERIALS, SEC. 40)

$P_o = 56{,}000$, $P_I = 0$ $a = 0.110$ IN, $b = 0.281$ IN., $\nu = 0.3$

$$(\delta_R)_b = \frac{-b P_o}{E_H}\left(\frac{a^2+b^2}{b^2-a^2} - \nu_H\right)$$

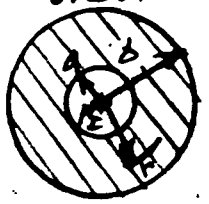

FLEXIBILITY AND STRESS IN SOFT SEAL

INNER WALL

$$(\delta_R)_b = \frac{-(0.281)(56{,}000)}{32\times10^6}\left[\frac{0.0121+0.0790}{0.0791-0.0121}-0.3\right] = -0.000521 \text{ IN.}$$

$$\text{RADIAL FLEXIBILITY} = C_3 = \frac{521\times10^{-6}\text{ IN}}{56{,}000\text{ psi}} = 9.31\times10^{-9}\ \frac{\text{IN}}{\text{psi}}$$

ELASTIC STRESSES AT $r=b$:

$$f_r = \frac{-P_0 b^2}{b^2-a^2}\left(1-\frac{a^2}{r^2}\right) = \frac{(-56000\text{ psi})(.0791)}{.0791-0.0121}\left(1-\frac{.0121}{.0791}\right)$$

$$= -56{,}000 \text{ psi.}$$

$$f_T = \frac{-P_0 b^2}{b^2-a^2}\left(1+\frac{a^2}{r^2}\right) = \frac{(-56000\text{ psi})(.0791)}{.0791-0.0121}\left(1+\frac{.0121}{.0791}\right)$$

$$= -76{,}500 \text{ psi.}$$

MARGINS AT 75°F.

$$(M.S.)_y = \frac{150{,}000}{1.0(56{,}000)} - 1 = \underline{+1.68}$$

$(M.S.)_{ULT}$ = NOT MEANINFUL IN COMPRESSION

ELASTIC STRESSES $r=a$:

$$f_r = 0$$

$$f_T = -\frac{2P_0 b^2}{b^2-a^2} = \frac{-2(56000)(.0791)}{.0791-0.0121} = -132{,}200 \text{ psi.}$$

$$(M.S.)_y = \frac{150{,}000}{1.0(132{,}200)} - 1 = \underline{+0.13}$$

FLEXIBILITY AND STRESS IN SOFT SEAL

OUTER WALL THICK CYLINDER STRESSES

$P_O = 0$ psi., $P_I = 56{,}000$ psi., $a = .3225$, $b = .499$ IN.

$$(\delta_R)_{r=a} = \frac{+a P_I}{E_H}\left(\frac{a^2+b^2}{b^2-a^2} + \nu_H\right) = \frac{+(.3225)(56000)}{32\times10^6}\left[\frac{0.1044+.249}{.249-.145} + 0.3\right]$$

$$= +1.204 \times 10^{-3}$$

$$\text{RADIAL FLEXIBILITY} = C_4 = \frac{1204\times10^{-6}\ \text{IN}}{56{,}000\ \text{psi}} = 21.5\times10^{-9}\ \frac{\text{IN}}{\text{psi.}}$$

ELASTIC STRESSES at $r=a$

$$f_r = \frac{a^2 P_I}{b^2-a^2}\left(1-\frac{b^2}{r^2}\right) = \frac{(.104)(56000)}{.249-.104}\left(1-\frac{.249}{.104}\right)$$

$$= -56000 \text{ psi.}$$

$$f_T = \frac{a^2 P_I}{b^2-a^2}\left(1+\frac{b^2}{r^2}\right) = \frac{.104(56000)}{.249-.104}\left(1+2.40\right)$$

$$= +2.44(56000) = +136{,}700 \text{ psi.}$$

SINCE PART IS UNDER COMBINED TENSION-COMPRESSION FIND DISTORSION ENERGY EQUIVALENT STRESS:

$$f_E = \frac{1}{\sqrt{2}}\sqrt{f_r^2+(f_T-f_r)^2+f_T^2} = 0.707\left[3140+37{,}100+18{,}670\right]^{1/2}$$

$= 171{,}000$ PSI. WHICH WOULD INDICATE AN OUTER WALL YIELD ZONE.

THIS ANALYSIS NEGLECTS THE REINFORCING EFFECT OF THE UNLOADED OUTER WALL ADJACENT TO THIS SECTION. NO WELL ESTABLISHED METHOD EXISTS FOR CALCULATING THIS EFFECT IN THICK SHELLS, SO A THIN SHELL METHOD WILL BE USED:

FLEXIBILITY AND STRESSES IN SOFT SEAL

OUTER WALL BENDING ANALYSIS

ANALYSE AS CYLINDER UNDER RADIAL LINE LOAD, $V_0 = (56{,}000\ psi)(.060\ IN) = 3360\ \frac{LB}{IN}$ (OUTWARD)

APPLY ROARK, TABLE XIII, CASE 10.

$\bar{R} = \frac{1}{2}(1.3225 + .499) = 0.411$, $t = 0.176\ IN.$

$$\lambda = \left[\frac{3(1-\nu^2)}{R^2 t^2}\right]^{1/4} = \frac{1.286}{\sqrt{.411(.176)}} = \frac{1.286}{.269} = 4.78\ IN^{-1}$$

$$D = \frac{Et^3}{12(1-\nu^2)} = \frac{32\times10^6(5.45\times10^{-3})}{12(.91)} = 15.97\times10^3\ psi.$$

$$(\delta_r)_{AT\ END} = \frac{-V_0}{2D\lambda^3} = \frac{-(3360)}{2(15.97\times10^3)(109.0)} = 0.000965\ IN.$$

$$C_4 = \frac{0.965\times10^{-3}}{56000} = 17.22\times10^{-9}\ IN/PSI.$$

$$(f_T)_{END} = \frac{-2V_0}{t}\lambda R = \frac{-2(3360\ \frac{LB}{IN})}{(0.176\ IN)}(4.78)(0.411\ IN)$$

$= +75{,}000\ psi.$ (THIN SHELL SOLN. WITHOUT BENDING $f_T = \frac{PR}{t} = \frac{56000(.411)}{.176} = 131{,}000\ psi$)

$$(f_A)_{AT\ x=0.060} = \pm\frac{6M}{t^2},\quad M = \frac{1}{\lambda}V_0 e^{-\lambda x}\sin\lambda x\ \Big|_{\lambda x = .287}$$

$$(f_A)_{0.06} = \frac{6(3360)(.751)(.283)}{(.031)(4.78)} = \pm 28{,}900\ psi.$$

$$f_E = 0.707\left[(f_A - f_t)^2 + (f_t - f_T)^2 + (f_T - f_A)^2\right]^{1/2}$$

$$= 0.707\left[(-28.9 + 56)^2 + (-56 - 75)^2 + (75 + 28.9)^2\right]^{1/2}$$

$$= 120{,}000\ psi.$$

PREPARED _____
CHECKED _____
MODEL _____

FLEXIBILITY AND STRESSES IN SOFT SEAL

OUTER WALL

MARGINS AT 75°F (HIGHER AT −300°F)

$$(M.S.)_Y = \frac{150}{1.0(120)} - 1 = \underline{+0.25}$$

$$(M.S.)_{ULT} = \frac{18.0}{(1.5)(120)} - 1 = \underline{0.0}$$

∴ OUTER WALL THICKNESS IS JUST ADEQUATE FOR 56,000 psi RADIAL SEAL STRESS. SUBSEQUENT PLASTIC ANALYSIS TO FOLLOW SHOWS RADIAL SEAL STRESS LESS THAN −56000 psi AXIAL STRESS, SO MARGINS ARE ADEQUATE. IF AXIAL SEALING STRESS WERE LATER INCREASED BASED ON FUTURE TESTING, A THICKER OUTER WALL SHOULD BE CONSIDERED.

FLEXIBILITY AND STRESSES IN SOFT SEAL

AS IN THE PRELIMINARY ANALYSIS, THE SOFT MATERIAL WILL PLASTICALLY FLOW ONLY TO THE EXTENT THAT THE CONFINING HARD MATERIAL WALLS DEFLECT. CONSIDERING AN ELEMENT OF THE SOFT MATERIAL ORIENTED TO THE AXIAL, RADIAL AND TANGENTIAL DIRECTIONS:

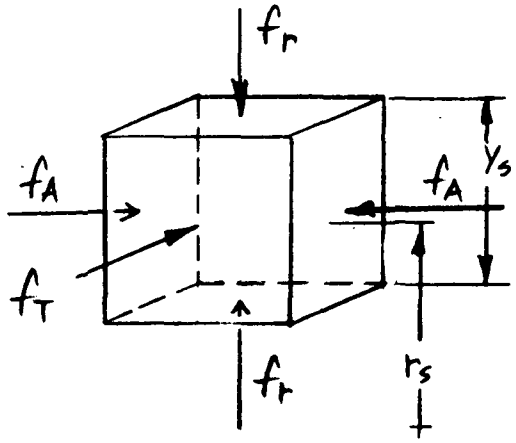

$$\epsilon_A = \frac{1}{E_s}\left[f_A - \nu(f_r + f_T)\right] \qquad (1)$$

$$\epsilon_r = \frac{1}{E_s}\left[f_r - \nu(f_T + f_A)\right] = C_r f_r \qquad (2)$$

$$\epsilon_T = \frac{1}{E_s}\left[f_T - \nu(f_A + f_r)\right] = C_T f_r \qquad (3)$$

WHERE THE RADIAL AND TANGENTIAL STRAIN FLEXIBILITIES C_r & C_T ARE FOUND FROM:

DEFLECTION OF SOFT SEAL ℓ:

$$\Delta r_s = \frac{1}{2} f_r (C_4 - C_3)$$

$$\epsilon_T = \frac{-2\pi \Delta r_s}{2\pi r_s} = \frac{1}{2}\left(\frac{C_4 - C_3}{r_s}\right) f_r = \frac{-1}{2}\left(\frac{17.22 - 9.31\times10^{-9}}{0.302\ IN}\right)$$

$$= -13.1\times10^{-9} f_r = C_T f_r$$

$$\epsilon_r = \frac{\Delta y_s}{y_s} = \left(\frac{C_4 + C_3}{y_s}\right) f_r = \frac{(17.22 + 9.31\times10^{-9}) f_r}{(0.042\ IN)}$$

$$= -631\times10^{-9} f_r = C_r f_r$$

FLEXIBILITY AND STRESSES IN SOFT SEAL

(3) $f_T = C_T f_r E_s + \nu(f_A + f_r) = \nu f_A + (\nu + C_T E_s) f_r$

(2) $(1 - C_r E_s) f_r = +\nu(f_T + f_A) = \nu f_A + \nu\left[\nu f_A + (\nu + C_T E_s) f_r\right]$

$$f_r = \frac{\nu(1+\nu) f_A}{1 - C_r E_s - \nu^2 - \nu C_T E_s}$$

THE SOLUTION OF THIS SET OF EQUATIONS IS NECESSARILY ITERATIVE AS $E_s = \frac{f_e}{\epsilon_e}$ IS A FUNCTION OF f_r, f_T & f_A. THE RANGE OF LIKELY SECANT MODULI FOR HIGHLY YIELDED CRYOGENIC ALUM IS INDICATED AS P_1 & P_2 ON P. 4.

AS FIRST TRIAL TAKE HYDROSTATIC ASSUMPTION AS TRUE, FIND STRAINS THEN FIND DISTORSION ENERGY EQUIVALENT STRAIN. USE THIS STRAIN TO ENTER STRESS STRAIN CURVE TO FIND E_s & ν.

$f_A = 56{,}000$ psi AND IF HYDROSTATIC $= f_r = f_T$

$\epsilon_T = -13.1 \times 10^{-9}(56000) = +734 \times 10^{-6}$ IN/IN

$\epsilon_r = -631 \times 10^{-9}(-56{,}000) = +3530 \times 10^{-6}$ IN/IN

$\epsilon_A = \epsilon_{ELAS} + \epsilon_{PLAS} = \left[1 - \frac{2\nu_E^2}{1-\nu_E}\right]\frac{f_A}{E} - \epsilon_T - \epsilon_r = \frac{-0.674(56)}{32\times10^6} - 4264\mu$

$= -1180 - 4264 = -5444\,\mu$ IN/IN.

FOR INITIALLY TIGHT GAPS, THESE ARE LARGEST STRAINS THAT COULD OCCUR.

ELEXIBILITY AND STRESSES IN SOFT SEAL

DISTORSION ENERGY EQUIVALENT STRAIN =
(REF BAKER, SHELL ANALYSIS MANUAL, N 68-24802, P. 449)

$$\epsilon_e = \frac{\sqrt{2}}{3}\left[(\epsilon_A-\epsilon_r)^2+(\epsilon_r-\epsilon_T)^2+(\epsilon_T-\epsilon_A)^2\right]^{1/2}$$

$$= 0.471\left[(-5444-3530)^2+(3530-734)^2+(734+5444)^2\right]^{1/2}$$

$$= 0.471\left[80.5\times10^6+7.8\times10^6+38.2\times10^6\right]^{1/2} = 5300\ \mu\ IN/IN.$$

$f_e \leq 11{,}000$ psi. FOR $\epsilon_e = 5300\ \mu$.
(DEPENDS ON DEGREE OF WORK HARDENING.)

$$E_s = \frac{11{,}000\ psi}{5300\ \mu\frac{IN}{IN}} = 2\times10^6\ psi.\ (1/10\ TH\ ELASTIC\ VALUE)$$

$$\nu \cong \frac{\epsilon_E}{\epsilon_{TOT}}(.3)+\frac{\epsilon_P}{\epsilon_{TOT}}(.5) = \frac{344\mu}{5300\mu}(.3)+\frac{4954\mu}{5300\mu}(.5)$$

$$= 0.48$$

SUBSTITUTING INTO PRECEDING EQUATIONS:

$$f_r = \frac{\nu(1+\nu)f_A}{1-C_r E_s-\nu^2-\nu C_T E_s} = \frac{.48(1.48)(-56{,}000)}{1-.230+1.262+0.013}$$

$$= -19{,}500\ psi.$$

$$f_T = \nu f_A+(\nu+C_T E_s)f_r = .48(-56000)+(.48-0.026)(-19500)$$

$$= -26{,}900-8850 = -35{,}750\ psi.$$

FURTHER ITERATION MIGHT IMPROVE ACCURACY OF SOLN.

FLEXIBILITY AND STRESSES IN SOFT SEAT

TRANSVERSE FRICTIONAL CONDITION BETWEEN HARD AND SOFT SEALS:

AS BEFORE, WHEN THE SEATING STRESS f_A IS REDUCED TO ZERO, THE PLASTIC PART OF f_m (AND f_T) CANNOT RELIEVE UNLESS THE HARD CONFINING WALLS CAN RETURN TO THEIR ORIGINAL POSITIONS. AS f_r & f_T REMAIN LESS THAN ~28000psi, LITTLE RELIEF WILL TAKE PLACE.
COEFFICIENT OF FRICTION OF ALUMINUM ON MILD STEEL, $\mu = 0.6$. μ FOR ALUM 1060-0 ON INCO-718 MUST BE MEASURED.
∴ SOLVE FOR $\mu = 0.2$ AND $\mu = 1.0$ (NORMAL RANGE)

RADIAL CONTACT AREA $= 3.14(.645\text{IN})(.060\text{IN})$
$= 0.1215\ \text{IN}^2$.

$f_r \cong -19{,}500$ psi.

$L_U\Big|_{\mu=1.0} = 19{,}500(.1215)(1.0) = 2370\ \text{LB}$

FOR $\mu = 0.6$, $L_U = 1420\ \text{LB}$, FOR $\mu = 0.2$, $L_U = 474\ \text{LB}$.

THUS THE NOMINAL 50 LB BELLEVILLE SPRING WILL NOT BE SUFFICIENT TO ADVANCE THE HARD OVER THE SOFT SEAL IN THE VALVE OPEN POSITION. AS THIS FRICTIONAL STICKING CANNOT INTERFERE WITH VALVE OPENING, THIS IS ACCEPTABLE.

FLEXIBILITY AND STRESSES IN SOFT SEAT

SHOULD EROSION OF THE SOFT SEAL FACE OCCUR, THE SEATING LOAD OF 1344 LB. WILL NOT BE SUFFICIENT TO ADVANCE THE SOFT SEAL RELATIVE TO THE HARD IN THE VALVE CLOSED POSITION FOR A NOMINAL COEFFICIENT OF FRICTION $\mu = 0.6$.

A DESIGN CHANGE FROM A 0.060 INCH CONTACT LENGTH TO A 0.050 LENGTH WILL CORRECT THIS. THEN

$$L_U\Big|_{\mu=0.6} = 1420\left(\frac{.05}{.06}\right) = 1180 \text{ LB} < 1344 \text{ LB}.$$

APPENDIX E
THERMAL PILOT VALVE DESIGN

Jeff 6-10-72

THERMAL PILOT VALVE DESIGN

CONFIGURATION

- EXPANSION TUBE
  LENGTH 3 ½" — 2" HEATED LENGTH
  .75" UNHEATED EARTH END

  OD .125
  ID .105
  WALL .010 — MATL 321 CRES

- INNER JACKET TUBE
  LENGTH 3 ½"

  OD .145 — MATL 321 CRES
  ID .125
  WALL .010

- PRESS SEAT DIA .090 — .003 WIDTH
- VENT SEAT DIA .060 — .004 WIDTH
- POPPET BALL DIA .125
- POPPET LOADING SPRING FORCE 25 LBS
- OUTER JACKET
  OD .562 — MATL 321 CRES
  WALL .032
- DESIGN TEMP RISE 400 °F
- EXPANSION TUBE STROKE = .006
  VENT OPEN .002 AT -320 °F
  VENT CLOSED AT -150 °F
  PRESSURE SEAT OPEN .004 − .0008 = .0032
  AT 80 °F

6-10-72

1. POPPET SEAT LOADING

ASSUME LOADING TO YIELD STRENGTH OF 321 CRES ANNEALED = 35000 PSI

SEAT DIA = .060 X .004 WIDTH

AREA = .060 π (.004) = .000752 in^2

LOAD = 35000 (.000752) = 26.3 #

PRESSURE LOADING OF SEAT

DIA .090 PRESS 400 PSI

F = .00636 (400) = .0255 # (NEGL.)

2. POPPET STROKE

TEMP RISE 400°F USE -320 °F BASE
HEATED LENGTH 2" (CONSERVATIVE)
PER ML-TDR-64-280 AF CRYO DATA BOOK
EXPANSION FROM -320 TO +80 °F = .003 IN/IN

FOR 2" HEATED LENGTH STROKE = .006

3. EXPANSION TUBE STRENGTH

HOOP .0123 − .0086 = .0037

AXIAL STRESS AT 25# LOAD

$\frac{25}{.0037}$ = 6750 PSI

6-10-72

COLUMN STRENGTH

NEGLECT JACKET TUBE

SLENDERNESS RATIO $r = \left[\frac{1}{4}(.0625^2 + .0525^2)\right]^{\frac{1}{2}}$

$= \left[\frac{1}{4}(.0039 + .0027)\right]^{\frac{1}{2}}$

$= \left(\frac{.0066}{4}\right)^{\frac{1}{2}} = (.0016)^{\frac{1}{2}} = .04$

$\frac{L}{r} = \frac{3.5}{.04} = 87.5$ (LONG COLUMN)

$P = \frac{A\pi^2 E}{\left(\frac{L}{r}\right)^2}$ $C = 1$ ROUND ENDS

$= \frac{\pi^2 (28\times10^6).0035}{(87.5)^2} = \frac{9.89(28\times10^6)(.0035)}{7660}$

$= 128\#$ COLUMN STRENGTH SIMPLE

STRAIN IN TUBE UNDER 25# LOAD

$\frac{6750(3.5)}{28\times10^6} = .000845$

6-10-72

THERMAL CHARACTERISTICS

HEAT REQ'D TO RAISE ESTIMATED MASS FROM -320 TO 80°F
(400° RISE)

TUBE $2.5(.145)(\pi)(.020) = .0228$
HTR $5(.00302) = .0151$
MISC $.0100$
TOTAL $.0479\ IN^3$
$WT = .3(.048) = .0144\ \#$

$HEAT = .0144(400).12 = .69\ BTU$

THERMAL LOSSES

CONDUCTIVE HEAT LOSS THRU TUBE ENDS
ASSUME: FULL Δt ACROSS TUBE
TUBE END LENGTH .75 (2 ENDS)
TUBE CROSS SECTION $.0165 - .0086 = .0079\ IN^2$

$$q = \frac{KA\Delta t}{L} = \frac{111\left(\frac{.0079}{144}\right)400}{.75} = 3.25\ BTU/HR$$

FOR BOTH ENDS $= 2(3.25) = 6.5\ BTU/HR$

CONDUCTION THRU HEATER CONNECTION
.062 DIA $A = .00302$
$K = 300\ BTU/HR/°F/FT^2/IN$ (AVG)
2 LEADS 1.0 LONG

$$q = \frac{300\left(\frac{.00302}{144}\right)400}{1.0} = 2.52\ BTU/HR$$

FOR BOTH ENDS $= 5.04\ BTU/HR$

6-10-72

RADIATION LOAD
VACUUM INSULATION

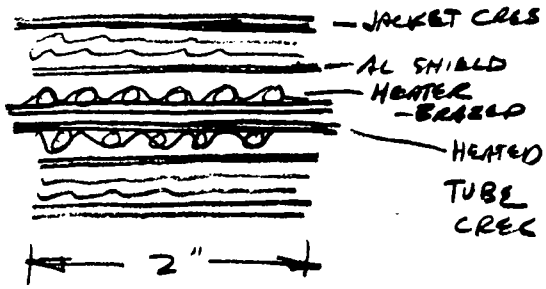

$$Q = \frac{\sigma A}{1/\epsilon_1 + \frac{A_1}{A_2}\left[\frac{1}{\epsilon_2} - 1\right]}\left(T_2^4 - T_1^4\right)$$

$$= \frac{5.076 \times 10^{-10}(1.18)}{\frac{1}{.03} + 1.5\left(\frac{1}{.03} - 1\right)}\left(856 \times 10^8\right)$$

$$\frac{6 \times 10^{-10}}{33.3 + 48.5}\left(856 \times 10^8\right)$$

$$= \frac{51.2}{81.8} = .627 \text{ WATTS}$$

$$= .627(3.415) = 2.14 \text{ BTU/HR}$$

ϵ_1 AL .03
ϵ_2 BRAZE .03
$T_1 = 140^\circ R$
$T_2 = 540^\circ R$
T_1^4 3.85×10^8
T_2^4 860×10^8
$\frac{A_1}{A_2} = 1.5$
$A = .188\pi(2) = 1.18 \text{ IN}^2$
$\sigma = 5.076 \times 10^{-10} \text{ WATTS/FT}^2$

TOTAL HEAT LOAD

TUBE ENDS	6.5
HTR CONNECT.	5.04
RADIATION	2.14
	13.68 BTU/HR

$$\frac{13.68}{3.415} = 4 \text{ WATTS}$$

TEMPERATURE RISE RATE AT 10 WATTS

6-10-72

10 - 4 = 6 WATTS AVAILABLE FOR HEATING

6 (3.415) = 20.5 BTU/HR

TIME TO HEAT MASS 40° F

$\frac{.69}{20.5}(60) = 2.02$ MIN